Technische Universität Braunschweig
Institut für Mikrobiologie

Twincore – Zentrum für Experimentelle und
Klinische Infektionsforschung
Institut für Molekulare Bakteriologie

Helmholtz Zentrum für Infektionsforschung
Abteilung Molekulare Bakteriologie

Analysis of antibiotic resistance determinants in *Pseudomonas aeruginosa* – a transcriptomic approach

Von der Fakultät für Lebenswissenschaften

der Technischen Universität Carolo-Wilhelmina

zu Braunschweig

zur Erlangung des Grades einer

Doktorin der Naturwissenschaften

(Dr. rer. nat.)

genehmigte

D i s s e r t a t i o n

von Ariane Alwine Khaledi
aus Braunschweig

1. Referent: Professor Dr. Michael Steinert
2. Referentin: Professor Dr. Susanne Häußler
eingereicht am: 28.04.2014
mündliche Prüfung (Disputation) am: 17.07.2014

Druckjahr 2014

Vorveröffentlichungen der Dissertation

Teilergebnisse aus dieser Arbeit wurden mit Genehmigung der Fakultät für Lebenswissenschaften, vertreten durch den Mentor der Arbeit, in folgenden Beiträgen vorab veröffentlicht:

Publikationen

Dötsch A., Eckweiler D., Schniederjans M., Zimmermann A., Jensen V., Scharfe M., Geffers R., Häussler S. (2012) The *Pseudomonas aeruginosa* transcriptome in planktonic cultures and static biofilms using RNA sequencing. PLoS One. 7(2):**e**31092.

Pohl S., Klockgether J., Eckweiler D., Khaledi A., Schniederjans M., Chouvarine P., Tümmler B., Häussler S. (in print) The extensive set of accessory *Pseudomonas aeruginosa* genomic components. Im Druck bei *FEMS Microbiology Letters,* April 2014.

Tagungsbeiträge

Zimmermann, A., Schniederjans, M., Dötsch, A., Häußler, S. Analysis of antibiotic resistance determinants in *Pseudomonas aeruginosa.* (Vortrag) 3rd Public Retreat HZI Graduate School, Bad Bevensen (2012).

Zimmermann, A., Schniederjans, M., Dötsch, A., Häußler, S. Wanna be a superbug? – Analysis of antibiotic resistance determinants in *Pseudomonas aeruginosa.* (Poster) International Summer School on Infection Research, Rügen (2012).

Zimmermann, A., Schniederjans, M., Dötsch, A., Häußler, S. Analysis of β-lactam resistance determinants in *Pseudomonas aeruginosa.* (Poster) 5th Congress of European Microbiologists (FEMS), Leipzig (2013).

It has long been an axiom of mine
that the little things
are infinitely the most important.

Sir Arthur Conan Doyle,
Sherlock Holmes - A Case of Identity

Summary

During this work, a *Pseudomonas aeruginosa* optimized, strand-specific RNA-sequencing method was developed to allow for multiplexed transcriptome data acquisition on Illumina next generation sequencing systems. This technique was used to obtain global sequence and expression information from 149 clinical isolates of different sample origins and with diverse antibiotic resistance profiles (most of them multidrug resistant). The received fraction of up to 75 % mapped mRNA reads per sample, resulting in up to 90 % total genome coverage, was sufficient for in depth data analysis at the single nucleotide level. This data was successfully used to determine high resolution taxonomic relatedness of the isolates and screen for genetic determinants correlating with β-lactam resistance phenotypes of phylogenetically unrelated strains. A combination of *de novo* assembly and coverage determination was used to search for acquired resistance genes and led to the identification of nine different β-lactamases in overall 19 isolates. Furthermore, unbiased statistical comparisons were developed and integrated in a publically available database for the analysis of core genetic alteration enrichments (SNPs, stops, gene expression) in phenotypically related groups of isolates. Thereby, six genes of significance in ceftazidime and two in meropenem non-susceptible isolates were identified. Detailed single gene investigation revealed that more than 95 % of the isolates harbored known, dominant genetic resistance determinants which, apart from acquired enzymes, were displayed by constitutive intrinsic *ampC* overexpression or lack of OprD porin due to expression repression or nonsense mutation. Penicillin binding proteins did not seem to be involved in ceftazidime or meropenem resistance of clinical isolates.

Furthermore, the effects of low-level sub-inhibitory concentrations of bactericidal antibiotics from different compound classes on the transcriptome of PA14 wild type cells were investigated, revealing a variety of specific responses (DNA repair, cell envelope modification, ribosome regulation), but also common ones as SOS response and the induction of denitrification pathways. These results could be connected to global metabolic reactions as a consequence of intracellular reactive oxygen stress. Using isotope labelling studies, we detected an enhanced biosynthesis of amino acids which are directly derived from tricarboxylic acid cycle dependent or closely related NAD+ and NADP+ dependent pathways. This suggests common impacts of low-level bactericidal antimicrobials on bacterial cellular systems, regardless of their chemical structure, with a likely connection to respiration hyperactivation.

Zusammenfassung

Im Verlauf dieser Arbeit wurde eine für *Pseudomonas aeruginosa* optimierte, Strang-spezifische Sequenziermethode entwickelt, die das Multiplexen verschiedener cDNA-Proben in einem einzigen gemeinsamen Illumina Sequenzieransatz ermöglicht sowie die nachträgliche probenspezifische Zuordnung der einzelnen Transkriptomdatensätze. Diese Technik wurde genutzt um globale Sequenz- und Expressionsinformationen von 149 klinischen Isolaten unterschiedlicher geografischer Herkunft und variierender Antibiotikaresistenzprofile (in der Mehrzahl multiresistent) aufzunehmen. Mit einem Anteil von bis zu 75 % mRNA pro Probe konnte eine Gesamtgenomabdeckung von bis zu 90 % erzielt werden, welche ausreichend für detaillierte, sequenzspezifische Analysen auf Einzelnukleotidebene war. Diese Daten wurden dazu genutzt, die Verwandtschaftsbeziehungen der verschiedenen Isolate hoch-auflösend darzustellen und nach genetischen Markern zu suchen, welche in nicht verwandten Stämmen in Zusammenhang mit β-Lactam-Resistenz standen. Durch eine Kombination aus *de novo assembly* und Analyse der relativen Genabdeckung konnten insgesamt neun verschiedene erworbene β-Lactamasen in zusammen 19 Isolaten detektiert werden. Des Weiteren wurden datenbankintegrierte Hilfsmittel für statistische Vergleiche entwickelt um die Anreicherungen intrinsischer genetischer Marker (SNPs, Stopps, Expressionsdifferenzen) in phänotypisch ähnlichen Gruppen von Isolaten zu ermöglichen. Hiermit konnten sechs signifikante Gene in Ceftazidim und zwei in Meropenem resistenten Isolaten identifiziert werden, die insgesamt zusätzlich Hinweise auf erworbene Kreuzresistenzen und kompensatorische Anpassungen lieferten. Eine detaillierte Untersuchung ausgewählter Gene zeigte zudem, dass in über 95 % die jeweilige erworbene β-Lactam-Resistenz auf bekannte Hauptmarker wie erworbenen Resistenzenzyme, eine Überexpression der intrinsischen β-Lactamase *ampC* oder ein Fehlen des OprD porins zurückzuführen war (Penicillin bindende Proteine schienen hingegen nicht nennenswert beteiligt).

Weiterhin wurde der Effekt von geringen, sub-inhibitorischen Konzentrationen bakterizider Antibiotika auf Wildtyp Zellen untersucht. Hierbei konnten neben spezifischen transkriptionellen Anpassungen eine Reihe von globalen Stressadaptionen wie die Induktion der SOS Antwort und des Denitrifikationsstoffwechsels beobachtet werden, die vermutlich aufgrund erhöhter intrazellulärer Sauerstoffradikalkonzentrationen auftraten. Mit Hilfe von Isotopenmarkierungen konnte eine Verbindung zu globalen metabolischen Veränderungen aufgezeigt werden. Diese führten unabhängig vom eingesetzten Antibiotikum zu einer erhöhten Biosynthese von Aminosäuren, die in direkter Abhängigkeit zum Zitratzyklus oder nahe verwandten NAD+ und NADP+ bedingten Prozessen standen. Somit lässt sich eine Überstimulation der Atmungskette als unabhängige Stressantwort auf geringe Antibiotikakonzentrationen vermuten.

Table of Contents

List of Figures

List of Tables

List of Abbreviations

ATP	adenosine triphosphate
CAZ	ceftazidim
CDC	U.S. Center for Disease Control
cDNA	complementary DNA
CF	cystic fibrosis
CFU	colony forming unit
CIP	ciprofloxacin
Cys	cysteine
D-Ala	D-alanine
ddC	dideoxycytidine
dH_2O	deionized water
DMSO	dimethyl sulfoxide
DNA	deoxyribonucleic acid
dNTP	deoxynucleotide triphosphate
DSN	duplex-specific nuclease
dT	deoxythymidine
DTT	dithiothreitol
EDTA	ethylenediaminetetraacetic acid
ESBL	extended spectrum β-lactamase
et al	*et alii*
FDA	Food and Drug Administration
FDR	false-discovery rate
GC	gas chromatography
GlcNAc	N-acetylglucosamine
H2DCFDA	2',7'-dichlorodihydrofluorescein diacetate
HEPES	4-(2-hydroxyethyl)-1-piperazineethanesulfonic acid
ICU	intensive care unit
LB	Luria-Bertani
LC-MS/MS	liquid chromatography - tandem mass spectrometry
log_2FC	logarithmic two fold change
LPS	lipopolysaccharide
MBL	metallo-β-lactamase
MDR	mutidrug resistant
MEM	meropenem
Met	methionine
Mex	multidrug efflux
MFP	membrane fusion protein
MIC	minimal inhibitory concentration
MOPS	3-(N-morpholino)propanesulfonic acid
MRGN	multi-resistant Gram-negative
mRNA	messenger RNA
MurNAc	N-acetylmuramic acid
nd	not determined

nrpk	normalized reads per kilobase
OD	optical density
OMF	outer membrane factor
padj	adjusted p-value
PAGE	polyacrylamide gel electrophoresis
PBP	penicillin binding protein
PBS	phosphate buffered saline
PCR	polymerase chain rection
PIP	piperacillin
PVDF	polyvinylidene fluoride
RNA	ribonucleic acid
RND	resistance-nodulation-division efflux pump
ROS	reactive oxygen species
rpg	reads per gene
rRNA	ribosomal RNA
SDS	sodium dodecyl sulfate
SLS	sodium lauryl sarcosinate
SNP	single nucleotide polymorphisms
sRNA	small RNA
TCA	tricarboxylic acid
TE	Tris-EDTA
TEX	terminator-5’-phosphate-dependent exonuclease
TOB	tobramycin
Tris	tris(hydroxymethyl)aminomethane
tRNA	transfer RNA
TSS	transcriptional start site
UPLC	ultra performance liquid chromatography
v/v	volume per volume
w/v	weight per volume
WGS	whole genome sequencing
wt	wild-type
WTS	whole transcriptome sequencing

1 Introduction

1.1 *Pseudomonas aeruginosa* as a model organism

Pseudomonas aeruginosa is probably the best characterized member of the genus *Pseudomonas,* which belongs to the class of γ-Proteobacteria. This diverse genus was first described in 1894 by the German botanist Walter Migula and served as a collecting pond for rod-shaped, polar-flagellated Gram-negative bacteria, which gained energy through oxygen dependent respiration [1]. Modern molecular taxonomy based on DNA-DNA-, rRNA-DNA-hybridization and, most importantly, 16S rRNA similarity has greatly improved phenotype independent classification [2,3]. At present, the genus comprises 230 species and subspecies [4].

Due to their metabolic flexibility, *P. aeruginosa* is able to thrive in diverse ecological niches and can thus be found ubiquitously in soil and water habitats [5]. The bacterium favors oxygen as a terminal electron acceptor within the respiratory chain, but can as well generate ATP under anaerobic conditions using nitrate or nitrite as alternative electron acceptors [6,7]. In the absence of a terminal electron acceptor, *P. aeruginosa* is able to ferment the amino acids arginine and pyruvate [8-10]. However, this metabolic pathway does not support cell growth and proliferation, but merely long-term survival under anaerobic conditions. Furthermore, *P. aeruginosa* is capable of degrading various carbon sources as sugars, fatty acids, alcohols, glycols, aromatic compounds, amines and amino acids [11], although it prefers the degradation of organic acids, e.g. acetic acid. Of note, when *P. aeruginosa* metabolizes glucose, this is, as opposed to most other bacteria, usually not done by glycolysis (Embden-Meyerhoff-Parnas pathway), or the pentose-phosphate pathway, but by the Entner-Doudoroff pathway (ED) [12]. This pathway uses 6-phosphogluconate dehydratase and 2-keto-3-deoxyphosphogluconate aldolase to create pyruvates from glucose [13].

Besides its free-living, environmental lifestyle, the catabolic adaptability and metabolic versatility allows *P. aeruginosa* likewise to colonize various plants and animal surface tissues, as well as human skin, where it may behave as an opportunistic pathogen. Interestingly, the bacterium uses the same repertoire of virulence factors in all hosts [14-16].

1.2 *Pseudomonas aeruginosa* as an opportunistic nosocomial pathogen

Despite its ubiquitous appearance, *P. aeruginosa* is rarely found in the normal human microbial flora and usually does not colonize and infect healthy individuals [17]. However, it can cause severe infections in immunocompromised people, were colonization rates can increase from nearly zero to

over 50 % during hospitalization [18]. As a consequence, this bacterium is responsible for 9 % of all hospital acquired infections in the USA, designating it one of the leading nosocomial pathogens [19]. Especially catheterized patients and burn wound victims are prone to life threatening infections, and *P. aeruginosa* is the leading cause of nosocomial pneumonia in the United States (51,000 cases in 2013) [20,21]. Most frequently, lung infections of *P. aeruginosa* occur in patients suffering from cystic fibrosis (CF). CF is an autosomal, recessively passed genetic disorder in which mutations of the cystic fibrosis transmembrane regulator (CFTR) lead to a reduction of the sodium and chloride ion transport across the epithelium. This results in increased mucus viscosity and promotes bacterial colonization of the lung. As a consequence, chronic *P. aeruginosa* infections establish, which represent the leading cause of lung function decline and ultimate mortality in CF patients [22-24]. Effective treatment and bacterial eradication proves to be difficult as *P. aeruginosa* is able to form biofilms and possesses complex virulence and protection systems, including pili for adhesion, siderophores for the acquisition of extracellular iron and mechanism for the secretion of exotoxins, phenazines and rhamnolipids [25-29].

However, the most evident threat poses the frequent occurrence of single and multiple antimicrobial resistant variants. While the overall *P. aeruginosa* infection rates in intensive care units (ICU) remained more or less stable during the past 30 years, there has been an alarming increase in drug resistant isolates [20]. About 13 % of severe healthcare-associated *Pseudomonas aeruginosa* infections (6,700 cases, resulting in 440 deaths in the USA in 2013) were caused by multidrug resistant (MDR) bacteria [21]. MDR defines acquired non-susceptibility to at least one agent in three or more antimicrobial categories, in this case the important anti-pseudomonal antibiotics aminoglycosides, fluoroquinolones and β-lactams [30]. Recently, a further nomenclature for multidrug resistant Gram-negative rods including *Pseudomonas aeruginosa* was introduced by the Robert Koch-Institut for improved risk management in hospitals. It suggested additional classification of the bacteria as 3MRGN or 4MRGN (for multi-resistant Gram-negative), when they display resistance to three or four of the following classes of antibiotic, respectively: penicillins, cephalosporins, carbapenems, and fluoroquinolones [31]. Drug-resistance in *P. aeruginosa* is associated with significant increases in morbidity, mortality, need for surgical intervention, length of hospital stay, and thus overall health care costs [32-35].

1.3 Antibiotics: past and present

Although the antimicrobial properties of certain extracts from molds and plants had been recognized as treatments of infections already over 2000 years ago, it was not until the early 20th century that antibiotics truly revolutionized modern medical therapy [36]. This new era was launched in 1928 by

the Scottish scientist and Nobel laureate Alexander Fleming who made an unexpected discovery during his work at St. Mary's Hospital in London: *Staphylococcus* colonies on a culture plate were destroyed in the neighborhood of a fungus contamination by a substance with an obvious antimicrobial activity. Fleming named this substance *Penicillin*, which only a decade later went into successful large-scale production [37]. Selman Waksman finally introduced the term "antibiotic" in a journal article in 1947, describing any substance produced by a microorganism that is antagonistic to the growth of other microorganisms in high dilution [38].

Subsequently, the use of antibiotics constituted a dramatic improvement in the treatment of life-threatening bacterial diseases as compared to the pre-antibiotic era characterized by the absence of adequate therapy [39]. As one example, the mortality rate of acute meningococcal meningitis was lowered from 70-90 % to 10 % [40]. Between 1940 and 1962 more than 20 new classes of antibiotics were marketed worldwide [41].

However, in the succeeding decades the more cost-efficient production of semisynthetic drug analogues gained increasing importance with only two novel classes discovered since [41]. Today, the overall yearly number of new antibiotic approvals by the Food and Drug Administration (FDA) is in a constant decline (Figure 1.1)[21].

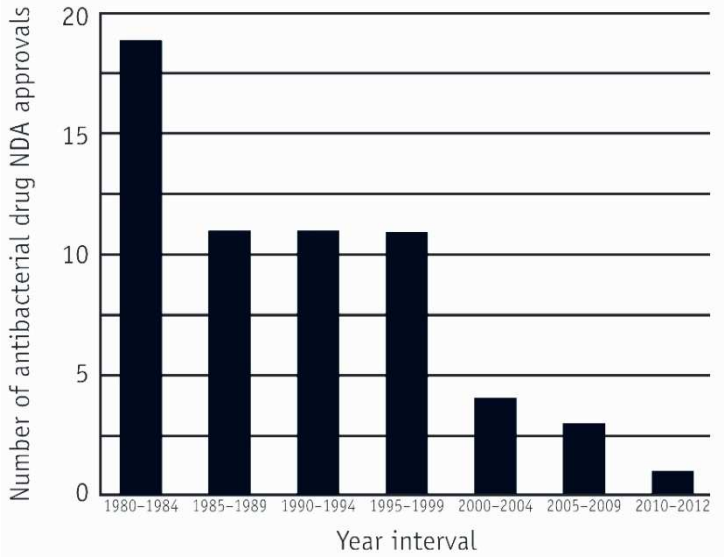

Figure 1.1 Number of new drug applications (NDA) approvals per year interval.

Intervals from 1980-2009 are 5-year intervals; 2010-2012 is a 3-year interval. Drugs are limited to systemic agents. Data of FDA's Center for Drug Evaluation and Research (CDER). Figure taken from [21].

Today's antibiotics can be divided into two groups based on their biological activity: *bactericidal* agents which induce cell death and *bacteriostatic* agents which merely stall bacterial growth and proliferation [42]. Further classification is done based on their cellular targets. Most current bactericidal antibiotics inhibit DNA, RNA or cell wall synthesis, while bacteriostatic ones usually halt

protein production (with the exception of the bactericidal aminoglycosides) [43]. Three bactericidal classes of antibiotics are of particular clinical relevance in the treatment of *P. aeruginosa* infections: aminoglycosides, fluoroquinolones and β-lactams [44].

Aminoglycosides bind to the 30S subunit of the bacterial ribosome and impair the incorporation of amino acids into elongating peptides, which leads to the production of misfolded proteins [45]. Fluoroquinolones interfere with changes in DNA supercoiling by binding to complexes of DNA and either one of the two target enzymes DNA gyrase and topoisomerase IV, and thus inhibit DNA replication [46]. The third group, β-lactams, induces lytic cell death by intervening with the synthesis of the bacterial cell wall [47].

1.3.1 β-lactams – inhibitors of cell wall biosynthesis

β-lactam antibiotics belong to one of the three largest classes of antibiotics and represent over 65 % of the world's antibiotic market [48]. They gain their antibiotic activity by interfering with the biosynthesis of the bacterial cell wall and can be used for the treatment of a variety of Gram-positive and Gram-negative infections [49].

The bacterial cell wall is composed of stabilizing layers of peptidoglycan, which plays a key role in maintaining cell shape and counteracting internal osmotic pressure [50]. Peptidoglycan is a covalently cross-linked polymer matrix consisting of two alternating amino sugars, namely N-acetylglucosamine (GlcNAc) and N-acetylmuramic acid (MurNAc), which are connected by β-(1,4)-glycosidic bonds. Adjacent MurNAc chains are further interlinked with each other by peptide cross-connections [51]. These cross-connections are accomplished by the activity of the penicillin-binding-proteins (PBPs) which recognize a natural D-Ala-D-Ala motive in the MurNAc adherent peptide chain [52]. β-lactams are analogues of the D-Ala-D-Ala dipeptide. They bind irreversibly to the active site of the PBPs instead, and thus prevent the cross-linking of the peptidoglycan units by inhibiting the peptide bond formation [53]. Most bacterial species have various types of PBPs. They differ in their molecular weight, enzymatic activity and affinity for binding penicillin or other β-lactam antibiotics [52].

Besides affecting the peptidoglycan stability per se, the inhibition of PBPs causes a build-up of peptidoglycan precursors. This rearrangement within the cell wall triggers a stress response which results in the autolytic hydrolysis of the existing peptidoglycan and promotes production of new peptidoglycan, and consequently further enhances the bactericidal activity of the antibiotic [42].

All β-lactam antibiotics commonly share the molecular β-lactam ring structure, but are classified into different subgroups according to additionally varying core structures. Members of four of these subgroups are administered to treat *P. aeruginosa* infections, the penicillins (penams), monobactams, cephalosporins (cephems) and carbapenems (Figure 1.2) [48].

Two β-lactams with particularly high anti-pseudomonal activity which are commonly used in the clinics, are the third generation cephalosporin ceftazidime (CAZ) and the carbapenem meropenem (MEM) [44].

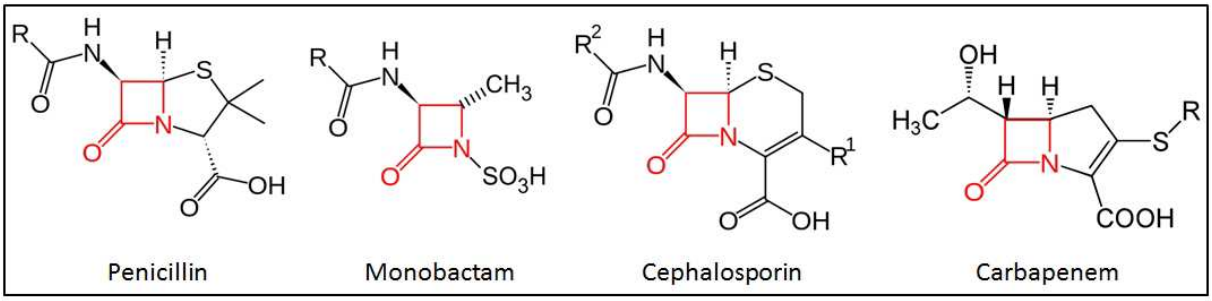

Figure 1.2 Core structure of the different classes of β-lactams.

The characteristic β-lactam ring structure is marked in red. β-lactams fused to thiazolidine rings are named penicillins, if they contain a 3,6-dihydro-2H-1,3-thiazine ring, cephalosporins. Carbapenems incorporate a 2,3-dihydro-1H-pyrrole, while monobactams do not contain any additional ring structure. Figure adapted from [48].

1.4 Antibiotic resistance in *Pseudomonas aeruginosa*

In 2013 *Pseudomonas aeruginosa* was classified as "a serious concern to public health, requiring prompt and sustained action" by the U.S. Center for Disease Control (CDC), due to its MDR antibiotic resistance profile [21]. Selection of adequate antibiotics becomes increasingly complicated, since *P. aeruginosa* does not only harbor a variety of intrinsic resistance mechanisms, but also a great capacity to acquire new ones by additional gene uptake or mutation. The latter is a particular threat during ongoing antibiotic medication, which can easily promote resistance development and MDR phenotypes, and thus increase the risk of treatment failure [54,55]. Resistance rates for β-lactams, fluoroquinolones and aminoglycosides from patients' isolates ranged up to 32 %, 35 % and 22 %, respectively in 2002, while MDR strains were isolated in 26 % of the cases [18].

Often a combination of chromosomally encoded mechanisms, including over time evolved chromosomal changes, and the acquisition of mechanisms imported on mobile genetic elements is responsible for the respective resistance phenotype [56].

1.4.1 Chromosomally encoded β-lactam resistance mechanisms affecting antibiotic influx and efflux

P. aeruginosa intrinsically exhibits low susceptibility towards a broad range of different antimicrobial classes. Two reasons for this are the low outer membrane permeability and the expression of several pump systems, which passively decreases the influx and actively increases the efflux of antimicrobial

substances to reduce drug accumulation inside the cell [57,58]. The low permeability is achieved by the asymmetric bilayer of the outer membrane with its variable lipopolysaccharide (LPS) which acts as an effective barrier against the rapid penetration of lipophilic antibiotics, and the lack of high-permeability porins for hydrophilic agents which are present in most other Gram-negatives [59].

1.4.1.1 Multidrug efflux systems

Additionally to its low membrane permeability, *P. aeruginosa* possesses nine multidrug efflux (Mex) pump systems of the resistance-nodulation-division (RND) family which are responsible for the extrusion of antibiotics (Table 1.1) [18].

Table 1.1 Overview of RND efflux pumps in *Pseudomonas aeruginosa.*

Modified from Lister and colleagues [18].

Efflux system	Regulators		Antibiotic substrates
	Direct	Indirect	
MexAB-OprM	MexR, NalD	NalC	β-lactams, fluoroquinolones, tetracyclines, chloramphenicol, macrolides, novobiocin, trimethoprim, sulfonamides
MexCD-OprJ	NfxB		β-lactams, fluoroquinolones, tetracyclines, chloramphenicol, macrolides, novobiocin
MexEF-OprN	MexT	MexS, MvaT	fluoroquinolones, chloramphenicol, trimethoprim
MexXY-OprM/Opm-x	MexZ		β-lactams, fluoroquinolones, aminoglycosides, tetracyclines, chloramphenicol, macrolides
MexJK-OprM/OpmH	MexL		tetracycline, erythromycin
MexGHI-OpmD	SoxR		fluoroquinolones
MexVW-OprM			fluoroquinolones, tetracyclines, chloramphenicol, erythromycin
MexPQ-OpmE			fluoroquinolones, tetracyclines, chloramphenicol, macrolides
MexMN-OprM			cloramphenicol, triamphenicol

x, the efflux system MexXY may use OpmB, OpmG, OpmH and/or OmpI

RND efflux pumps typically consist of three individual components: a periplasmic membrane fusion protein (MFP), a cytoplasmic membrane transporter (RND), and an outer membrane factor (OMF). MFP and RND are obligatorily co-transcribed in one operon, while the OMF can optionally be a part of the same operon or be an individually transcribed component (Figure 1.3). Regulation of the operons occurs by adjacent, direct regulators (usually transcriptional repressors) and partly in combination with secondary, indirect regulators [18]. Members of the RND family are secondary active transporters and gain their energy required for substrate extrusion from proton motive force [60].

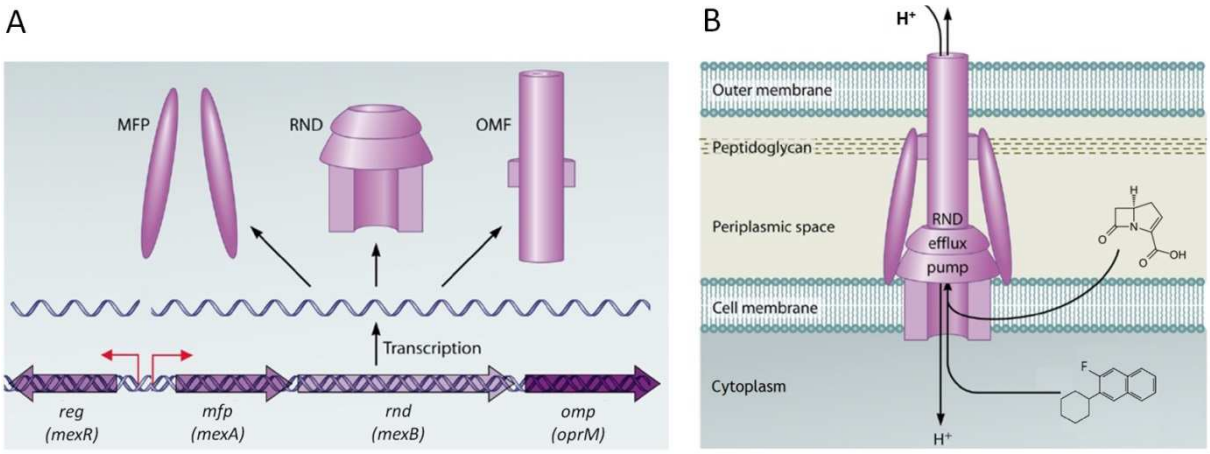

Figure 1.3 Structure and function of RND efflux pumps in *Pseudomonas aeruginosa*.

A: RND pumps typically exist in a tripartite system consisting of an RND cytoplasmic membrane transporter (RND), a membrane fusion protein (MFP), and an outer membrane factor (OMF). Genes encoding for MFP and RND are always transcribed from the same operon, while the OMF gene may be part of the same operon. Primary regulation is usually mediated by an adjacently transcribed regulator *(reg).* **B:** The RND complex forms a channel spanning the entire cell envelope (including outer membrane, peptidoglycan, periplasm and inner cell membrane), which allows for the proton-driven transport of lipophilic and amphiphilic substances from the cytoplasm to the outside of the cell. The RND efflux pumps can also extrude drugs from the periplasmic space before they cross the cytoplasmic membrane. Figure modified from [18].

Although antimicrobial agents do not appear to be their natural substrates, RND efflux pumps show broad substrate specificity toward various classes of antibiotics [61-63]. However, only MexAB-OprM is expressed at sufficient levels to influence intrinsic multidrug susceptibility in wild-type cells [64]. In the case of the remaining Mex pumps, up-regulation has to be triggered by mutational disruption of the corresponding repressors. This can occur via non-synonymous single nucleotide polymorphisms (SNPs) or, more frequently, via unspecific short insertions or deletions within the repressing regulator gene that lead to the expression of a non-functional protein [65-67]. As during antibiotic treatment adaptive mutations which induce drug tolerance are strongly selected, alterations within efflux regulatory genes are an important step towards initial bacterial survival [68]. However, RND systems are only able to confer low level antibiotic resistance. Thus, more specific antibiotic target mutations have to follow promptly to conquer high level antibiotic exposure [69].

Three Mex pump systems, namely MexAB-OprM, MexCD-OprJ, and MexXY have been described previously to export β-lactam antibiotics [18]. However, the latter two have only a very narrow substrate profile. MexCD-OprJ prefers fourth generation cephalosporins as cefepime, cefpirome and cefozopran and shows no significant activity towards meropenem, and the extent of activity of MexXY for meropenem and ceftazidime is not completely clear, but MIC changes range among low susceptibility values and are generally lower for carbapenems than cephalosporins [70-72]. MexAB-

OprM on the other hand exhibits broad substrate specificity among β-lactams, including the clinically relevant third generation cephalosporins and meropenem, and has a more pronounced effect on the respective susceptibility phenotype [18,73,74].

1.4.1.2 Porins and β-lactam resistance: OprD

The outer membrane of Gram-negative bacteria is a semipermeable construct and functions as a barrier to direct the uptake of environmental substances. Permeability varies among different bacterial species and is decreased by 92 % in *P. aeruginosa* compared with *E. coli* [75]. Nevertheless, bacteria have to ensure sufficient nutrient uptake into the cell, which is achieved by a collection of water-filled protein channels, the porins. These porins play an important role in the transport of sugars, amino acids, phosphates, divalent cations, and siderophores [75]. However, since porins are non-specific or only contain stereospecific binding sites, they also allow the passage of hydrophilic antibiotics, as β-lactam, across the membrane [76-78]. Genome sequencing revealed 64 known or predicted porins in *P. aeruginosa* of which 19 belong to the family of OprD porins with 46 % to 57 % amino acid sequence similarity to the OprD protein [75,79].

OprD is a 443 amino acid long porin, specific for the uptake of basic amino acids, for example arginine, small peptides containing these amino acids, and respective analogues as carbapenem antibiotics for which it is the preferential entry portal [80,81]. Consequently, a decreased expression of functional OprD can increase carbapenem resistance [82,83]. Interestingly, due to the competition of carbapenems and amino acids passing through the channel, environmental conditions providing high concentrations of different amino acids, such as in serum or culture medium, can alter carbapenem MIC values by up to 2-fold [84,85]. However, mutants lacking OprD are not necessarily compromised in growth, since other porins can counteract the loss and take over specific amino acid transporting activities, as OpdP in the case of arginine [86,87].

The pathway of OprD mediated resistance can involve transcriptional repression or mutational disruption of the gene inducing conformational changes or premature translational stops, both frequently occurring during carbapenem treatment [88-90].

As other typical porin proteins, OprD contains a transmembrane β-barrel structure comprising 16 strands interconnected with seven short periplasmic turns, acting as hinges, and eight external loops [91,92]. X-ray crystal structures even suggest an 18-stranded β-barrel with nine external loops [93]. This particular structure is essential for the semi-selective substance transport, as it was shown by deletion experiments that the different external loops specifically interact with putative substrates, and missing amino acids can increase or decrease the susceptibility towards individual antibiotics or whole substance classes as carbapenems or other β-lactams [88,91,92,94-96].

Despite the importance of the external loops in substrate up-take, OprD shows a high natural variability, especially within these regions, also among carbapenem susceptible strains and particularly clinical isolates [92,96,97]. One reason could be selective pressure upon specific environmental conditions, as the immune system for example recognizes bacteria first by distinct surface markers, in particular outer membrane proteins. Thus, high porin surface variability influences host pathogen interactions and aids in immune evasion [98].

Besides mutational disruption, transcriptional repression of *oprD* is a key principle in carbapenem resistance. However, regulation of *oprD* comprises a complex network and is not yet completely understood. Transcription of *oprD* can be initiated from two start sites, 23 and 71 bases upstream of the gene, which are both used with equal frequencies [18]. Ochs and colleagues even described a third start site at position -89 and additionally identified the arginine responsive regulator ArgR as one of the direct transcription inducers [99]. They also proposed a second amino acid dependent induction mechanism, as glutamate as carbon source triggers *oprD* expression independently of ArgR.

On the other hand, multiple ways of transcriptional repression are known as well, which include trace metal (particularly zinc and copper) dependent repression via CrcS, CrzR, and the two component regulatory system CopR-CopS [100-102]. Recently another two-component regulatory system, ParR-ParS which is also involved in MexXY regulation was described to possibly influence imipenem susceptibility by repressing *oprD* expression [103]. Synergistic regulation of OprD and efflux pumps seems to be of general importance, as this has also been described for the MexEF-OprN efflux pump. The *mexEF-oprN* operon is, amongst other factors, controlled by the adjacently transcribed transcriptional activator MexT, which was shown to not only positively regulate *mexEF-oprN* but also negatively regulate *oprD* expression [104,105]. However, it is not known so far, whether MexT directly interacts with the *oprD* promoter or rather stimulates indirect transcriptional regulation, and there is further evidence for MexT-mediated posttranscriptional effects [106].

1.4.2 β-lactamases – hydrolyzing enzymes

Besides controlling antibiotic influx and efflux, a third important β-lactam resistance mechanism in Gram-negative bacteria is the antibiotic degradation by corresponding enzymes, the β-lactamases [47]. β-lactamases are able to inactivate antibiotics by hydrolyzing the amide bond of their characteristic four-membered β-lactam core ring-structure [107,108]. Thus, they lose their PBP binding capacity and thereby their membrane destructive functions. In fact, hydrolysis of β-lactam antibiotics by β-lactamases is the most common mechanism of resistance for this class of antibacterial agents in clinically important Gram-negative bacteria [109]. By late 2009, 890 unique variants of these enzymes had been reported, but this number is constantly growing [109-113].

Depending on their different molecular structure, β-lactamases can be divided into two families, serine-β-lactamases and metallo-β-lactamases (MBL). While MBLs need zinc to be functionally active and are inhibited by metal chelators as EDTA, serine-β-lactamases remain unaffected [114]. Further classification is done based on the amino acid sequence similarities of these enzymes. To date, four classes are recognized (A-D): classes A, C, and D act by a serine-based mechanism, whereas class B contains the MBLs. Classes A, C and D show high substrate diversities including narrow and wide spectrum activity, including a few carbapenemases and extended spectrum β-lactamases (ESBLs). MBLs likewise display varying substrate specificities; however, they share the common features of potent carbapenemase activity, resistance to clinical β-lactamase inhibitors and lack of activity against monobactams [115-117]. For an overview on β-lactamase classification and properties, see Table 1.2.

Table 1.2 Classification and properties of β-lactamases.

Table modified from [47] with further modifications from [109,113,114,118].

Class	Type of enzyme	Preferred substrates	Inhibited by		Representative enzymes or enzyme families
			CA or TZB*	EDTA	
A	Penicillinase	Penicillins	yes	no	Penicillinases from Gram-positives
	RSBL	Penicillins, cephalosporins	yes	no	TEM-1, TEM-2, SHV-1
	ESBL	Penicillins, cephalosporins[a], monobactams	yes	no	SHV, TEM, CTX-M, PER-1, VEB, GES,
	IR β-lactamase	Penicillins, cephalosporins	no	no	TEM-30 to -41, -44, -45, -51, -54
	IR ESBL	Penicillins, cephalosporins[a]	no	no	TEM-50, -68, -80
	Carbapenemase	Penicillins, cephalosporins, carbapenems, monobactams; sometimes es-β-lactams[b]	some	no	SME, IMI, KPC, GES-2, SHV-38
B	Carbapenemase	Most β-lactams	no	yes	IMP, VIM, SPM, IND, NDM, GIM, AIM, FIM, SIM, DIM
C	Expanded-spectrum cephalosporinase	Penicillins, carbapenems, es-β-lactams[b] and 4th generation cephalosporins	no	no	CMY, LAT, MOX, FOX, ACT, MIR, DHA, CFE-1
D	Narrow-spectrum penicillinase	Penicillins, cloxacillin	some	no	OXA
	ESBL	Penicillins, cloxacillin, es-β-lactams[b], sometimes monobactams or cephalosporins[c]	some	no	several OXA-2 and -10 derivatives, OXA-18, -29, -30, -31, -32, -45
	Carbapenemase	penicillins, oxacillin, carbapenems	yes	no	several OXA-23 to -24, -48, -51, -55, -58, -60, -62 derivatives

[a] including narrow and extended spectrum cephalosporins; [b] extended spectrum beta-lactams; [c] 4th generation cephalosporins; * cluvanic acid and tazobactam; ESBL, extended spectrum beta-lactamase; RSBL, restricted spectrum beta-lactamase; IR, inhibitor resistant

1.4.2.1 Acquired β-lactamases

Horizontally acquired β-lactamases largely contribute to a rapid intra- and inter-species spread of β-lactam resistances among clinical isolates [119-122]. They are either plasmid encoded or associated with transposable genetic elements to facilitate mobility, including transfer across different bacterial genera [123]. The respective genes may be parts of single small mobile elements known as gene cassettes, which comprise the open reading frame (ORF) and a downstream recombination site, or be organized in large integrons, which are the major vectors of antibiotic multi-resistance in Gram-negative bacteria [124,125]. Integrons are genetic elements that harbor a number of different gene cassettes, usually commonly transcribed from one integron specific promoter [126]. Furthermore, an integron comprises an individually expressed, recombinase (e.g. IntI) that promotes the specific excision of genes cassettes and their integration at an adjacent *attI* site [127,128].

Among the acquired β-lactamases, ESBLs and carbapenemases pose a particular threat as they constitute broad resistance towards almost all β-lactam antibiotics. Although these enzymes show world-wide dissemination, epidemiological patterns differ country specific [114]. To date, seven types of MBL carbapenemases, IMP, VIM, NDM, SPM, GIM, AIM and FIM, and tree types of serine carbapenemases, GES, KPC and OXA have been described in *P. aeruginosa* [113,114,129]. However, MBLs are the most prevalent group of carbapenemases in this organism [129]. Among the ESBLs, CTX-M, VEB, and PER variants have the most widespread dissemination and, along with OXA ESBLs, have been found in clinical *P. aeruginosa* isolates [130-136].

1.4.2.2 *P. aeruginosa* endogenous β-lactamases: OXA-50 and AmpC

Besides the potential to acquire new β-lactamases from other bacteria, the *P. aeruginosa* genome also encodes for two endogenous β-lactamases, a constitutively expressed oxacillinase, OXA-50 (PoxB) and an inducible, expanded spectrum cephalosporinase, AmpC [137]. While OXA-50 has only very narrow substrate specificity and low hydrolysis potential, AmpC is capable of efficiently degrading all β-lactam antibiotics except carbapenems, whose hydrolysis only occurs upon specific mutational changes within AmpC [137-139]. However, AmpC is only produced at very low, basal levels in wild-type cells and resistance is dependent on induction or constitutive overexpression of the gene. This explains the effectiveness of anti-pseudomonal β-lactam antibiotics as ceftazidime and piperacillin, which lack sufficient AmpC induction activity (opposed to narrow spectrum cephalosporins and benzyl-penicillins) [138,140]. Interestingly, carbapenems are able to induce *ampC* expression, although they are not (or only marginally, as for imipenem) hydrolyzed by the native AmpC enzyme [141,142].

Mutational induction of *ampC* overexpression is a common mechanism and of great clinical significance, as it has previously been described that bacteremia patients with AmpC overproducing *P. aeruginosa* were 67 times more likely to receive inappropriate empiric antibiotics and were thus likewise more prone to acquire persistent bacteremia (45 % vs. 6 %) [143-145]. However, the mutational sites where such mutations can occur are diverse due to the complex *ampC*-regulatory network.

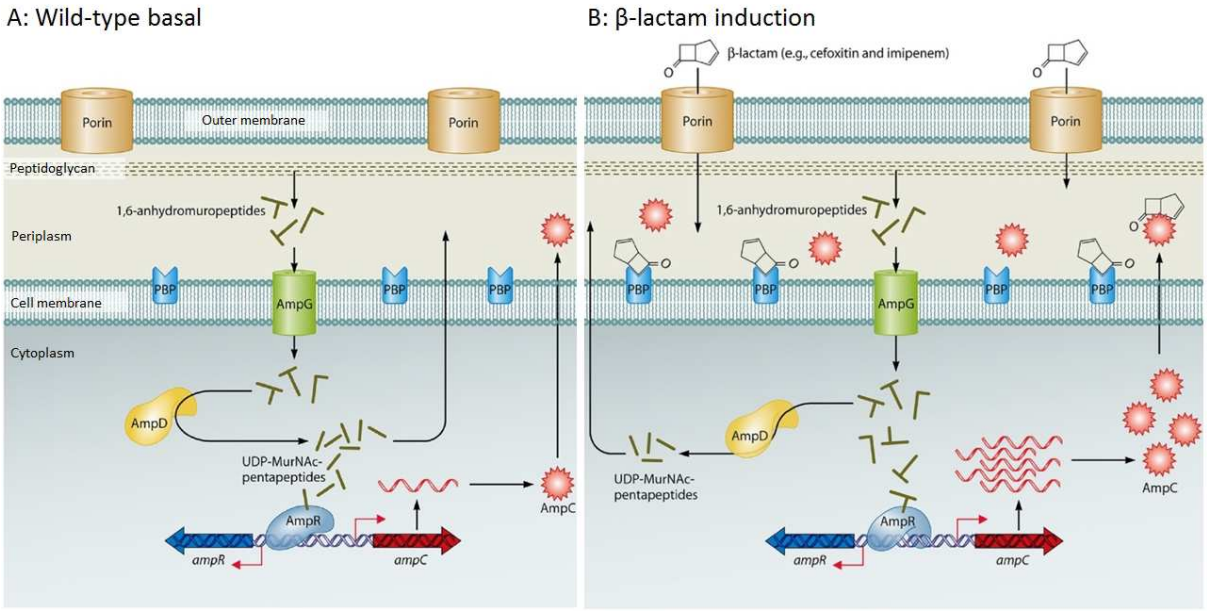

Figure 1.4 Mechanisms involved in *ampC* expression regulation.

A: Wild-type basal expression of *ampC*. During normal cell wall recycling, 1,6-anhydromuropeptides (AHMPs) are removed from the cell wall and transported into the cytoplasm via the AmpG permease. The AHMPs are cleaved by AmpD, and later converted into UDP-MurNAc-pentapeptides (UDP-PPs). These UDP-PPs interact with AmpR bound to the *ampR-ampC* intergenic region, creating a conformation that represses transcription of *ampC*, resulting in only low, basal levels of AmpC. **B:** β-lactam induction of *ampC* expression. Inducing β-lactams enter the periplasmic space and interact with target PBPs. This leads to an increase in cell wall fragment (AHMPs), which AmpD is unable to process efficiently. The AHMPs (inducing peptides) replace UDP-PPs (suppressing peptides) bound to AmpR, causing a conformational change that converts AmpR into a transcriptional activator. Thus, *ampC* is expressed at higher levels. Figure modified from [18].

Direct regulation of *ampC* expression is controlled by the transcriptional regulator AmpR, which binds to the *ampR-ampC* intergenic region. Whether AmpR activates or represses *ampC* expression is dependent on the type of additional cofactor and is tightly interlinked with the process of peptidoglycan precursor recycling, as depicted in Figure 1.4 [18,107]. During normal cell wall synthesis, muropeptides are produced, which enter the cytoplasm through the permease AmpG [146]. In the cytoplasm, they are modified by AmpD and UDP is added [50,147,148]. These UPD-

peptides have a repressing function when binding AmpR, resulting in only low level basal expression of *ampC* [149]. When inducing β-lactams enter the cell, they lead to an increased production of muropeptides, which AmpD is not able to handle anymore [150]. Thus, these muropeptides bind AmpR instead of the UPD-peptides. This leads to a conformational change in AmpR, which now activates high expression of *ampC* [149]. Once the level of β-lactams has decreased again due to degradation by AmpC, wild-type *ampC* expression is automatically restored [18].

Constitutive overexpression (de-repression) of *ampC* can result from a modification of any of the involved regulatory components. However, some AmpC-overproducing *P. aeruginosa* strains do not exhibit mutations in either *ampR, ampD*, or the *ampR-ampC* intergenic region and do not exhibit changes in the level of *ampD* expression [151,152]. Therefore it is suggested that further factors for AmpC regulation exist, possibly including AmpD homologues – *P. aeruginosa* exhibits two additional AmpD homologues, AmpDh2 and AmpDh2 – , AmpE or PBP4 [153-155].

1.5 How antibiotics affect bacteria – from specific targets to global networks

Most investigations on how bactericidal antibiotics affect bacteria and induce cell death are centered on the antibiotic's primary targets. Aminoglycosides stall translation by binding the ribosomes, quinolones prevent DNA replication by interfering with gyrase and topoisomerase, and β-lactams inhibit cell wall biosynthesis. However, in recent studies secondary mechanisms beyond primary targets have been described as important contributors to antibiotic tolerance. In these publications, large collections of *P. aeruginosa* transposon mutants were screened for susceptibility to different antibiotics (ciprofloxacin, tobramycin, amikacin, meropenem, imipenem, ceftazidime, tetracycline and polymixins), identifying genes of diverse functions, which are not related to efflux systems or cell envelope composition, but often involved in the bacterial metabolism [156-160]. While the identified genes are often unique for a particular substrate, there are also overlaps across structurally different classes of antibiotics, as *ftsK,* encoding for a protein involved in cell division, was shown to be involved in low level resistance to quinolones and β-lactams [157,159].

Even more overlaps could be detected in the case of the catabolite repression control regulator Crc. Crc is a post-transcriptional repressor that regulates the use of carbon sources in nutrient complex environments [161]. Inhibition of Crc makes *P. aeruginosa* less virulent and more susceptible to antibiotics in planktonic culture and biofilms, emphasizing the influence of global regulatory networks on antibiotic resistance [162,163].

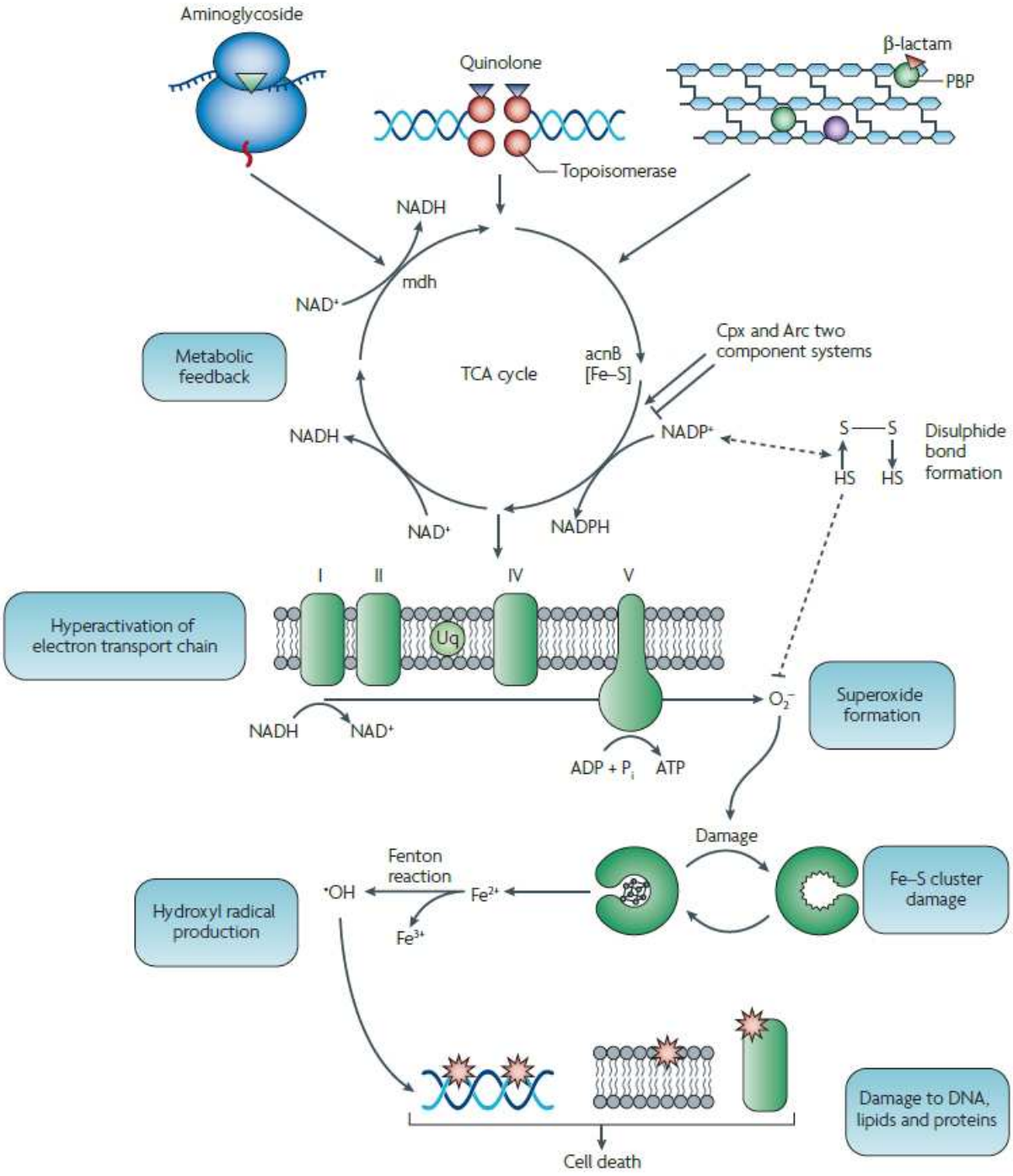

Figure 1.5 Common mechanism of cell death induced by bactericidal antibiotics.

The primary drug-target interaction (aminoglycosides with ribosomes, quinolones with gyrase/topoisomerase, and β-lactams with PBPs) stimulates the oxidation of NADH through the electron transport chain, which is dependent on the tricarboxylic acid (TCA) cycle. Hyperactivation of the electron chain stimulates superoxide (O_2^-) formation, which damage iron-sulfur clusters. This leads to the formation of hydroxyl radicals ($^{\bullet}OH$) by the Fenton reaction which damage DNA, proteins and lipids and thus contributes to antibiotic-induced cell death. Another mechanism to trigger hydroxyl radical formation is through two component systems, as the redox responsive Arc system or the envelope responsive Cpx system, and it is suggested that redox sensitive proteins containing disulphides might also contribute to this mechanism. Figure from [42].

Kohanski and colleagues even went a step further when they introduced their model of cell death by bactericidal antibiotics in 2007 [164]. Hence it is proposed that not only interconnected antibiotic tolerance mechanisms exist, but that there is also a common mechanism of killing by these antibiotics, regardless of their structural class and primary target.

In this proposed model a common downstream cascade upon primary drug-target interaction is described which leads to the production of lethal doses of reactive oxygen species (ROS) (Figure 1.5). When the antibiotics bind their targets, they stimulate a metabolic feedback that conducts the oxidation of NADH by the electron transport chain within the tricarboxylic acid (TCA) cycle. A hyperactivation of this electron chain stimulates the formation of superoxides which damage iron-sulfur clusters and thus make free iron available for oxidation through hydrogen peroxide by in the Fenton reaction. As a result, hydroxyl radicals are formed that damage DNA, proteins and lipids and thus promote antibiotic-induced cell death [164]. However, this model is still widely discussed with several recent approving and rejecting studies [165-169].

1.6 Recent progress in next generation sequencing

The “genomic era” started with the first complete bacterial genome which was sequenced using Sanger sequencing technology in 1995 [170]. Although sequencing greatly progressed during the following years, mostly due to the human Genome Project, the complete sequencing of one single genome still required years of time and very large budgets. Ten years later, in 2005, the introduction of “next generation sequencing” finally led to significant advances towards more cost efficient, high-throughput technologies [171,172]. In recent years, the sequencing capability has even been doubling every 6 to 9 months – much faster than Moore’s law [173,174]. As one example, while there were only 11 publically available unique and complete *Pseudomonas aeruginosa* sequences released between 2000 and 2012, this number had increased to 21 by January 2014 [175].

Next generation sequencing technologies include a number of different methods [176-178] that vary in costs, sequencing time, read lengths, and accuracy, but all of them comprise the three steps of template library preparation, sequencing, and data analysis [179]. Sequencing techniques can contain the detection of bioluminescent or up to four colors fluorescent signals, and usually include the immobilization of spatially separated template sites either on beads in emulsion (Roche/Life Technologies) or on solid phase (Illumina/Pacific Biosciences) [179].

Besides whole genome sequencing, next generation technologies also revolutionized transcriptome analysis, as they show clear advantages compared with the before widely used microarrays. Transcriptome sequencing (RNA-seq) provides sequence and expression information at the same time and thus allows for *de novo* sequence assembly instead of hybridization to a predefined tiling

array matrix [180]. This facilitates the detection of previously unannotated genes and sequences. Furthermore, RNA-sequencing offers a higher dynamic range and increased sensitivity for low abundant transcripts, as well as single nucleotide resolution of transcript boundaries [181,182]. These benefits over microarrays have recently made RNA-sequencing a valuable tool for determining the transcriptomes of a variety of prokaryotes [183-185].

Furthermore, it is suggested that rapid and cheap sequencing could, besides basic research, also transform clinical microbiology. On the one hand by providing innovative molecular diagnostic tools to apply customized, targeted treatment approaches and thus avoid treatment failure, on the other hand by seeking for a comprehensive understanding of the genomic background and evolutionary biology of pathogens [186,187]. Here, RNA-sequencing provides a considerable advantage over DNA-sequencing as the additional gene expression data facilitate the detection of adaptive mutations within the diverse genetic background of clinical isolates [188].

1.7 Aims of the thesis

The frequency of antibiotic resistance in bacterial pathogens is steadily increasing around the world, resulting in a growing threat to public health. While the widespread and empirical use of antibiotics further promotes the expansion of resistance phenotypes and the occurrence of multi-drug resistance, at the same time adequate treatment options are diminishing due to the constantly declining approval rate of novel antibiotic compounds. Besides the promotion of drug discovery and approval, the continuing rapid evolution and spread of antibiotic resistances thus call for alternative strategies to combat bacterial infections.

One major concern in this context is the treatment of multi-drug resistant *Pseudomonas aeruginosa* infections. This nosocomial pathogen is of particular importance since is does not only feature a large repertoire of intrinsic resistances, but also a great capacity to incorporate acquired ones. Thereby, not only the import of resistance mechanisms on mobile genetic elements is a growing concern, but also the bacteria's impressive ability to develop resistance during the course of an infection through adaptive chromosomal mutational changes. While many direct antibiotic targets have already been described, their complex regulatory networks, cross-resistance interplay, and predisposing factors are still largely unknown and call for further, detailed investigation.

The overall aim of this thesis was to shed more light on the *P. aeruginosa* resistome and evaluate potential targets for molecular diagnostic approaches and optimized treatment strategies. To achieve this goal, we aimed at using a cost efficient RNA-sequencing method to investigate the transcriptomes of large amounts of clinical *P. aeruginosa* isolates from diverse geographical and infection site origins in respect to their β-lactam antibiotic resistance determinants. Thereby global phenotype-genotype correlations should be applied to uncover all known as well as potentially knew core genetic resistance markers and identify their nature, dimension, and interaction. Furthermore, the accessory transcriptome of these isolates was to be analyzed for mobile, acquired genetic elements.

To gain more insight into the evolution of resistance and cooperating regulatory networks, we also aimed to explore the impact of low, sub-lethal antibiotic exposure and its effects on transcriptional and metabolic profiles. In this regard it was particularly of interest, if different antibiotics from diverse substance classes and with variable direct cellular targets induce similar or divergent cellular responses.

2 Materials and Methods

2.1 Bacterial strains and growth conditions

The bacterial strains used in this study are listed in Tables 2.1-2.2. All strains were maintained at -70 °C as 15 % (v/v) glycerol stocks. *Escherichia coli* strain DH5α was used for all cloning steps, and strain S17-1 for conjugative DNA transfer. As *Pseudomonas aeruginosa* reference strain, the well-established and completely sequenced PA14 strain was used.

All *P. aeruginosa* and *E. coli* strains were cultured at 37 °C in Luria-Bertani broth (LB; 1 l = 5 g yeast-extract, 7.5 g NaCl, 10 g tryptone), shaking (180 rpm), unless indicated differently. LB medium was solidified by addition of 1.6 % (w/v) agar.

When required for selection, the following antibiotics were used for *Pseudomonas* and *E. coli*, respectively: 100 µg/ml and 10 µg/ml tetracycline, 30 µg/ml and 15 µg/ml gentamycin, 400 µg/ml carbenicillin and 100 µg/ml ampicillin. Oligomers used for cloning and RNA-sequencing (Table 2.3) were ordered from Eurofins MWG Operon. Primers for cloning were designed based on the PA14 genome sequence [189], and PCR amplifications were performed using PA14 genomic DNA as template. All obtained constructs were sequenced at Eurofins MWG Operon to rule out PCR errors.

Table 2.1 Bacterial strains used in this study (not including clinical isolates).

Strain	Relevant genotype	Reference
E. coli		
DH5α	F- endA1 glnV44 thi-1 recA1 relA1 gyrA96 deoR nupG Φ80dlacZ M15 (lacZYA-argF)U169, hsdR17(rK-mK+), λ-	[190]
S17-1	C600::RP-4 2-(Tc::Mu) (Kn::Tn7) thi pro hsdR hsdM+recA	[191]
P. aeruginosa		
PA14 wt		[192]
PA14Δ*mexS*	*mexS* knock-out mutant constructed in the PA14 wt strain	This study
PA14Δ*oprD*	*oprD* knock-out mutant constructed in the PA14 wt strain	This study
PA14Δ*mexR*	*mexR* knock-out mutant constructed in the PA14 wt strain	[69]
PA14Δ*mexZ*	*mexZ* knock-out mutant constructed in the PA14 wt strain	[69]
PA14Δ*nfxB*	*nfxB* knock-out mutant constructed in the PA14 wt strain	[69]
PA14Δ*oprD*Δ*mexR*	*oprD* / *mexR* double knock-out mutant constructed in PA14Δ*mexR*	This study

2.1.1 Clinical strain collection

The 149 in this study investigated clinical *P. aeruginosa* isolates were provided by different clinics and research institutions. In total, 87 isolates were collected at the Hannover Medical School (MHH), 40 isolates were from a strain collection provided by the University of Freiburg (sampled in numerous countries across Europe), 14 isolates were received from the Robert-Koch-Institute in Wernigerode, and 8 isolates were provided by the National Reference Centre for multidrug-resistant Gram-negative Bacteria in Bochum. The resulting strain-collection contained a cross-sectional distribution with diverse sample origins (Table 2.2). Most of the isolates were categorized as multidrug-resistant (resistant to three or more antimicrobial classes, according to Magiorakos *et al.,* [30]). The antibiotic susceptibility data were either hospital- or institution-derived or determined in house using the Vitek2 system (bioMérieux) or E-tests (bioMérieux).

Table 2.2 Clinical isolates used in this study.

Origin	Strain	CF	Material	City, country	RNA-seq pool and barcode	CAZ MIC		MEM MIC	
Strain collection of the National Reference Centre (NRZ), Bochum, Germany	B197	nd	nd	nd	clinical_pool_11_bc3	8	S	16	R
	B214	nd	nd	nd	clinical_pool_11_bc4	8	S	8	I
	B266	nd	nd	nd	clinical_pool_11_bc6	16	I	16	R
	B271	nd	nd	nd	clinical_pool_11_bc5	1	S	0.5	S
	B337	nd	nd	nd	clinical_pool_11_bc8	1	S	8	I
	B34	nd	nd	nd	clinical_pool_11_bc1	265	R	0.25	S
	B428	nd	nd	nd	clinical_pool_11_bc9	8	S	32	R
	B445	nd	nd	nd	clinical_pool_11_bc10	1	S	32	R
Hannover Medical School, Germany	MHH10047	no	tonsil swab	Hannover, Germany	clinical_pool_6_bc18	8	S	1	S
	MHH10049	yes	nasal swab	Hannover, Germany	clinical_pool_6_bc19	8	S	2	S
	MHH10660	yes	lung transplant donor	Hannover, Germany	MHH-pool-04_bc20	256	R	16	R
	MHH10978	yes	tonsil swab	Hannover, Germany	clinical_pool_7_bc7	32	R	4	S
	MHH11148	no	tonsil swab	Hannover, Germany	clinical_pool_7_bc10	16	I	1	S
	MHH11444	yes	tonsil swab	Hannover, Germany	MHH-pool-05_bc6	8	S	16	R
	MHH11445	yes	tonsil swab	Hannover, Germany	MHH-pool-05_bc7	8	S	4	S
	MHH11540	no	midstream urine	Hannover, Germany	clinical_pool_9_bc6	32	R	8	I
	MHH11572	no	midstream urine	Hannover, Germany	clinical_pool_8_bc23	256	R	16	R
	MHH11785	yes	lung transplant donor	Hannover, Germany	MHH-pool-04_bc11	256	R	8	I
	MHH11935	no	bronchoalveolar lavage	Hannover, Germany	clinical_pool_8_bc1	8	S	8	I
	MHH11989	yes	tonsil swab	Hannover, Germany	clinical_pool_7_bc8	8	S	8	I
	MHH12178	no	catheter swab abdomen	Hannover, Germany	clinical_pool_6_bc9	16	I	16	R
	MHH12207	yes	bronchoalveolar lavage	Hannover, Germany	MHH-pool-05_bc3	32	R	8	I
	MHH12269	yes	sputum	Hannover, Germany	MHH-pool-05_bc4	32	R	16	R
	MHH12274	no	bronchoalveolar lavage	Hannover, Germany	clinical_pool_7_bc9	16	I	0.5	S
	MHH13062	no	permanent catheter urine	Hannover, Germany	clinical_pool_9_bc7	8	S	4	S
	MHH13224	no	bronchial rinsing	Hannover, Germany	clinical_pool_9_bc2	8	S	8	I

Hannover Medical School, Germany	MHH13305	yes	bronchial secrete	Hannover, Germany	clinical_pool_7_bc11	32	R	16	R
	MHH13395	no	bronchoalveolar lavage	Hannover, Germany	MHH-pool-05_bc5	8	S	8	I
	MHH13428	no	swab intraop abdomen	Hannover, Germany	clinical_pool_9_bc4	32	R	2	S
	MHH13633	no	tracheal secrete	Hannover, Germany	MHH-pool-04_bc12	2	S	1	S
	MHH13682	yes	lung transplant donor	Hannover, Germany	clinical_pool_6_bc8	256	R	8	I
	MHH13684	yes	lung transplant recipient	Hannover, Germany	clinical_pool_9_bc5	256	R	4	S
	MHH13714	no	permanent catheter urine	Hannover, Germany	clinical_pool_7_bc1	8	S	0.25	S
	MHH14088	no	perfusate	Hannover, Germany	clinical_pool_7_bc2	8	S	2	S
	MHH14103	no	swab heel	Hannover, Germany	clinical_pool_7_bc5	32	R	8	I
	MHH14322	no	bronchial rinsing	Hannover, Germany	clinical_pool_7_bc3	8	S	0.5	S
	MHH14387	yes	lung transplant recipient	Hannover, Germany	clinical_pool_7_bc6	4	S	4	S
	MHH14449	no	bronchial secrete	Hannover, Germany	clinical_pool_7_bc4	16	I	16	R
	MHH6827	no	midstream urine	Hannover, Germany	MHH-pool-02_bc12	32	R	8	I
	MHH6829	no	midstream urine	Hannover, Germany	MHH-pool-02_bc1	16	I	16	R
	MHH6870	no	midstream urine	Hannover, Germany	MHH-pool-02_bc2	32	R	8	I
	MHH6887	no	tracheal secrete	Hannover, Germany	clinical_pool_6_bc10	32	R	0.125	S
	MHH6938	no	bronchoalveolar lavage	Hannover, Germany	MHH-pool-05_bc1	16	I	4	S
	MHH6964	no	wound swab abdomen	Hannover, Germany	MHH-pool-02_bc3	8	S	8	I
	MHH7032	no	venous catheter	Hannover, Germany	MHH-pool-04_bc13	16	I	8	I
	MHH7055	no	bronchoalveolar lavage	Hannover, Germany	MHH-pool-03_bc1	4	S	8	I
	MHH7084	no	permanent catheter urine	Hannover, Germany	MHH-pool-03_bc2	32	R	8	I
	MHH7091	yes	lung transplant recipient	Hannover, Germany	MHH-pool-04_bc5	4	S	0.5	S
	MHH7125	no	tonsil swab	Hannover, Germany	MHH-pool-04_bc14	8	S	4	S
	MHH7135	no	bronchial secrete	Hannover, Germany	MHH-pool-04_bc9	4	S	4	S
	MHH7176	no	midstream urine	Hannover, Germany	MHH-pool-04_bc15	32	R	8	I
	MHH7200	yes	tonsil swab	Hannover, Germany	MHH-pool-03_bc4	32	R	4	S
	MHH7252	no	tracheal secrete	Hannover, Germany	MHH-pool-03_bc7	2	S	4	S
	MHH7261	no	permanent catheter urine	Hannover, Germany	MHH-pool-02_bc10	32	R	8	I
	MHH7313	no	tracheal secrete	Hannover, Germany	MHH-pool-01_bc6	4	S	8	I
	MHH7368	no	nasal swab	Hannover, Germany	MHH-pool-02_bc11	16	I	8	I
	MHH7444	yes	bronchoalveolar lavage	Hannover, Germany	MHH-pool-03_bc3	32	R	8	I
	MHH7508	yes	bronchial secrete	Hannover, Germany	MHH-pool-02_bc4	32	R	8	I
	MHH7818	yes	tracheal secrete	Hannover, Germany	MHH-pool-02_bc7	8	S	4	S
	MHH7823	no	tonsil swab	Hannover, Germany	MHH-pool-03_bc5	32	R	8	I
	MHH7863	no	bronchial secrete	Hannover, Germany	MHH-pool-03_bc6	32	R	8	I
	MHH8044	yes	tracheal secrete	Hannover, Germany	MHH-pool-02_bc8	32	R	8	I
	MHH8349	no	midstream urine	Hannover, Germany	MHH-pool-01_bc1	32	R	8	I
	MHH8478	no	midstream urine	Hannover, Germany	MHH-pool-01_bc2	32	R	1	S
	MHH8481	yes	bronchial secrete	Hannover, Germany	MHH-pool-04_bc16	256	R	32	R
	MHH8482	yes	bronchial secrete	Hannover, Germany	MHH-pool-01_bc9	32	R	8	I
	MHH8607	no	sputum	Hannover, Germany	clinical_pool_6_bc13	32	R	16	R
	MHH8613	no	ear swab	Hannover, Germany	MHH-pool-03_bc8	32	R	2	S
	MHH8614	no	midstream urine	Hannover, Germany	MHH-pool-01_bc3	32	R	1	S
	MHH8627	no	drainage bile duct	Hannover, Germany	MHH-pool-01_bc4	16	I	32	R
	MHH8697	no	rectal swab	Hannover, Germany	MHH-pool-02_bc9	1	S	16	R
	MHH8931	yes	lung transplant donor	Hannover, Germany	MHH-pool-05_bc17	256	R	16	R
	MHH9157	no	wound swab abdomen	Hannover, Germany	MHH-pool-01_bc5	32	R	1	S

Hannover Medical School, Germany	MHH9229	no	tonsil swab	Hannover, Germany	MHH-pool-01_bc10	16	I	4	S
	MHH9460	nd	tracheal secrete	Hannover, Germany	MHH-pool-01_bc7	32	R	8	I
	MHH9481	no	bronchial rinsing	Hannover, Germany	clinical_pool_8_bc13	32	R	4	S
	MHH9484	no	tonsil swab	Hannover, Germany	MHH-pool-01_bc8	8	S	8	I
	MHH9509	nd	tracheal secrete	Hannover, Germany	MHH-pool-01_bc11	32	R	8	I
	MHH9534	no	bronchial secrete	Hannover, Germany	MHH-pool-05_bc18	32	R	8	I
	MHH9536	nd	tracheal secrete	Hannover, Germany	MHH-pool-01_bc12	32	R	16	R
	MHH9561	nd	tonsil swab	Hannover, Germany	MHH-pool-03_bc13	32	R	16	R
	MHH9604	nd	bronchial secrete	Hannover, Germany	MHH-pool-03_bc14	32	R	8	I
	MHH9619	nd	tonsil swab	Hannover, Germany	MHH-pool-03_bc15	32	R	8	I
	MHH9639	nd	tonsil swab	Hannover, Germany	MHH-pool-03_bc16	32	R	8	I
	MHH9652	no	drainage liquid	Hannover, Germany	clinical_pool_6_bc14	32	R	8	I
	MHH9674	no	bronchoalveolar lavage	Hannover, Germany	clinical_pool_6_bc15	2	S	0.125	S
	MHH9678	nd	tonsil swab	Hannover, Germany	clinical_pool_7_bc12	32	R	8	I
	MHH9709	nd	tonsil swab	Hannover, Germany	MHH-pool-05_bc8	32	R	8	I
	MHH9717	no	tracheal secrete	Hannover, Germany	MHH-pool-04_bc10	8	S	16	R
	MHH9748	no	tonsil swab	Hannover, Germany	MHH-pool-05_bc16	4	S	4	S
	MHH9830	no	tracheal secrete	Hannover, Germany	MHH-pool-05_bc9	32	R	8	I
	MHH9847	nd	tracheal secrete	Hannover, Germany	MHH-pool-05_bc10	32	R	8	I
	MHH9854	yes	nasal swab	Hannover, Germany	clinical_pool_6_bc17	256	R	8	I
	MHH9923	nd	tracheal secrete	Hannover, Germany	clinical_pool_6_bc11	32	R	8	I
	MHH9924	nd	swab intraoperative	Hannover, Germany	clinical_pool_6_bc12	32	R	8	I
Strain collection University of Freiburg, Germany	Psae0613	nd	nd	nd	PSAE_1_PE_bc1	8	S	0.25	S
	Psae1152	nd	drainage catheter	Stuttgart, Germany	PSAE_1_PE_bc10	128	R	64	R
	Psae1471	nd	respiratory tract	Berlin, Germany	PSAE_1_PE_bc3	2	S	0.5	S
	Psae1640	nd	urine	Munich, Germany	clinical_pool_9_bc12	8	S	2	S
	Psae1646	nd	urine	Munich, Germany	clinical_pool_10_bc5	4	S	16	R
	Psae1655	nd	respiratory tract	Munich, Germany	clinical_pool_10_bc2	4	S	8	I
	Psae1657	nd	respiratory tract	Munich, Germany	clinical_pool_10_bc7	8	S	16	R
	Psae1659	nd	respiratory tract	Munich, Germany	clinical_pool_10_bc8	16	I	8	I
	Psae1660	nd	respiratory tract	Munich, Germany	clinical_pool_10_bc6	8	S	16	R
	Psae1661	nd	respiratory tract	Freiburg, Germany	clinical_pool_8_bc17	64	R	128	R
	Psae1688	nd	urine	Limburg, Germany	clinical_pool_10_bc9	4	S	8	I
	Psae1695	nd	respiratory tract	Bremen, Germany	clinical_pool_10_bc15	4	S	1	S
	Psae1711	nd	nd	Regensburg, Germany	PSAE_1_PE_bc7	1	S	0.5	S
	Psae1715	nd	respiratory tract	Freiburg, Germany	clinical_pool_10_bc10	4	S	8	I
	Psae1716	nd	blood	Freiburg, Germany	clinical_pool_8_bc16	32	R	8	I
	Psae1747	nd	respiratory tract	Freiburg, Germany	PSAE_1_PE_bc2	64	R	16	R
	Psae1758	nd	respiratory tract	Limburg, Germany	PSAE_1_PE_bc6	2	S	0.25	S
	Psae1766	nd	respiratory tract	Bremen, Germany	PSAE_1_PE_bc8	8	S	16	R
	Psae1775	nd	respiratory tract	Ruedesheim, Germany	clinical_pool_10_bc11	4	S	8	I
	Psae1793	nd	respiratory tract	nd	clinical_pool_10_bc4	8	S	32	R
	Psae1807	nd	respiratory tract	Berlin, Germany	clinical_pool_10_bc12	64	R	8	I
	Psae1829	nd	respiratory tract	Regensburg, Germany	clinical_pool_10_bc13	4	S	8	I
	Psae1875	nd	respiratory tract	Berlin, Germany	PSAE_1_PE_bc9	4	S	16	R
	Psae1892	nd	respiratory tract	Gera, Germany	clinical_pool_9_bc11	4	S	2	S

Strain collection University of Freiburg, Germany	Psae1910	nd	respiratory tract	Regensburg, Germany	clinical_pool_9_bc13	1	S	0.25	S
	Psae1928	nd	respiratory tract	Bremen, Germany	clinical_pool_9_bc14	32	R	2	S
	Psae1950	nd	respiratory tract	Bremen, Germany	clinical_pool_9_bc8	0.5	S	1	S
	Psae2134	nd	respiratory tract	Timisoara, Rumania	clinical_pool_9_bc9	16	I	32	R
	Psae2136	nd	respiratory tract	Timisoara, Rumania	PSAE_1_PE_bc12	64	R	16	R
	Psae2162	nd	nd	Catania, Italy	PSAE_1_PE_bc11	128	R	32	R
	Psae2180	nd	urine	nd	clinical_pool_8_bc18	128	R	64	R
	Psae2302	nd	respiratory tract	Rozzano, Italy	clinical_pool_8_bc15	64	R	8	I
	Psae2305	nd	respiratory tract	Sassari, Italy	clinical_pool_9_bc10	4	S	0.25	S
	Psae2307	nd	respiratory tract	Sassari, Italy	clinical_pool_8_bc19	128	R	32	R
	Psae2319	nd	nd	Palermo, Italy	clinical_pool_8_bc22	128	R	64	R
	Psae2324	nd	respiratory tract	Neubrandenburg, Germany	PSAE_1_PE_bc4	2	S	4	S
	Psae2326	nd	urine	Neubrandenburg, Germany	clinical_pool_8_bc14	32	R	16	R
	Psae2328	nd	urine	Neubrandenburg, Germany	PSAE_1_PE_bc5	2	S	16	R
	Psae2335	nd	urine	Trencin, Hungary	clinical_pool_8_bc20	256	R	128	R
	Psae2338	nd	respiratory tract	Bari, Italy	clinical_pool_8_bc21	128	R	64	R
Strain collection Robert Koch Institute, Wernigerode, Germany	RKI_100_12	nd	nd	nd	clinical_pool_12_bc9	32	R	32	R
	RKI_12_11	nd	nd	nd	clinical_pool_11_bc12	8	S	32	R
	RKI_24_11	nd	nd	nd	clinical_pool_12_bc13	32	R	32	R
	RKI_339_12	nd	nd	nd	clinical_pool_12_bc20	256	R	32	R
	RKI_359_11	nd	nd	nd	clinical_pool_12_bc24	32	R	32	R
	RKI_360_11	nd	nd	nd	clinical_pool_12_bc7	16	I	32	R
	RKI_37_11	nd	nd	nd	clinical_pool_12_bc16	16	I	32	R
	RKI_392_11	nd	nd	nd	clinical_pool_12_bc10	8	S	0.25	S
	RKI_395_11	nd	nd	nd	clinical_pool_12_bc15	32	R	8	I
	RKI_53_11	nd	nd	nd	clinical_pool_12_bc18	32	R	4	S
	RKI_82_10	nd	nd	nd	clinical_pool_12_bc22	32	R	32	R
	RKI_96_12	nd	nd	nd	clinical_pool_11_bc14	32	R	8	I
	RKI_98_12	nd	nd	nd	clinical_pool_12_bc11	4	S	16	R
	RKI_99_12	nd	nd	nd	clinical_pool_12_bc17	32	R	16	R

CF, patients diagnosed with cystic fibrosis; nd, not determined

2.2 Plasmids and Oligomers

Plasmids used for cloning can be found in the respective materials and methods section (Constructions of *mexS* and *oprD* knock-out mutants), a list of all oligomers used in this study is presented below, in Table 2.3.

Table 2.3 Oligomers used for PCR and RNA-sequencing.

Oligoname	Sequence*	Classification	Used for
R	5' AAAAAAAAAAAAAAAAAAAGAGCCGACATCGAGGTGCCAAAC 3'	Capture oligomer	rRNA removal
4Pse	5' AAAAAAAAAAAAAAAAAAGGGTTGCGCTCGTTACGGGACTT 3'	Capture oligomer	rRNA removal
4R	5' AAAAAAAAAAAAAAAAAAACTTACCCGACAAGGAATTTCGC 3'	Capture oligomer	rRNA removal
1R	5' AAAAAAAAAAAAAAAAAATGGACTACCAGGGTATCTAATCC 3'	Capture oligomer	rRNA removal
807-R	5' Biotin-GAGCCGACATCGAGGTGCCAAAC 3'	Capture oligomer	rRNA removal
111-4Pse	5' Biotin-GGGTTGCGCTCGTTACGGGACTT 3'	Capture oligomer	rRNA removal
195-4R	5' Biotin-ACTTACCCGACAAGGAATTTCGC 3'	Capture oligomer	rRNA removal
251-1R	5' Biotin-TGGACTACCAGGGTATCTAATCC 3'	Capture oligomer	rRNA removal
2-PolyA	5' AAAAAAAAAAAAAAAAAAGCTCCCTTCATCCGCTCGACTT 3'	Capture oligomer	rRNA removal
9-PolyA	5' AAAAAAAAAAAAAAAAAAGTGCTTTACAATCCGAAGACCT 3'	Capture oligomer	rRNA removal
27-PolyA	5' AAAAAAAAAAAAAAAAAATACTAGCGATTCCGACTTCACG 3'	Capture oligomer	rRNA removal
3-PolyA	5' AAAAAAAAAAAAAAAAAAACTACTAAGGGAATCTCGGTTGA 3'	Capture oligomer	rRNA removal
10-PolyA	5' AAAAAAAAAAAAAAAAAATTCCGCGCAGGCCGACTCGACTA 3'	Capture oligomer	rRNA removal
RT	5' GCTGAACCGCTCTTCCGATCT 3'	Reverse transcription	RNA-sequencing
Primer A	5' AATGATACGGCGACCACCGAGATCTACACTCTTTCCCTACACGAC GCTCTTCCGATCT 3'	PCR primer	RNA-sequencing
Primer B	5 'CAAGCAGAAGACGGCATACGAGATCGGTCTCGGCATTCCTGCTG AACCGCTCTTCCGATCT 3'	PCR primer	RNA-sequencing
B2	5' P-AGAUCGGAAGAGCGGUUCAGC-ddC 3'	RNA-Adapter (3' Adapter)	RNA-sequencing
BC6-1	5' UACACGACGCUCUUCCGAUCUACGAGA 3'	RNA-Adapter (5' Adapter)	RNA-sequencing
BC6-2	5' UACACGACGCUCUUCCGAUCUACUUGC 3'	RNA-Adapter (5' Adapter)	RNA-sequencing
BC6-3	5' UACACGACGCUCUUCCGAUCUAUCUGG 3'	RNA-Adapter (5' Adapter)	RNA-sequencing
BC6-4	5' UACACGACGCUCUUCCGAUCUCAUACG 3'	RNA-Adapter (5' Adapter)	RNA-sequencing
BC6-5	5' UACACGACGCUCUUCCGAUCUCGUCAU 3'	RNA-Adapter (5' Adapter)	RNA-sequencing
BC6-6	5' UACACGACGCUCUUCCGAUCUGGUUAC 3'	RNA-Adapter (5' Adapter)	RNA-sequencing
BC6-7	5' UACACGACGCUCUUCCGAUCUGUACCU 3'	RNA-Adapter (5' Adapter)	RNA-sequencing
BC6-8	5' UACACGACGCUCUUCCGAUCUGUCAAG 3'	RNA-Adapter (5' Adapter)	RNA-sequencing
BC6-9	5' UACACGACGCUCUUCCGAUCUUCUCUG 3'	RNA-Adapter (5' Adapter)	RNA-sequencing
BC6-10	5' UACACGACGCUCUUCCGAUCUUGGUUC 3'	RNA-Adapter (5' Adapter)	RNA-sequencing
BC6-11	5' UACACGACGCUCUUCCGAUCUUUCCGA 3'	RNA-Adapter (5' Adapter)	RNA-sequencing
BC6-12	5' UACACGACGCUCUUCCGAUCUUUGCAG 3'	RNA-Adapter (5' Adapter)	RNA-sequencing
BC6-13	5' UACACGACGCUCUUCCGAUCUAAUCGG 3'	RNA-Adapter (5' Adapter)	RNA-sequencing
BC6-14	5' UACACGACGCUCUUCCGAUCUAGAGAC 3'	RNA-Adapter (5' Adapter)	RNA-sequencing
BC6-15	5' UACACGACGCUCUUCCGAUCUAGUCUC 3'	RNA-Adapter (5' Adapter)	RNA-sequencing
BC6-16	5' UACACGACGCUCUUCCGAUCUAUUGCC 3'	RNA-Adapter (5' Adapter)	RNA-sequencing
BC6-17	5' UACACGACGCUCUUCCGAUCUCCAUCG 3'	RNA-Adapter (5' Adapter)	RNA-sequencing
BC6-18	5' UACACGACGCUCUUCCGAUCUCGACCA 3'	RNA-Adapter (5' Adapter)	RNA-sequencing
BC6-19	5' UACACGACGCUCUUCCGAUCUGACCUG 3'	RNA-Adapter (5' Adapter)	RNA-sequencing
BC6-20	5' UACACGACGCUCUUCCGAUCUGCUAGG 3'	RNA-Adapter (5' Adapter)	RNA-sequencing
BC6-21	5' UACACGACGCUCUUCCGAUCUGUCGGU 3'	RNA-Adapter (5' Adapter)	RNA-sequencing
BC6-22	5' UACACGACGCUCUUCCGAUCUUAAGCG 3'	RNA-Adapter (5' Adapter)	RNA-sequencing
BC6-23	5' UACACGACGCUCUUCCGAUCUUCCAAC 3'	RNA-Adapter (5' Adapter)	RNA-sequencing
BC6-24	5' UACACGACGCUCUUCCGAUCUUUGGCU 3'	RNA-Adapter (5' Adapter)	RNA-sequencing
mexS_FP1_XbaI	5' ACATCATCTAGAAGCACAACCCAAGCGATCAA 3'	PCR primer	*mexS* knock-out

mexS_RP1+20bp	5' ATGCACTGCAGAGGTTTGCGCGGGTATTCGAGTTCGACCAG 3'	PCR primer	*mexS* knock-out
mexS_FP2+20bp	5' TGGTCGAACTCGAATACCCGCGCAAACCTCTGCAGTGCATC 3'	PCR primer	*mexS* knock-out
mexS_RP2_HindIII	5' ACATCAAAGCTTAGGTGGGCGAAGATTTCCTG 3'	PCR primer	*mexS* knock-out
oprD_FP1_XbaI	5' ACATCATCTAGAGCAGGTACAGGCGTTGATCC 3'	PCR primer	*oprD* knock-out
oprD_RP1+20bp	5' AAACCAAAGGAGCAATCACACGACTATCCGCTGTCGATCC 3'	PCR primer	*oprD* knock-out
oprD_FP2+20bp	5' GGATCGACAGCGGATAGTCGTGTGATTGCTCCTTTGGTTTTGA 3'	PCR primer	*oprD* knock-out
oprD_RP2_HindIII	5' ACATCAAAGCTTGCAACCAACCCTTGAAGCAG 3'	PCR primer	*oprD* knock-out
SeqPr_Oxa224_R	5' TTATAAATTTAGTGTGTTTAGAATGGTG 3'	PCR primer	β-lactamase amplification
SeqPr_Oxa224_F	5' ATGAAAAACACAATACATATCAACTTC 3'	PCR primer	β-lactamase amplification
SeqPr_Vim2_R	5' ATGTTCAAACTTTTGAGTAAGTTATTGG 3'	PCR primer	β-lactamase amplification
SeqPr_Vim2_F	5' CTACTCAACGACTGAGCGATTTG 3'	PCR primer	β-lactamase amplification
SeqPr_Vim1_R	5' ATGTTAAAAGTTATTAGTAGTTTATTGG 3'	PCR primer	β-lactamase amplification
SeqPr_Vim1_F	5' CTACTCGGCGACTGAGCGATT 3'	PCR primer	β-lactamase amplification
SeqPr_Imp7 _F	5' ATGAAAAAGTTATCAGTATTCTTTATGTTTTT 3'	PCR primer	β-lactamase amplification
SeqPr_Imp7 _R	5' TTAGTTACTTGGTTTTGATAGCTTTTTAC 3'	PCR primer	β-lactamase amplification
SeqPr_ctx123 _F	5' ATGGTTAAAAAATCACTGCGC 3'	PCR primer	β-lactamase amplification
SeqPr_ctx123 _R	5' TTTCCGCTATTACAAACCGT 3'	PCR primer	β-lactamase amplification

* Restriction sites are underlined, barcode sequences are marked in orange.

2.3 DNA transfer techniques

2.3.1 Transformation of chemically competent *E. coli*

For the preparation of chemically competent *E. coli,* 50 ml LB were inoculated 1:1000 from an overnight culture of the respective strain and cultivated to an OD_{600} of 0.3-0.5. To prevent further growth, the culture was chilled on ice for 15 min before harvesting the cells by centrifugation at 4 °C at 3,200xg for 15 min. Subsequent steps were carried out on ice. The pellet was resuspended in 18 ml RF1 buffer (100 mM RbCl; 50 mM $MnCl_2$; 30 mM potassium acetate; 10 mM $CaCl_2$; pH 5.8). After a second centrifugation step, cells were resuspended in 2 ml ice-cold RF2 buffer (10 mM RbCl; 10 mM MOPS; 75 mM $CaCl_2$; 15 % (v/v) glycerol; pH 5.8) and incubated on ice for 15 min. The competent cells were aliquoted 125 µl each, frozen in liquid nitrogen and stored at -70 °C. For transformation, competent cells were gently thawed on ice for 15 min, mixed with the respective DNA and further incubated on ice for 20 min. After a heat shock for 90 s at 42 °C, 800 µl LB was added and the cells were incubated shaking at 37 °C for 1 h. Thereafter, 100 µl of the transformation reaction was plated on LB agar containing antibiotics for selection of transformants. The plates were incubated overnight at 37 °C.

2.3.2 Electroporation of *P. aeruginosa*

To prepare electrocompetent *P. aeruginosa* cells, a thick lawn of cells from an overnight grown LB agar plate was used. Half of the plate was harvested with an inoculation loop and resuspended in 1 ml 0.3 M sucrose solution. The bacteria were collected by centrifugation (16,000xg for 2 min) and washed 3 additional times with sucrose solution to remove extracellular matrix compounds. Finally, the pellet was resuspended in 100 µl deionized water, mixed with 100 ng plasmid DNA, and transferred to an electroporation cuvette (2 mm electrode gap). The electroporation was carried out in a Gene Pulser II (Bio-Rad) with settings 2.45 kV voltage, 25 µF capacitance and 200 Ω resistance. 1 ml pre-warmed LB was added directly after the discharge, the cells were transferred to a microfuge tube and incubated for 1.5 h at 37 °C. To select for transformants, 100 µl of cells were plated on LB agar containing antibiotics and incubated overnight at 37 °C. Electrocompetent *P. aeruginosa* cells were freshly prepared each time before use.

2.3.3 Plasmid transfer by diparental mating (conjugation)

When pex18AP constructs were used to create knock-out mutants, plasmids were introduced by conjugation with *E. coli* S17-1 as the donor strain. For conjugation experiments, the *P. aeruginosa* recipient was grown in 5 ml LB broth for 20 h at 42 °C, while the *E. coli* donor carrying the respective pex18AP construct was grown in 10 ml LB broth, supplemented with ampicillin for 6 h at 37 °C. Bacterial cultures were mixed in a 1:10 ratio, using 100 µl *P. aeruginosa* and 1 ml *E. coli* suspension. The cell-mix was harvested by centrifugation (6,000xg, 5 min), washed twice with LB and finally resuspended in 100 µl LB, before it was applied as a single drop on an LB agar plate. After 16 h of incubation at 37 °C, the drop was thoroughly washed off the agar plate with 2 ml PBS, and 100 µl of the suspension was plated on LB agar plates containing carbenicillin (400 µg/ml) and nalidixic acid (10 µg/ml) to counter select the *E. coli* donor cells and any *P. aeruginosa* which did not take in the pex18AP. To promote plasmid loss, single colonies were picked, cultivated overnight in 5 ml NaCl free LB broth containing 10 % sucrose, and passaged in this medium 3 times with 50 µl inoculum and an incubation time of 8-16 h for each passage. After the final passage, cells were diluted to obtain single colonies when plated on LB agar supplemented with 10 % sucrose. Successful mutation integration was screened for by checking the growth of single colonies on selective LB agar plates containing antibiotics.

2.4 Antibiotic susceptibility testing

2.4.1 E-test

Antibiotic susceptibility for selected clinical isolates was determined by E-test (bioMérieux) according to the manufacturer's guidelines. From an overnight culture of the respective strain incubated at 37 °C, 180 rpm in LB broth, 2 ml suspension of an OD_{600} of 0.132 (≙ McFarland standard 0.5) were prepared in PBS. Approximately 100 µl of this suspension were thoroughly applied to a Mueller-Hinton agar plate by streaking it three times with a cotton swab. Once the remaining liquid was absorbed by the agar, the E-test stripe was applied to the plate. MIC values were determined after 18 h of incubation at 37 °C.

2.4.2 Broth dilution

Antibiotic susceptibility and MIC values are specific for the applied culturing conditions, bacterial inoculation amount and media. Thus, to define suitable sub-inhibitory antibiotic concentrations in LB broth, MIC values for the PA14 wt were determined in liquid culture. Therefore, bacterial overnight pre-cultures were diluted to an OD_{600} of 3 (≙ $3*10^8$ CFU/ml) and 0.01 (≙ $1*10^6$ CFU/ml), respectively in LB broth, and 100 µl culture was mixed with 100 µl antibiotic in 96 well plate format. Antibiotic stock concentrations as listed in Table 2.4 were used to prepare five 1:1 serial dilutions in LB broth. Bacterial growth was monitored in triplicates after 12 h incubation at 37 °C, shaking.

Table 2.4 Stock concentrations of antibiotics for MIC determination in liquid culture.

Antibiotic	Stock concentration
Meropenem (MEM)	4 µg/ml
Ciprofloxacin (CIP)	0.5 µg/ml
Piperacillin (PIP)	64 µg/ml
Ceftazidim (CAZ)	32 µg/ml
Tobramycin (TOB)	4 µg/ml

2.5 RNA-sequencing – sample preparation

2.5.1 Culturing conditions and harvesting

Whole, single nucleotide transcriptome-sequencing was performed using a custom-made protocol with 5'-barcoded RNA-libraries to enable a pooled sequencing of numerous samples at once [193].

For each strain, three main cultures were inoculated in 10 ml LB from individual overnight pre-cultures to an OD_{600} of 0.02. Of note, the cells used for inoculation were beforehand collected by centrifugation, and resuspended in LB. If not indicated differently, the main cultures were cultivated

until OD_{600} of 2 ± 0.1 at 37 °C, 180 rpm. The three individual bacterial cultures were pooled and 4 ml culture was collected to the same amount RNAprotect (Qiagen). After 10 min incubation at room temperature, the suspension was centrifuged 5 min at 6,000xg and the supernatant was carefully removed. Pellets were stored at -70 °C for no longer than 4 weeks before processing them further.

2.5.2 RNA-extraction and DNA removal

After thawing, the pellet was centrifuged again for 5 min at 6,000xg to remove any residual supernatant. The pellet was thoroughly resuspended in 100 µl TE buffer (10 mM Tris-HCl; 1 mM EDTA, pH 8) supplemented with 800 µg Lysozyme per 1 ml by pipetting, vortexing and 10 min incubation at room temperature. Following, 350 µl of RLT buffer (Qiagen) supplemented with 10 µl per 1 ml β-mercaptoethanol was added and the suspension was frozen for 30 min at -70 °C and thawed again for additional cell destruction. Total RNA was extracted with Qiashredder columns (Qiagen) and the RNeasy plus kit (Qiagen) according to the manufacturer's instructions and the total RNA was collected in a final 50 µl. Residual DNA was removed by DNAse (Ambion) treatment (1 µl DNase per 50 µl total RNA, incubated for 30 min at 37 °C).

2.5.3 rRNA removal by hybridization using oligo$(dT)_{25}$ beads

To evaluate the rRNA reduction rate by indirect hybridization, four polyadenylated capture oligos (R, 1R, 4R and 4PSE; see Table 2.3, *Pseudomonas* specific sequences were obtained from Ambion) were used in combination with oligo$(dT)_{25}$ magnetic beads (Dynabeads, Invitrogen). 200 µl of well resuspended bead-suspension was applied to a new tube and beads were collected by a magnetic rack to remove the supernatant, before they were resuspended in 100 µl binding buffer (20 mM Tris-HCl, pH 7.5 supplemented with 1 M LiCl and 2 mM EDTA). Separately, 5 µg total PA14 RNA were incubated with a mix of 1 µl of each capture oligo in 100 µl binding buffer. After short vortexing, the sample was incubated at 65 °C for 2 min to dissolve RNA secondary structure, before it was directly added to the 100 µl of prepared beads. For oligo binding and subsequent capture by the poly-T beads, the mix was incubated rotating at room temperature for 10 min. Following, the beads were removed with the help of a magnetic rack and the supernatant containing the enriched mRNA was stored on ice. Residual, unintentionally captured mRNA was removed from the beads in an additional washing step using 100 µl washing buffer (10 mM Tris-HCl, pH 7.5 supplemented with 0.15 M LiCl and 1 mM EDTA). Beads were mixed in the washing buffer by slowly tapping the tube and thoroughly collected in a magnetic rack, before the supernatant was carefully removed and pooled with the initial mRNA fraction.

2.5.4 rRNA removal by hybridization using streptavidin tagged magnetic beads

For the removal of rRNA by biotin-streptavidin binding, the same rRNA complementary oligos were used as in 2.5.3, but in a biotinylated instead of the polyadenylated version, now named 807-R, 111-4Pse, 195-4R and 251-1R (Table 2.3). Correspondingly, removal was performed using streptavidin tagged magnetic beads (M-280 Dynabeads, Invitrogen). Before use, 50-100 µl beads were pre-washed several times with 100 µl of the following solutions: 3 x buffer B&W, 2 x solution A, 1 x solution B. Following, the beads were resuspended in the same amount of B&W buffer. Meanwhile, 5 µg of total bacterial RNA (PA14 wt) were prepared in 100 µl B&W buffer and mixed with 4 µl of capture oligos (25 µM each). The RNA-oligo suspension was incubated for 10 min at 70 °C to dissolve secondary structures, followed by 15 min at 37 °C to allow oligo-rRNA binding. Thereafter, the pre-washed beads were added and incubated for another 15 min either at 37 °C, shaking, or room temperature, rotating, to capture the oligos' biotin tag. To collect the beads and separate them from the supernatant containing mRNA, a magnetic rack was used. Solution compositions were as follows: B&W buffer (5mM Tris-HCl, pH 7.5; 0.5 mM EDTA; 1 M NaCl), solution A (0.1 M NaOH, 0.05 M NaCl), solution B (0.1 M NaCl).

2.5.5 rRNA removal by hybridization using MICROBExpress

If not indicated differently, rRNA was depleted from total RNA by the use of magnetic beads with the MICROBExpress Kit (Ambion). According to the manufacturer's instructions, 7 µg total RNA were prepared in 15 µl TE, mixed with 200 µl binding buffer, 4 µl capture oligo-mix and 50 µl magnetic beads, and mixed by tapping. The suspension was incubated for 10 min at 70 °C to denature RNA secondary structures and incubated for 1 h at 37 °C for hybridization. The oligo-mix consisted of 4 polyadenylated capture oligomers (25 µM each), R, 1R, 4R and 4PSE (Table 2.3), which were mixed to equal amounts. Beads were pre-washed before use, once with nuclease free water and once with binding buffer, before resuspension in binding buffer (50 µl each) and pre-adjustment to 37 °C. To gather the mRNA containing supernatant, the beads were collected for separation in a magnetic rack. Any unintentionally bound mRNA was eluted from the beads during an additional washing step with 100 µl pre-warmed wash solution. After gentle vortexing, the supernatant was again aspirated in a magnetic rack and pooled with the previously collected fraction.

2.5.6 Enzymatic rRNA removal by terminator-5'-phosphate-dependent exonuclease

In order to access the applicability of enzymatic rRNA removal in *P. aeruginosa*, terminator-5'-phosphate-dependent exonuclease (TEX, Epicentre) was used according to the manufacturer's instructions. Initial amount of RNA, enzyme, incubation time and buffer are specifically indicated separately for every corresponding experiment.

2.5.7 rRNA removal by duplex-specific nuclease (DSN)

In order to maximize mRNA content of the samples, a second rRNA removal step was applied before sequencing, additional to the preceding hybridization-based rRNA depletion of the *P. aeruginosa* clinical isolates and PA14 wt under varying environmental conditions. This second removal step was based on DSN (duplex-specific nuclease, Evrogen) treatment and conducted according to Illumina's "DSN Normalization Sample Preparation Guide" after pooling the final cDNA libraries for sequencing. The DSN enzyme is supposed to degrade duplex DNA in preference to single stranded DNA and can thus be used to normalize the relative transcript abundance in favor of mRNA derived cDNA fragments. DSN treatment of cDNA libraries had been shown previously to efficiently decrease rRNA transcripts while at the same time preserving the original relative abundance of mRNA species in bacterial cells [194].

2.5.8 RNA clean up and concentration by precipitation and chloroform-phenol purification

Whenever RNA needed to be concentrated to smaller volumes or it was necessary to remove residual chemicals, this was done by sodium acetate/ethanol precipitation adding 1/10 volume 3 M sodium acetate, 1/50 volume glycogen and 3 volumes of ethanol. The sample was thoroughly vortexed and incubated for 1 h at -70 °C for precipitation. Following, the precipitant was collected by centrifugation at 4 °C (10,000xg, 30 min) and residual sodium acetate was removed by washing the RNA pellet twice with 750 µl 70 % (v/v) ethanol.

If protein remains had to be removed as well, chloroform-phenol purification was applied prior to precipitation. In order to extract the proteins, the sample volume was adjusted to 200 µl with RNase free water and vigorously mixed by shaking with the same amount of phenol-chloroform-isoamyl alcohol (25:24:1, Roth) in MaXtract High Density tubes (Qiagen). After centrifugation (5 min, 10,000xg) the upper, aqueous phase was removed and its RNA precipitated.

2.5.9 cDNA library construction

cDNA library construction from mRNA was a multistep procedure. The principle of the custom created method (original idea developed by Andreas Dötsch, Helmholtz Centre for Infection Research) is shown in Figure 2.1, while detailed protocol description can be found in this text.

First, the mRNA obtained after MICROBExpress rRNA removal (if not indicated differently) was mechanically fragmented to a median size of ~200 nt by sonication (S2 single tube system, Covaris) with settings 150 s processing time, intensity 5, duty cycle 10 %. As fragmentation required specific buffer conditions, the mRNA was afore precipitated and the pellet resuspended in 130 µl TE (10 mM Tris-HCl, pH 8; 1 mM EDTA). For concentrating the RNA fragments after shearing, a second precipitation was performed, after which the pellet was resuspended in 15 µl RNase free water.

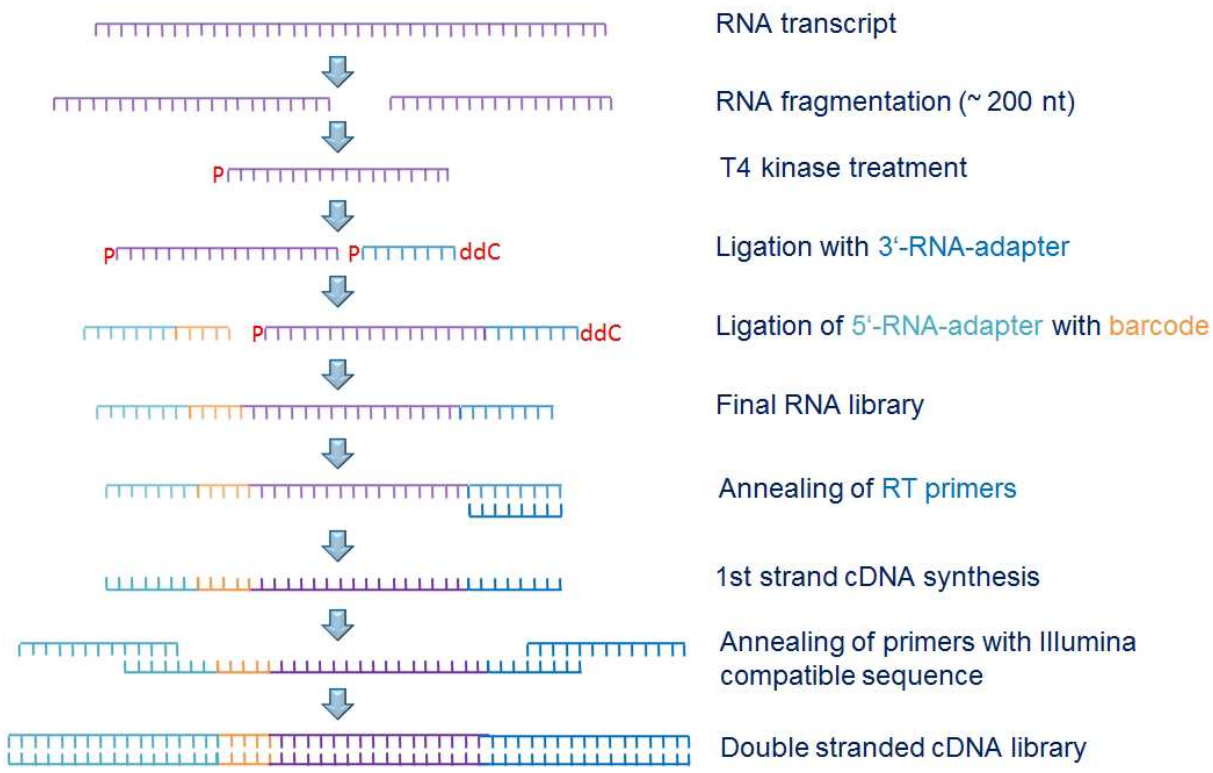

Figure 2.1 Principle of cDNA library construction by a custom made protocol.

Bacterial mRNA was fragmented by sonication and treated with T4 kinase to ensure 5'-phosphorylation (P) and 3'-dephosphorylation of every fragment. To ligate adapters specifically to 3'- and 5'-ends of the fragments, a 3'-RNA-adapter with 5'-phosphorylation and 3'-protection by dideoxycytidine (ddC) was used. In contrast, the afterwards ligated 5'-RNA-adapter was not modified, but because of the ddC only able to attach to the phosphorylated 5'-end of the RNA fragments. Furthermore, the 5'-adapter included a 6 nt specific sequence (barcode) to enable strand-specificity of the protocol and allow multiplexing of several samples for sequencing. After RNA-adapter ligation, cDNA was transcribed using 3'-RNA-adapter complementary primers for reverse transcription. First strand cDNA was amplified to create a double-stranded cDNA library in a maximum of 15 cycles (to minimize PCR bias) by DNA primers matching the RNA adapter sequences and containing additional Illumina flowcell compatible parts.

To prepare the RNA fragments for adapter ligation, 5'-phosphorylation and 3'-dephosphorylation was carried out by incubation with T4 polynucleotide kinase (T4 Pnk, Fermentas) for 25 min at 37 °C (using 1x buffer A, 10 U T4 Pnk and 5 mM ATP). Before, 3'- and 5'-RNA-adapter oligonucleotides (Table 2.3) were ligated, the RNA was purified by phenol-chloroform purification and additional ethanol precipitation. Adapter ligation was conducted over night at 16 °C with 10 U T4 RNA ligase (Thermo Scientific) in a total volume of 20 µl containing 5 mM ATP and an access of 50 pmol adapter. After 3'- and 5'-RNA-adapter ligation, RNA was purified using the RNeasy MinElute cleanup kit (Qiagen) to remove unbound adapter oligomers. Strand-specific cDNA libraries were generated by

reverse transcription using SuperScript II or III (Invitrogen) together with a DNA primer complementary to the 3'-adapter sequence to generate first-strand cDNA (RT primer), followed by 15 cycles PCR amplification with Herculase II polymerase (Agilent Technologies) in combination with PCR primers matching Illumina specific regions for compatibility with Genome Analyzer flowcells. Herculase polymerase was shown previously to produce barely amplification bias due to length or GC % variations, in contrast to other polymerases as Phusion, Pfu or Taq [195].

Samples were pooled to equal amounts and a maximum of 12 samples per pool. Before sequencing on an Illumina Genome Analyzer IIx, DSN treatment was applied to each pool (see "rRNA removal by duplex-specific nuclease (DSN)"). Quality and size distributions of the samples were checked throughout the library preparation process on an Agilent 2100 Bioanalyzer Pico Chip (Agilent).

Sequencing was performed either in paired-end mode, generating reads with a length of 76 or 110 nt (clinical isolates) or single-end mode, generating 36 nt reads (PA14 wt at varying environmental conditions).

2.6 RNA-sequencing – raw data processing

The dataset obtained from Illumina sequencing was analyzed using a custom bioinformatical pipeline (developed by Andreas Dötsch, HZI, Braunschweig), starting with the sorting of the raw sequence reads obtained in Illumina FASTQ-format by their expected barcode sequence. For successfully sorted reads, the barcode and adapter sequences were removed, while reads containing a barcode sequence with more than one error were discarded. The reads were mapped to the PA14 reference genome, which is available for download from the Pseudomonas Genome database (http://v2.pseudomonas.com, [189]). Mapping was performed using *stampy,* a short-read aligner that allows for gapped alignments [196], for quantification of gene expression, and SAMtools [197] was utilized for sequence variation calling. The reads per gene (rpg) values of all genes were calculated from the SAM output files. Testing for differential expression against PA14 wt was performed with DESeq [198], an R software package that uses a statistical model based on the negative binomial distribution. All short sequence read data have been deposited at the National Center for Biotechnology Information sequence read archive (http://www.ncbi.nlm.nih.gov/sra) under the accession number SRP034661. Library preparation, sequencing and raw data analysis of the 149 clinical isolates was performed in equal amounts together with Monika Schniederjans (Helmholtz Centre for Infection Research).

2.7 Detection of acquired resistance enzymes

For the analysis of the accessory genome and the detection of acquired resistance genes, a *de novo* transcriptome assembly was applied using Oases [199] (version 0.2.06) with settings kmin = 25, kmax = 29, minimal transcript length = 100. As Oases input, the clipped FASTQ files of each paired-end sample were merged into one and shuffled. The following generated contigs were aligned with BlastN against a custom file containing a collection of 658 transposable resistance genes, including 514 β-lactamases (genelist downloadable from Bactome (see chapter 2.9) in FASTA format). The results were filtered for redundancy, displaying only the top hit for every detected gene (regarding fragment length and sequence match).

Additionally, a second approach was performed using the custom resistance gene collection as an "artificial genome" against which the sequencing reads were mapped. This method allows calculating the relative sequence coverage of each resistance gene. Both approaches were compared and their results combined to improve prediction correctness for the presence of acquired enzymes.

To verify the bioinformatical prediction, primers were designed for the multiplexed amplification of previously detected resistance genes and the amplified DNA was subsequently Sanger sequenced. PCR settings, tested clinical isolates and amplifiable genes for each pair of primers are listed in Table 2.5. Alignments for primer design were created using MultAlign [200].

Table 2.5 Resistance gene amplification.

Primer	Ta*	Template DNA	Fragment sizes/amplifiable genes
SeqPr_Oxa224_R SeqPr_Oxa224_F	62 °C	PSAE2136, PSAE1747	831 bp/*oxa224, oxa4*
SeqPr_Vim2_R SeqPr_Vim2_F	65 °C	PSAE1716, PSAE1747, PSAE2307	801bp/*vim2-3,6,8-11,15-18,23-24;* 741 bp/*vim30*
SeqPr_Vim1_R SeqPr_Vim1_F	59 °C	PSAE1152, PSAE1661, PSAE2162, PSAE2180, PSAE2319, PSAE2338	801bp/*vim1,4,14,19,26-27,32*
SeqPr_Imp7 _F SeqPr_Imp7 _R	64 °C	PSAE2335	741 bp/*imp7*
SeqPr_ctx123 _F SeqPr_ctx123 _R	64 °C	PSAE2326	~885 bp/*ctx-m-1,3,10-12,15,22-23,28-30,32-34,36-37,42,52-58,60-62,66,68-69,71-72,79-80,82,88,96,101,114,116*

* Ta, annealing temperature

2.8 Phylogeny

The phylogenetic tree was created using a total of 214 genes that were ≥ 90 % covered with sequencing reads from all clinical isolates and also had orthologs in all five *Pseudomonas aeruginosa* reference strains used here (PA14, PAO1, LESB58, PACS2, PA7). The ortholog information was

obtained from a pre-computed *Pseudomonas* genome alignment with Mauve (http://www.pseudomonas.com/mauve.jsp, [189]). To extract the gene sequences of the clinical isolates, consensus sequences were created using the SAMtools package. From the consensus sequences and the reference genomes, the 214 gene sequences were extracted using the annotation information, resulting in one concatenated sequence per strain. Phylogenetic distances between the strains were calculated using a k-mer approach developed by Ole Lund and Rolf Kaas (Technical University of Denmark, personal communication). The sequences were split into 17-mers, which were then compared between the strains. The resulting distance matrix (created by Sarah Pohl, Helmholtz Centre for Infection Research) was used to build a neighbor-joining tree in R using the package ape [201]. The tree was then visualized in Dendroscope [202] and supplemental information, as antibiotic resistance phenotype or acquired resistance genes, was added and visualized using iTOL (http://itol.embl.de, [203]).

2.9 Data display: the Bactome database

The Bactome ("Bacterial Genome") database was developed as a comprehensive project data resource and result storage system and programmed by Klaus Hornischer (Helmholtz Centre for Infection Research). By the end of 2013, Bactome consisted of 135 cDNA-sequenced *P. aeruginosa* clinical isolates, including information on their transcriptomes and phenotypes, and information on the *P. aeruginosa* PA14 reference genome for comparative analysis. The basic information for Bactome is extracted from RefSeq [204] files and additional annotation is imported from public data sources as Entrez [205] and UniProt [206]. Configurable program tools as protein domain annotation with Pfam/HMMER [207] create additional annotation. The content of the database is constantly updated through an automatic system of programs. Access to the data stored in Bactome is achieved through a system of web services, which offer tools for the display of the data, e.g. in form of a "Gene Feature Card", or for the processing of data sets with statistical analysis in R. The Bactome database is implemented on a Linux-based Apache web server and consists of data stored in a MySQL database system. Programs are written in Python, web pages in HTML with JavaScript functionality. Bactome stores the basic sequence information in flat files, whereas all of the annotation is contained in the MySQL database.

2.9.1 SNP matrix calculation

SNP matrices for statistical comparisons were created based on SAMtools .flt.vcf files and read coverage information for every position. For the “SNP-wise” approach, the annotated SNPs of all isolates defined for a particular group comparison in Bactome and with a SNP quality score above the

defined threshold were individually extracted via the Bactome database. Next, the read coverage for every SNP was examined and any SNP above the in Bactome defined read coverage threshold was regarded to be definitive positive. SNPs which did not fulfill the custom set coverage criteria were marked as uncertain. From this information a matrix was created, consisting of “0” for no SNP, “1” for definitive SNP and “NA” for uncertain SNP, which was then used for subsequent statistical analysis.

The same method was applied for the "Gene-wise” SNP calculations with the exception that “1” indicates that at least one definitive SNP was found within the whole sequence of a gene and "NA" that exclusively uncertain SNPs were found.

2.9.2 Stop matrix generation

For the determination of those clinical isolates, in which a mutation caused the generation of a stop codon (and thus resulted in a truncated protein sequence), the PA14 reference coding sequence was extracted and used to generate two individual sequences. In the first sequence, only nucleotide exchanges of SNPs above defined quality and coverage thresholds were introduced, thus resulting in a mutated gene sequence with a minimal likelihood of false positive results. The second nucleotide sequence was created based on all detected SNPs, not considering quality or coverage thresholds. Next, both mutated sequences and the reference gene sequence were individually translated into the corresponding peptides, automatically cutting off residues beyond a predicted stop site. To generate a stop matrix to be used for the statistical analysis, the length of each mutated peptide sequence was compared to the reference peptide’s length. Same length peptides in both mutated cases are defined as “0”, while shortened first sequences are defined “1” and second sequences are defined “NA”.

2.9.3 Gene expression matrix generation

The calculation of significant differential gene expression between two groups in Bactome was based on the reads per gene (rpg) generated from SAM output files, size factor normalized in DESeq. Further normalization based on individual gene length was performed to obtain normalized reads per kilobase (nrpk) for every gene.

2.9.4 Phenotype-genotype group comparisons

Group comparisons of clinical isolates for significant differential gene expression were performed using Student’s T-test and group specific accumulations of mutations (SNPs and intragenic stop codons) were analyzed with Fisher's exact test. In both cases, the Benjamini-Hochberg (bh) correction was used to calculate adjusted p-values (padj) to control the false-discovery rate (FDR) in the list of regulated genes. However, due to the general low abundance of intragenic stop codons,

the uncorrected p-values were also considered in the stop comparisons and should thus be interpreted as “scores”, indicating a probably significant accumulation.

2.10 Statistics for overall correlation

Pearson’s correlation (r) was used to test for linear coherence as gene expression and MIC values, and Kendall’s rank-correlation (τ) was used to analyze the dependence of MIC values on a single, distinct feature (e.g. occurrence of specific enzymes or mutations).

For the investigation of “optimal” (here maximizing true positives and minimizing false positive detection) expression thresholds to define binary resistance phenotype grouping (susceptible and non-susceptible), as in the case of *ampC*, a calculation of the receiver operating characteristic (ROC) curve was applied. In ROC analysis, the area under the curve (AUC) is the mean for correlation. To obtain information about the suitability of particular $\log_2$FC cutoffs, the rates of sensitivity (true positives) and specificity (false positives) were calculated for each expression value and compared to each other.

2.11 Carbapenemase activity assay

In order to verify the bioinformatical prediction of acquired carbapenemases, an enzymatic activity assay was performed as previously described by Lauretti and colleagues [208], with some modifications. Main cultures were inoculated in 5 ml LB broth with 300 µl bacterial suspension from overnight pre-cultures and cultivated for 4.5-5 h (early stationary growth phase) at 37 °C, 180 rpm. To harvest the cells, 1 ml culture was collected by centrifugation (2 min, 16,000xg) and resuspended in 500 µl 50 mM HEPES buffer (pH 7) supplemented with 10 µM $ZnSO_4$ for metallo-β-lactamase activity. The cells were broken by sonication (3 cycles à 20 sec, duty cycle 40 %, output control 3.5, Branson Sonicator S250 Analogue). Unbroken cells were pelleted by centrifugation (10 min, 10,000xg), while the remaining supernatant was collected in a fresh tube. Reactions were set up in duplicates for each measurement, mixing a total of 200 µl supernatant with 22 µl 150 mM MEM. The mix was incubated 20 min at 25 °C, before MEM hydrolysis was monitored at 297 nm and 300 nm using a NanoDrop spectrophotometer (Thermo Scientific). The values of both measurements from both duplicates were averaged to one and normalized to the respective total protein amount of the crude extracts as determined by Qubit Protein Assay (Invitrogen).

2.11.1 Carbapenemase assay with activity rescue

For some strains, the carbapenemase activity assay described above showed ambiguous results, possibly due to interfering substances at the monitored wave length. In these cases, the respective strains were instead analyzed for carbapenemase activity rescue by adding $ZnSO_4$ subsequent to incubation with EDTA. For this assay, the cells were grown and harvested as described above, with the exception of using 500 µl pure HEPES buffer for cell pellet resuspension. After lysis and the elimination of unbroken cells, 100 µl supernatant for each replicate was mixed in a new tube with 100 µl HEPES supplemented with 4 mM EDTA (2 mM final concentration) and 300 µM MEM (150 µM final concentration). After 20 min incubation at 25 °C, the base extinction was measured at 297 nm and 300 nm. Afterwards, 4 µl 100 mM $ZnSO_4$ was added (2 mM final concentration) to each sample, followed by a second 20 min incubation step at 25 °C and MEM hydrolysis monitoring at 297 nm and 300 nm. From these values, the base extinctions during EDTA incubation (which inhibits metallo-β-lactamase activity) were subtracted, before samples were again normalized to the total protein amount of the crude extracts.

2.12 Constructions of *mexS* and *oprD* knock-out mutants

To generate *mexS* and *oprD* knock-out mutants in the *P. aeruginosa* PA14 wt strain or a PA14ΔmexR mutant, respectively, mutagenesis was carried out by homologous recombination using the pEX18Ap plasmid [209]. Around 500 bp long, flanking regions upstream and downstream of the respective genes were amplified and an approximately 1000 bp fragment was created by overlap extension PCR as described previously [210], primers are listed in Table 2.3 and PCR parameters, using Phusion polymerase (Invitrogen) in Table 2.6. The fragment was introduced into pEX18Ap via *Hind*III/*Xba*I restriction sites and conjugated into PA14 with the help of *E. coli* S17-1. Mutant candidates were identified by plating on LB agar containing 0.25 µg/ml MEM (Δ*oprD*), and 1 µg/ml CIP (Δ*mexS*) and were further verified by PCR and Sanger sequencing.

Table 2.6 PCR parameters for overlap extension PCR to create *mexS* and *oprD* knock-out mutants.

PCR	Primer	PCR conditions* s_{mexS}, s_{oprD}, t_{ex}, T_a, t_a
1. PCR	FP1_XbaI RP1+20bp	517 bp, 470 bp, 30 s, 68 °C, 20 s
2. PCR	FP2+20bp RP2_HindIII	455 bp, 485 bp, 30 s, 68 °C, 20 s
3. PCR	FP1_XbaI RP2_HindIII	972 bp, 955 bp, 1 min 15 s, 68 °C, 30 s

* s_{mexS}, fragment size *mexS*; s_{oprD}, fragment size *oprD*; t_{ex}, extension time; T_a, annealing temperature; t_a, annealing time

2.13 OprD antibody generation

As OprD is an outer membrane protein, specific purification of sufficient soluble amounts of the protein as a whole provides a great challenge. Hence, we choose to use individual small peptides comprising parts of the *P. aeruginosa* PA14 OprD instead for antibody generation. Peptides suitable for synthetic production and subsequent antibody generation in rabbits had to fulfill the following criteria: 1) length of 10-13 amino acids, 2) a high number of hydrophilic amino acids for sufficient water solubility, 3) preferably at least one proline within the sequence to increase stability, 4) contain suitable epitope sites with high antibody binding specificity and sensitivity. The antibody binding parameters for linear B-cell epitopes of all parts of the OprD sequence were calculated with the BepiPred prediction tool, version 1.0b [211]. Two sequences which matched the above criteria and additionally were not mutated in any of the 135 phylogenetically unrelated clinical isolates were identified. These peptides were synthesized by Werner Tegge (Helmholtz Centre for Infection Research): peptide 1, amino acids 115-123 (NDGTPRDDYSR) and peptide 2, amino acids 329-340 (YSDFNGPGEKS). The immunization of rabbits with the synthesized peptides to gain antisera was performed at BioGenes, Berlin.

2.14 Antibody purification

Before use, the polyclonal antisera obtained from immunization with OprD peptides (peptide 1 = serum 1, peptide 2 = serum 2) were purified using the respective peptide conjugated sepharose. A total of 1 g cyanogen bromide activated sepharose (CNBr-activated-sepharose 4B, GE Healthcare)

was equilibrated for 15 min in 20 ml dH_2O and washed three times in a glass drip with 100 ml dH_2O, 200 ml 5mM HCl, and 200 ml borate buffer (0.1 M boric acid, 0.5 M NaCl, pH 8.4). Following, the sepharose was mixed with 10 mg of the respective peptide, dissolved in 2 ml borate buffer (additionally containing 500 µl DMSO for peptide 1 to prevent precipitation). The suspension was incubated rotating at 4 °C overnight to couple the peptide with the sepharose. The coupled sepharose was pelleted by centrifugation (5 min, 201xg), washed three times with 1.5 M Tris-HCl (pH 8.8), incubated for 1 h rotating with the same solution and subsequently washed twice with PBS (phosphate buffered saline, 137 mM NaCl; 2.7 mM KCl; 10 mM Na_2HPo_4; 2 mM KH_2PO_4; pH 7.4). Following, the coupled sepharose was resuspended in 50 ml solution of a 1:1 mix of serum and PBS. The suspension was incubated overnight, gently rotating at 4 °C to allow the antibody to bind its antigen peptide. To eliminate unspecific binding, the sepharose was first thoroughly collected on a PBS pre-equilibrated plastic drip (PD-10 columns, GE Healthcare) by applying the suspension and the three following flow-throughs on the drip, and subsequently washed twice with 100 ml PBS and 15 ml washing buffer (0.1 M acetate, 0.5 M NaCl, pH 4.8). The specifically bound antibodies were eluted with elution buffer (0.2 M acetate, 0.5M NaCl, pH 2.5) in ten 2 ml fractions. Protein concentrations were measured and fractions containing antibody were pooled, receiving 0.11 mg/ml antibody 1 and 1.26 mg/ml antibody 2. Both antibodies could be used diluted 1:500 in immunodetection assays.

2.15 OprD protein detection by Western Blot

For the detection of OprD protein with specific antibodies, cultures of *P. aeruginosa* clinical isolates and PA14 wt were inoculated from LB-agar plates and grown overnight at 37 °C in 5 ml LB broth. An amount of bacterial cells equivalent to 1 ml adjusted to OD_{600} = 2 was collected by centrifugation for 2 min at 16,000xg. The pellet was resuspended in 50 µl PBS, heat lysed, treated with Benzonase Nuclease (Novagen), and diluted 1:1 in SDS sample buffer. 10 µl were run on 10 % SDS-polyacrylamide gels and subsequently blotted to a PVDF membrane (Immobilon-P, Millipore). OprD protein was detected with purified, polyclonal anti-OprD serum (1:500), followed by a peroxidase conjugated secondary antibody (anti-rabbit-POD, B4C, 1:2000) and Lumilight (chemiluminescent peroxidase substrate, Roche, Mannheim) incubation.

2.16 Outer membrane protein visualization

Selected clinical isolates, PA14 wt and PA14Δ*oprD* mutant were grown overnight in 100 ml LB broth at 37 °C, 180rpm. The cultures were harvested by centrifugation (10,000xg, 4 °C, 20 min), washed twice with Tris-Mg buffer (10 mM Tris, 5 mM $MgCl_2$, pH 7.3), resuspended in 5 ml of the same buffer

and kept cooled on ice during further processing. To lyse the cells, sonication was used for 7 cycles, 2 min each at level 5 and duty cycle 50 % (Branson Sonicator S250 Analogue) and unbroken cells were removed by centrifugation (10,000xg, 4 °C, 10 min). Membranes were pelleted from the supernatant by ultracentrifugation (100,000xg, 4 °C, 1 h) and the outer membrane was purified by washing the pellet twice with Tris-Mg buffer containing 2 % sodium lauryl sarcosinate (SLS). All steps involving SLS were carried out at room temperature to prevent precipitation of the detergent. For every washing step, pellets were resuspended, incubated 20 min and centrifuged 1 h. The final pellet was resuspended in 500 µl dH_2O. Protein concentrations were measured and equally adjusted to 1.3 µg per µl. Each sample was diluted 1:1 in SDS sample buffer and heated to 95 °C for 5 min, before running 15 µl each on 10 % or 15 % SDS-polyacrylamide gels (SDS-PAGE). The bands were visualized with InstantBlue (Gentaur).

2.17 LC-MS/MS sample preparation

Sample preparation was conducted from InstantBlue strained SDS-polyacrylamide gels in the group of Cellular Proteomics at the Helmholtz Centre for Infection Research (Lothar Jänsch / Josef Wissing). For tandem liquid chromatography mass spectrometric analysis (LC-MS/MS), desired protein bands were cut from the gel and destained in a solution containing 30 % acetonitrile and 50 mM NH_4HCO_3. Following, the gel slices were reduced for 30 min at 56 °C with 20 mM DTT in 50 mM NH_4HCO_3, alkylated with 20 mM iodoacetamide in 50 mM NH_4HCO_3 and cut into small pieces. After two washings with 50 mM NH_4HCO_3, the gel pieces were dehydrated in acetonitrile and dried. For all procedures, the volume of the solutions was higher than 20 times the gel volume. Dried samples were rehydrated in 50 mM NH_4HCO_3 supplemented with 10 % acetonitrile and 1:20 sequencing grade modified trypsin (Promega). Digestion of the proteins was performed over night at 37 °C. Peptides were subsequently eluted several times (1 x H_2O; 1 x 1 % triflouroacetic acid; 2 x 30 % acetonitrile containing 0.1% triflouroacetic acid) and dried in a vacuum centrifuge. For LC-MS/MS the dried pellet was desalted using ZipTip RP18 Tips (Millipore), evaporated, and re-solubilized in 3 % acetonitrile containing 0.5 % formic acid.

2.18 LC-MS/MS data acquisition, data analysis and database searching

Liquid chromatography coupled mass spectrometric analysis was performed by Josef Wissing (Helmholtz Centre for Infection Research). LC-MS/MS was carried out on a Dionex UltiMate 3000 n-RSLC system connected to an LTQ Orbitrap Velos mass spectrometer (Thermo Scientific). Peptides were loaded onto a C18 pre-column (3 µm, Acclaim, 75 µm x 20 mm, Dionex) and washed for 3 min at a constant flow rate of 6 µl per min. Subsequently, peptides were separated on an analytical C18

column (3-µm, Acclaim PepMap RSLC, 75 µm x 25 cm, Dionex) at 350 µl per min via ultra performance liquid chromatography (UPLC) using a linear 120-min gradient from 100 % buffer A (0.1 % formic acid in H_2O) to 25 % buffer B (0.1 % formic acid in acetonitrile), followed by a 50 min gradient from 25 % buffer to 80 % buffer B. The LC system was operated with Chromeleon Software (Version 6.8, Dionex), which was embedded in the Xcalibur software (Version 2.1, Thermo Scientific). The effluent from the analytical column was electro-sprayed (Pico Tip Emitter Needles, New Objectives) into the mass spectrometer (Orbitrap Velos Pro), which was controlled by Xcalibur software and operated in the data-dependent mode with the automatic selection of a maximum of 10 doubly and triply charged peptides and their subsequent fragmentation. Peptide fragmentation was carried out using LTQ settings (Min signal 2000, Isolation width 4, Normalized collision energy 35, Default Charge State 4 and Activation time 10 ms). The obtained raw data files were processed via the Proteome Discoverer program (Version 1.4, Thermo Scientific) on a Mascot server (V. 2.3.02, Matrix Science) using a *Pseudomonas aeruginosa* PA14 or PAO1 database extracted from SwissProt. The following search parameters were used: enzyme, trypsin; maximum missed cleavages, 1; fixed modification: carbamidomethyl (Cys); variable modifications: oxidation (Met), peptide tolerance, 10 ppm; MS/MS tolerance, 0.4 Da.

2.19 Fluorescence detection by flow cytometry

Reactive oxygen species (ROS) were detected by flow cytometry using the cell-permeant fluorescent dye H2DCFDA (2',7'-dichlorodihydrofluorescein diacetate, Life Technologies). For sample preparation, the bacteria were cultivated in LB broth at an OD_{600} of 0.8, until the cultures were split into 10 ml each and treated with antibiotics or 50 µl DMSO (dimethyl sulfoxide) or 100 mM H_2O_2, respectively, as controls. Samples of 1 ml culture were harvested at time points one, two and three hours post treatment by centrifugation. The bacterial pellets were resuspended in 1 ml PBS, diluted 1:10 in PBS (final volume 1 ml) and incubated for 2 h at 37 °C, 180 rpm in the dark with 20 µl of 4 mM H2DCFDA, dissolved in DMSO. Measurement at the LSR II flow cytometer (BD Biosciences) and data analysis with FACSDiva software, version 6.1.3 were performed by Anne Lorenz (Helmholtz Centre for Infection Research).

2.20 Metabolic isotope analysis

Analysis of amino acid synthesis was carried out by Esther Surges and Wolf-Rainer Abraham (Helmholtz Centre for Infection Research). Samples were inoculated to an OD_{600} of 0.1 in 600 ml BM2 (7mM $(NH_4)_2SO_4$, 40 mM K_2HPO_4, 22 mM KH_2PO_4, 2mM $MgSo_4$, 0.01 mM $FeSo_4$, pH 7) supplemented with 50 mM glucose and grown until an OD_{600} of 0.8 before a final concentration of 2.5 mM

completely ^{13}C labeled glucose or 1,2 ^{13}C labeled acetate was added. Following, the culture was split by 50 ml each and treated with the respective antibiotic. Samples of 2 ml were harvested by centrifugation at 1 h, 2 h, and 3 h time points post antibiotic exposure and bacterial cell numbers were calculated from CFU counts. Isotope measurements were conducted using a mass spectrometer (IRMS MAT 253) equipped with a Trace GC Plus gas chromatograph via GC Isolink IV (Thermo Scientific). Pee Dee Belemnite (PDB) was used as standard for the relative calculation of ^{13}C incorporation into newly synthesized amino acids.

2.20.1 Amino acid extraction

Amino acids were extracted from a pellet of 2 ml bacterial culture by addition of 2 ml HCl and 24 h hydrolysis at 100 °C. The suspension was filtered (0.2 µm pore size, Whatman) to eliminate large unbroken particles, before the remaining acid was evaporated. The pellet was resuspended in 60 % (v/v) methanol if stored at -20 °C and evaporated again before further processing. For derivatization, in a first step 400 µl dichloromethane were added and subsequently evaporated to remove remaining water. The amino acids were esterified in 800 µl 5:1 isopropanol:acetyl chloride (v:v) for 45 min at 100 °C and the derivatizing agents removed by evaporation, followed by a second dichloromethane evaporation step. A second step of derivatization was performed with 400 µl 1:1 trifluoroacetate:dichloromethane (v:v) for 15 min at 100 °C. The derivatizing agents were carefully evaporated on ice and the amino acids were resuspended in ethyl acetate for GC measurement.

3 Results

3.1 An optimized protocol for cost efficient high-throughput transcriptome sequencing of *P. aeruginosa*

In order to establish a way for cost efficient, high-throughput transcriptome-sequencing of large amounts of clinical *P. aeruginosa* isolates, a customized protocol was used to create barcoded cDNA libraries which are compatible with Illumina flow cells. For this purpose, total bacterial RNA was extracted and ligated during library construction to RNA adapters, which were specifically designed for 5'- and 3'-end ligation of the extracted RNA. Hereby the 5'-end adapters contained an individually assigned 6 nucleotide sequence which facilitated 5'-recognition of a transcript and thus strand-specific sequencing, and multiplexing of several samples, as transcripts belonging to the same sample could be distinguished from each other by bioinformatical tools after sequencing. One limitation when multiplexing, however, is the necessity to obtain a sufficient sequencing depth with the desired transcripts, in this case, those from protein coding mRNA.

3.1.1 mRNA enrichment strategies

Bacterial total RNA comprises a variety of different types of RNA, including coding RNA (mRNA) and non-coding RNA (rRNA, tRNA, sRNA). The largest portion, which spans over 95 % of the total RNA, is made up by the non-coding RNAs, particularly rRNA. Conversely, valuable information on gene expression and gene transcript sequences is only present to less than 4 % in sequenced total bacterial RNA [212]. However, the efficient reduction of rRNA can shift the distribution in favor of the coding RNAs and increase the mRNA sequencing depth of individual samples, and thus also allow for multiplexing of several individual samples on one sequencing lane without immediate transcriptome coverage limitations. While rRNA depletion is rather unproblematic in eukaryotic material because of the natural polyadenylation of the mRNA, bacterial mRNA lacks this tag and therefore cannot be used for direct hybridization to immobilized poly-T sequences [213]. During this work, a variety of different indirect hybridization-based and enzymatic rRNA reduction methods were analyzed for their applicability and efficiency on *P. aeruginosa* rRNA depletion to maximize mRNA enrichment. Particularly a specific reduction of 16S and 32S rRNA was of importance, as the small 5S rRNA (120 nt) could be largely eliminated using size selecting columns during RNA extraction.

3.1.1.1 Hybridization-based rRNA depletion using magnetic beads

One option to increase the amount of mRNA from a sample of total bacterial RNA is the extraction of rRNA using magnetic beads. For this approach, rRNA complementary oligomers were designed with a specific tail which allowed the capture by compatible magnetic beads. Once the oligos bound the rRNA, this complex could thus be extracted with the help of magnets. Figure 3.1 shows the electropherograms obtained from Bioanalyzer for all tested conditions after removal treatment using hybridization methods. Further information on initially applied amounts of total RNA, the total RNA reduction after each approach and the 16S and 23S specific ratios can be found in the corresponding Table 3.1.

Table 3.1 rRNA reduction efficiencies using methods with rRNA complementary oligomers and magnetic beads.

Total RNA reduction percentage was calculated from the amount of RNA left after treatment (measured by NanoDrop), while 16S and 23S rRNA ratios were calculated from Bioanalyzer electropherograms, respectively.

Sample	Total RNA [µg]	RNA after treatment [ng total]	Total RNA Reduction [%]	16S [%]	23S [%]
Control	-	-	-	25.7	44.2
Oligo $(dT)_{25}$	5	500	90	20.7	39.4
Streptavidin 50 µl	10	6600	34	21.8	33.3
Streptavidin 2x 50 µl	10	3900	61	21.5	30.5
Streptavidin 100 µl	10	5000	50	19	30.7
Streptavidin 50 µl, rotating	5	2900	42	13.7	21.3
Ambion oligos4	5	675	86.5	4.4	3.7
Ambion oligos4	10	1450	85.5	7.5	20.5
Ambion oligos5	10	1600	84	2.2	37.2
Ambion oligos4+5	5	600	88	2	16.9
Ambion 2x: oligos4, oligos5	10	950	90.5	0	3.4

Figure 3.1 B depicts the result of an indirect hybridization approach using a mix of four different rRNA complementary capture oligos, each with a tail of 18 adenine residues (1R, 4R, R, and 4Pse; oligos4) in combination with matching oligo $(dT)_{25}$ magnetic beads (Dynabeads, Invitrogen). Interestingly, despite a total RNA reduction of 90 % (Table 3.1), this approach led only to marginal reduction of rRNA with amounts of 16S rRNA decreased from 25 % to 20 % and 23S rRNA from 44 % to 37 %, respectively, determined from Bioanalyzer electropherograms, compared to the untreated total RNA (Figure 3.1 A).

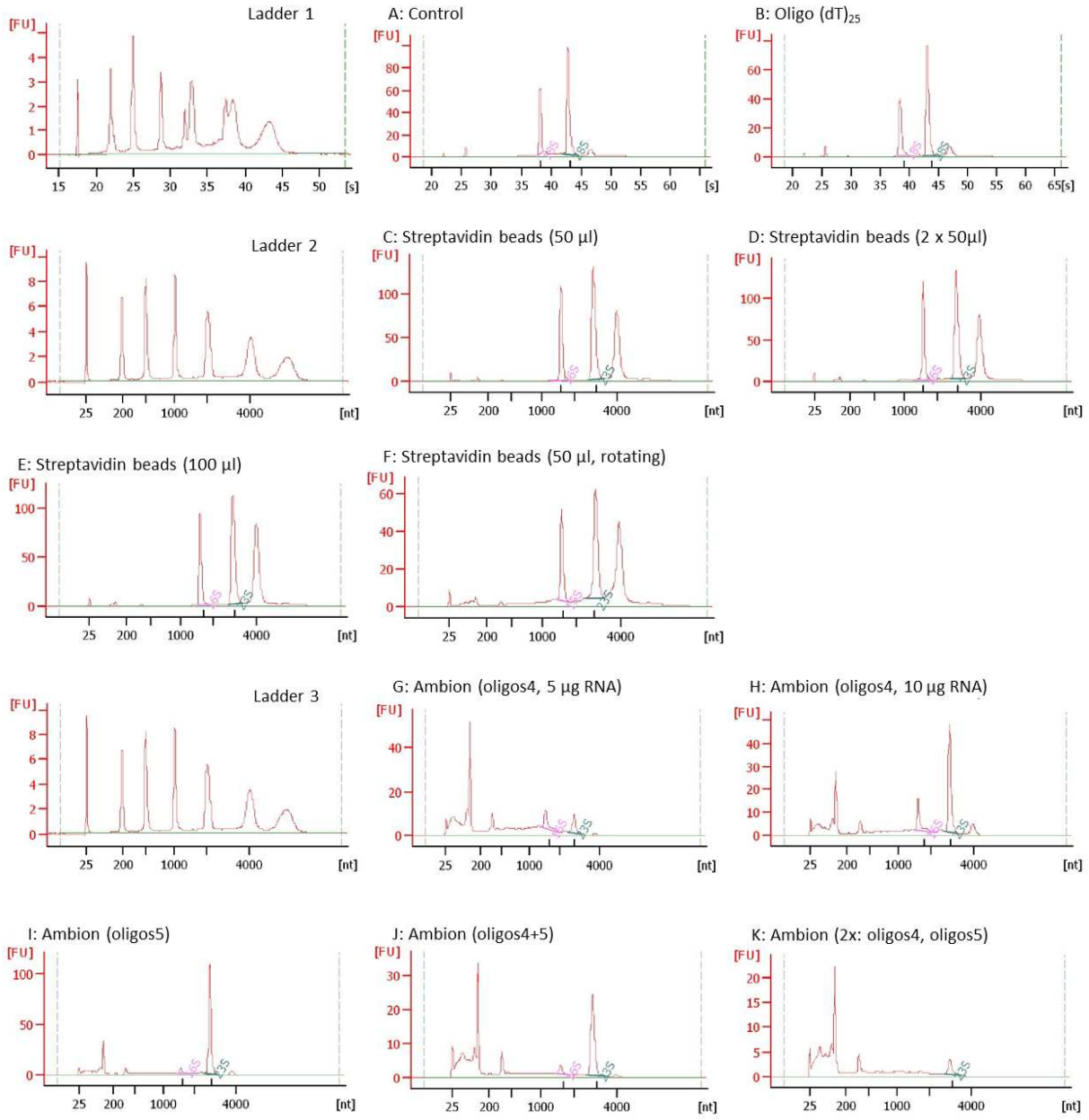

Figure 3.1 rRNA depletion by magnetic beads.

rRNA depletion of PA14 wt total RNA was performed using different methods based on the principles of rRNA complementary, tagged capture oligomers in combination with matching magnetic beads to capture the rRNA bound oligomers. A-K show the respective electropherograms obtained from Agilent 2100 Bioanalyzer. A: Untreated control (PA14 total RNA). B: Depletion using a mix of four specific, rRNA complementary oligomers with poly-A-tail (1R, 4R, R, and 4Pse) and matching oligo $(dT)_{25}$ magnetic beads. C-F: rRNA depletion performed with streptavidin magnetic beads and a mix of four rRNA complementary, biotinylated oligomers (251-1R, 195-4R, 807-R, and 111-4Pse). C: Sample was treated with 50 µl streptavidin magnetic beads. D: Two rounds of rRNA depletion as in (C) were applied after each other. E: Sample was treated with one round of rRNA depletion using the double amount of beads (100 µl) as in (C). F: Sample was rotated during treatment with magnetic beads, as opposed to C-E, were samples were kept shaking in a thermomixer. G-K: rRNA was depleted using the MICROBExpress kit (Ambion), which combines polyadenylated rRNA-complementary oligomers with

matching oligo (dT) magnetic beads. G: Four oligos (1R, 4R, R, and 4Pse) were used on 5 µg total RNA. H: The same oligos as in (G) were used on 10 µg total RNA. I: A mix of five oligos (2-PolyA, 9-PolyA, 27-PolyA, 3-PolyA, and 10-PolyA) was applied on 10 µg total RNA. J: A mix of nine oligos was used on 5 µg RNA, containing the oligos from (G) and (I) in equal amounts. K: 10 µg of total RNA were treated twice with the MICROBExpress kit using first four oligos as in (G), followed by a second round with five oligos as in (I).
Samples A-B (Ladder 1), C-F (Ladder 2), and G-K (Ladder 3) were run together on individual Bioanalyzer pico chips. Probable 16S and 23S fractions were marked in pink and green, respectively.

A similar output was obtained when using the same oligos in a biotinylated, instead of the polyadenylated version in combination with streptavidin-tagged magnetic beads (Dynabeads, Invitrogen), as shown in Figure 3.1 C. Here, the amount of 16S and 23S rRNA was reduced to 22 % and 33 %, respectively. Neither doubling the amount of oligos and beads, nor applying two individual rounds of rRNA removal after each other significantly affected the outcome (Figure 3.1 D-E). However, an improvement was made by rotating the sample instead of shaking, with a respective reduction to 14 % (16S) and 21 % (23S), which indicated that insufficient physical contact of rRNAs, oligos and beads under the selected conditions might have been one reason for the low removal efficiency. To optimize hybridization conditions, the commercially available MICROBExpress kit (Ambion) was used, which had previously been described to efficiently remove rRNA and provide samples with more than 40 % mRNA for selected organisms [214]. The MICROBExpress system is based on poly-T beads, thus the same oligo mix was used as for the Oligo $(dT)_{25}$ Dynabeads. Application of the MICROBExpress buffer and beads led under comparative experimental conditions to a significant increase in rRNA reduction rate to only 4 % residual 16S and 23S rRNA when applied on 5 µg total RNA (Figure 3.1 G). Depletion was a little less efficient, particularly for 23S rRNA, when 10 µg of total RNA were applied (Figure 3.1 H). To test whether the use of additional complementary oligos would further increase rRNA removal rates due to a greater number of rRNA target regions, five new oligos (2-PolyA, 9-PolyA, 27-PolyA, 3-PolyA, and 10-PolyA; oligos5) distinct from the first four were designed based on the *P. aeruginosa* rRNA sequence. rRNA depletion with these five oligos alone in combination with the MICROBExpress kit proved to be similarly efficient on 16S rRNA and only slightly less efficient on 23S rRNA compared to the previously tested oligo4 mix (Figure 3.1 I). However, a combination of all 9 (4+5) oligos in one mix could not provide more mRNA, but was on the contrary even slightly less efficient on 23S rRNA removal than application of only the oligos4 mix (Figure 3.1 J). Although the oligo sequences had afore been analyzed for inter- and intra-complementarity, possible molecular interference cannot be completely excluded and might be an explanation for this unexpected result. Thus, two individual MICROBExpress reduction rounds were performed after each other with oligos4 in the first and oligos5 in the second, to avoid any secondary effects. As shown in Figure 3.1. K, these two individual reduction rounds with distinct sets of oligos

indeed strongly decreased rRNA amounts, even from 10 µg of initial total RNA. While 16S rRNA was completely eradicated, only 3.4 % of 23S rRNA was left from the initial 25 % (16S) and 44 % (23S), according to Bioanalyzer calculation (Table 3.1). However, as the costs for one MICROBExpress run made up 33 % of the costs for library preparation as a whole and more than 10 % of the total sequencing costs of one sample, the increased multiplexing capacity by applying two rounds of rRNA reduction proved to be not economical compared to the additional costs. Therefore, the applicability of enzymatic rRNA removal for *P. aeruginosa* was investigated as a possible alternative option.

3.1.1.2 Enzymatic rRNA depletion by terminator-5´-phosphate-dependent exonuclease (TEX)

Besides the capture of rRNA by magnetic beads, another option to remove prokaryotic rRNA which has previously been described for bacterial species is the specific enzymatic degradation [214]. While bacterial mRNA lacks polyadenylation, it contains a 5'-triphosphate instead. Mature rRNA and tRNA on the contrary exhibit a 5'-monophosphate. This difference can be used by the enzyme terminator-5´-phosphate-dependent exonuclease (TEX) to specifically degrade non-mRNA transcripts.

Table 3.2 rRNA reduction efficiencies using enzymatic degradation by terminator-5'-phosphate-dependent exonuclease (TEX).

Samples were either treated with TEX enzyme alone or a combination of rRNA removal with Ambion magnetic beads (MICROBExpress) followed by TEX incubation (ATA, ATB). Samples TEX 150s b and T1A – ATB were Illumina sequenced and further analyzed (Figure 3.3). For sample TEX 180s no 16S and 23S ratios could be calculated due to overall fragmentation of the RNA (compare Figure 3.2).

Sample	Total RNA [µg]	RNA after treatment [ng total]	RNA Reduction [%]	TEX [U]	TEX [U/µg RNA]	Inkubation [min]	Buffer	16S [%]	23S [%]
Control	-	-	-	-	-	-	-	26.7	48.5
TEX 150s a	15	2575	82	7	0.47	150	A	1.9	40.8
TEX 150s b	7	975	86	6	0.85	150	A	1.3	33.8
TEX 180s	7	825	88	7	1	180	A	-	-
TEX 1U	2.5	1585	36	1	0.4	60	A	2.7	59.2
TEX 5U	2.5	407	83	5	2	60	A	2.4	46.2
T1A	2.5	780	68	1	0.4	60	A	nd	nd
T1B	2.5	1170	53	1	0.4	60	B	nd	nd
T5A	2.5	120	95	5	2	60	A	nd	nd
T5B	2.5	390	84	5	2	60	B	nd	nd
ATA	1.4	240	82	1	0.71	60	A	nd	nd
ATB	1.4	420	70	1	0.71	60	B	nd	nd

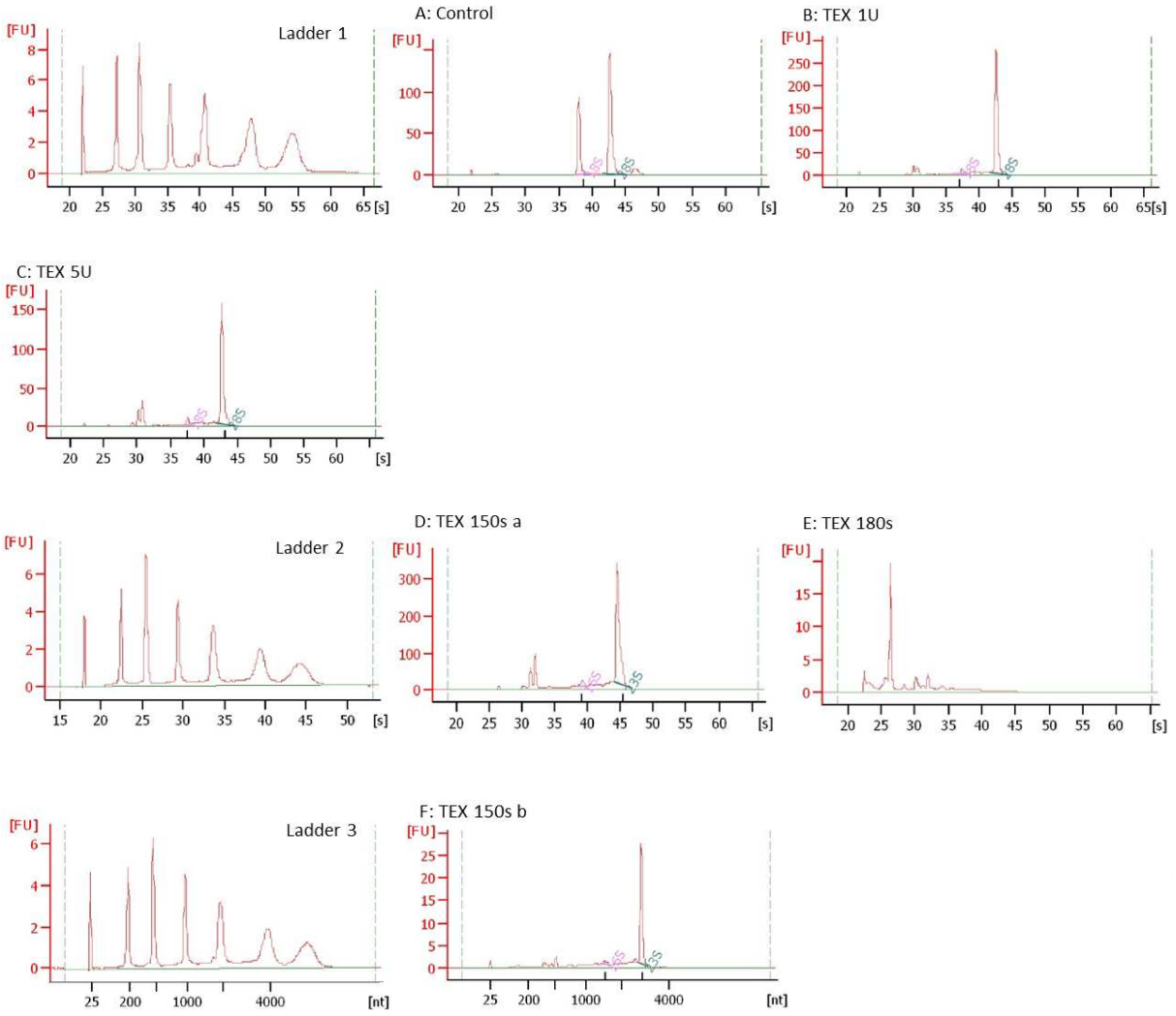

Figure 3.2 rRNA depletion by enzymatic degradation.

PA14 wt total RNA was treated by specific enzymatic degradation using terminator-5´-phosphate-dependent exonuclease (TEX) to reduce the amount of rRNA content. A-F show the respective electropherograms obtained from Agilent 2100 Bioanalyzer. A: Untreated control sample (total RNA). B-F: Samples treated with TEX enzyme using different concentrations and incubation times. Details for each reaction setup can be obtained from Table 3.2. Samples A-C (Ladder 1), D-E (Ladder 2), and F (Ladder 3) were run together on individual Bioanalyzer pico chips. Probable 16S and 23S fractions were marked in pink and green, respectively.

Figure 3.2 depicts the electropherograms obtained from Bioanalyzer for TEX treated samples with the influence of prolonged incubation and varied enzyme concentration. Further information on each sample set up, including initially applied amounts of total RNA and respective enzyme concentrations per µg RNA, as well as RNA reduction after each approach accompanied by the 16S and 23S specific ratios can be found in the corresponding Table 3.2.

While hybridization-based approaches showed only a minor increased preference for 16S over 23S rRNA, TEX dependent enzymatic degradation clearly favored the depletion of 16S rRNA (Figure 3.2 B). As increased enzyme concentration did not alter rRNA removal ratios (Figure 3.2 C), one possible

explanation was thought to be the size difference of 16S (1500 nt) and 23S (2900 nt) rRNA, which resulted in supposedly longer degradation time for 23S. Thus, the incubation time was stepwise increased from 60 s to 150 s and 180 s. While only slight improvement was obtained at 150 s to 1 % 16S and 34 % 23S rRNA compared to 27 % and 49 % for the control sample and 3 % and 46 % after 60 min incubation, severe overall RNA degradation was observed at 180 s (Figure 3.2 D-F).

To compare the effects of both, hybridization and enzymatic rRNA removal on the actually remaining proportion of mapped rRNA transcripts and examine method specific influences on the overall gene expression profile, one Ambion treated sample and one 150 s TEX treated sample were Illumina sequenced. Furthermore, four additional samples with varying TEX enzyme concentrations and reaction buffer conditions, and two samples treated with magnetic beads, followed by TEX incubation were investigated.

As shown in Figure 3.3 A, the Ambion MICROBExpress treatment clearly led to the highest amount of rRNA reduction with an increase to 40 % mRNA transcripts. Additional TEX incubation in either buffer A or B did not influence this ratio (samples ATA and ATB). On the other hand, TEX incubation alone still remained with 85-95 % mapped rRNA reads, regardless of the selected conditions, although the previously by Bioanalyzer determined overall rRNA reduction differed only from 40 % (Ambion oligos4) to 46 % (TEX 150s b). This discrepancy likely results from incomplete rRNA degradation, producing augmented smaller fragments, instead of effectively removing the rRNA. Thus, the respective remaining fragments are still amplified and mapped, and continue to affect mRNA sequencing depth.

Another interesting observation was the effect of enzymatic and hybridization dependent rRNA treatment on mRNA gene expression profiles, as depicted in Figure 3.3 B. As an example, the *oprD* gene was chosen, which is known to be initiated for transcription from at least two individual transcriptional start sites at -23 and -71 upstream of the gene [18]. Both start sites were clearly visible as significant, sharp peaks just before the *oprD* coding sequence, when rRNA was removed by hybridization. However, enzymatic TEX treatment, even as low as 0.4 U per µg total RNA (samples T1A and T1B), completely eradicated these significant start side peaks. Additionally, overall gene wide expression patterns differed greatly from the hybridization treated sample, particularly with increasing enzyme concentration, incubation duration and use of buffer B. It therefore appears that TEX dependent enzymatic rRNA degradation is not highly specific and as well affects mRNA transcripts.

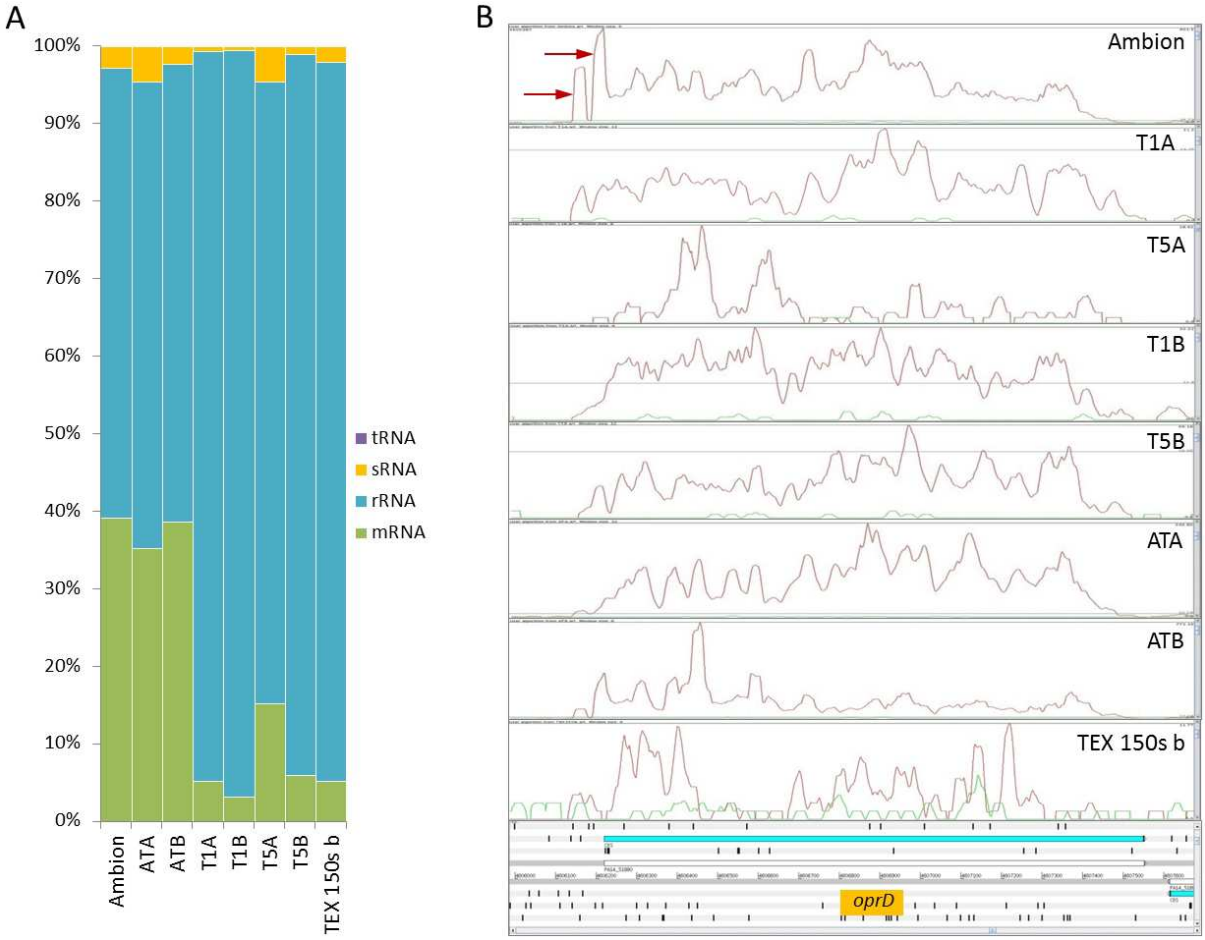

Figure 3.3 Transcript distribution and gene expression profiles after rRNA removal.

A: Abundance of mRNA, rRNA, sRNA and tRNA reads after mapping to the PA14 reference genome. B: Effects of different enzymatic and hybridization-based rRNA depletion protocols on mRNA transcripts (using the example of the *oprD* gene). Transcriptional start sites are indicated by red arrows. Expression profiles were visualized with Artemis genome browser [215], with gene expression of the plus strand shown in red and gene expression of the minus strand in green, respectively.

Concluding, best results in terms of rRNA reduction, integrity of the mRNA *in vivo* profile of *P. aeruginosa* and overall cost efficiency for high-throughput application were obtained from treatment with one round of rRNA removal by Ambion MICROBExpress in combination with oligos4. To remain with sufficient amounts of mRNA for library preparation after reduction and still maximize the removal impact, 7 µg of total bacterial RNA were initially used per sample for preparation of the sequenced clinical isolates.

3.2 Transcriptome sequencing of clinical *P. aeruginosa* isolates

Our study was designed to investigate the genetic modifications underlying antibiotic resistance phenotypes in *P. aeruginosa* clinical isolates. For this purpose, a cross-sectional study group was chosen with isolates sampled in different regions across Europe as well as diverse infection sites as wounds, catheters, urinary tract infections, and sections of the respiratory tract, including 30 samples from cystic fibrosis patients. Altogether, our sample collection comprised 149 clinical *P. aeruginosa* isolates, provided by the Hannover Medical School (87), the University of Freiburg (40), the Robert-Koch-Institute in Wernigerode (14), and the National Reference Centre for multidrug-resistant Gram-negative Bacteria in Bochum (8). To focus particularly on the subject of antibiotic resistances, the majority of the strains were selected because of their categorization as multidrug-resistant. All strains were cultivated, RNA-sequenced, and analyzed based on the sequencing data for gene expression and mutations.

3.2.1 Coverage and relative transcript abundance of clinical *P. aeruginosa* isolates

Since this study aimed to analyze not only the gene expression profiles but also the transcript sequences of different *P. aeruginosa* isolates in order to search for resistance determining mutations, a sufficient read coverage had to be assured. This was of particular importance with the intention to maximize multiplexing on the same sequencing lane, thereby exhausting the entire scope of Illumina sequencing capacity. A second important challenge was to determine the analysis strategy in favor of either read mapping to a reference genome or whole transcriptome *de novo* assembly.

Complete genome sequences of several *P. aeruginosa* isolates have already been made available to the community [79,216-218], and comparative analysis of the different strains discovered a mosaic genome. Approximately 90 % of the *P. aeruginosa* genome belongs to strongly conserved, ‘core’ genetic elements, interspread by only a small proportion of accessory genetic islands [219,220].

This allowed acquiring the vast majority of sequence and expression information by mapping the sequencing reads of the clinical isolates directly to the sequence of one known reference strain without the need for whole transcriptome *de novo* assembly. In this study, the clinical isolate UCBPP-PA14 was used as genetic reference [189].

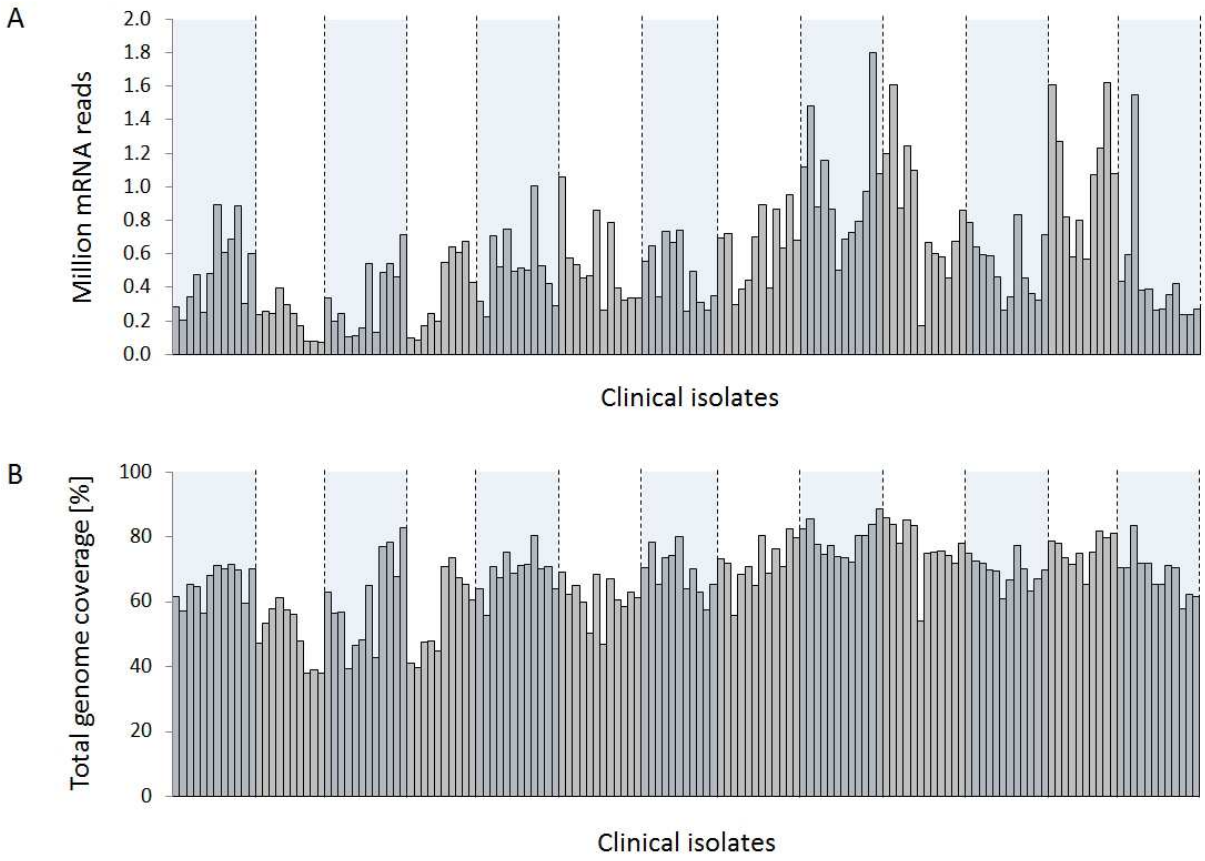

Figure 3.4 Individual read counts and genome coverage of 149 clinical *P. aeruginosa* isolates.

Clinical isolates are depicted from left to right in order of sample preparation and sequencing. A: Amounts of mapped reads (to the PA14 reference genome) obtained from RNA-sequencing per isolates. B: Whole genome coverage (nucleotide positions with ≥ 1 read) per sample. Different sequencing pools are separated by dashed lines.

Figure 3.4 A depicts the individual numbers of mRNA reads mapped to the PA14 reference genome for each of the 149 clinical isolates. Hereby the read origins, as coding or non-coding RNA were not taken into account. Additionally, the corresponding total genome coverage was calculated as determined by the amount of nucleotide positions with at least one mapped read (Figure 3.4 B). Interestingly, the amounts of mapped reads fluctuated much more strongly than the correspondingly calculated coverage. Further analysis revealed that read quantity and genome coverage only showed a clear, nearly linear correlation (r = 0.83) within the range of up to 0.8 million mapped mRNA reads, resulting in approximately 75-80 % genome coverage. Above this threshold, saturation occurred and only a slight further increase in coverage ranging from 70 % to a maximum of 90 % could be seen (r = 0.50), despite more than doubling read quantities of up to 1.8 million mapped mRNA reads per sample (Figure 3.5).

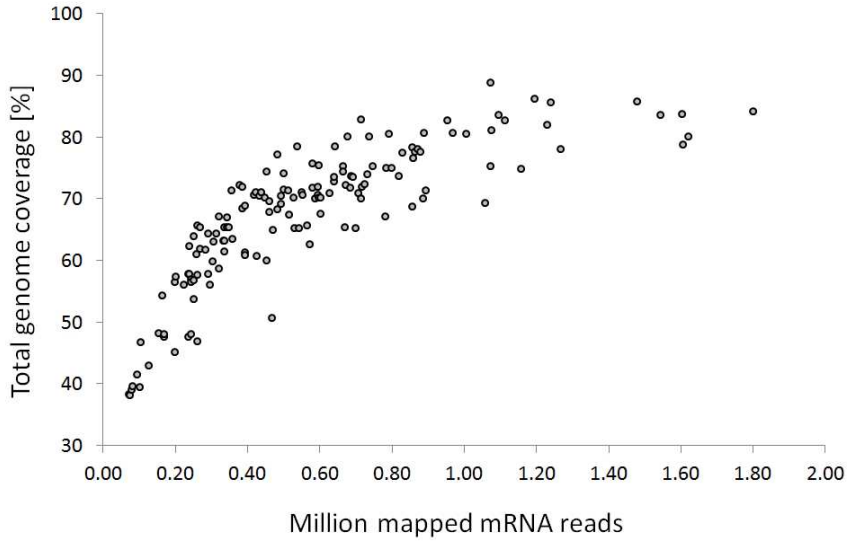

Figure 3.5 Correlation between numbers of mapped reads and genome coverage.

A clear linear correlation between the amount of mapped reads and the total genome coverage could be recognized until 0.8 million mRNA reads per sample (r = 0.83). Above this threshold, saturation was seen with only slight further increase in coverage despite doubling read numbers (r = 0.50).

Overall, multiplexing of up to twelve individual samples in equal amounts on one Illumina Genome Analyzer IIx lane provided between two and 13 million mapped reads, with an average of five million reads per sample (Figure 3.6 A). Only sequencing the transcriptomes of the clinical isolates, thus a total genome coverage ranging from 40 % up to 90 % could be obtained with an average of 67 % genome coverage across the samples (Figure 3.6 B). Furthermore, an averaged 49 % of the genomes were covered with at least three or more mapped reads. Of note, the total genome coverage of a paired end sequenced PA14 wt strain reached 70 %.

This coverage was sufficient to enable us to use the transcriptome data for gaining information about sequence variations as single nucleotide polymorphisms (SNPs) or larger mutations as insertions and deletions. We employed this sequence information both for phylotyping to evaluate clonal relatedness within the sequenced strain collection and resistance phenotype prediction accompanied by unbiased, global phenotype-genotype correlations.

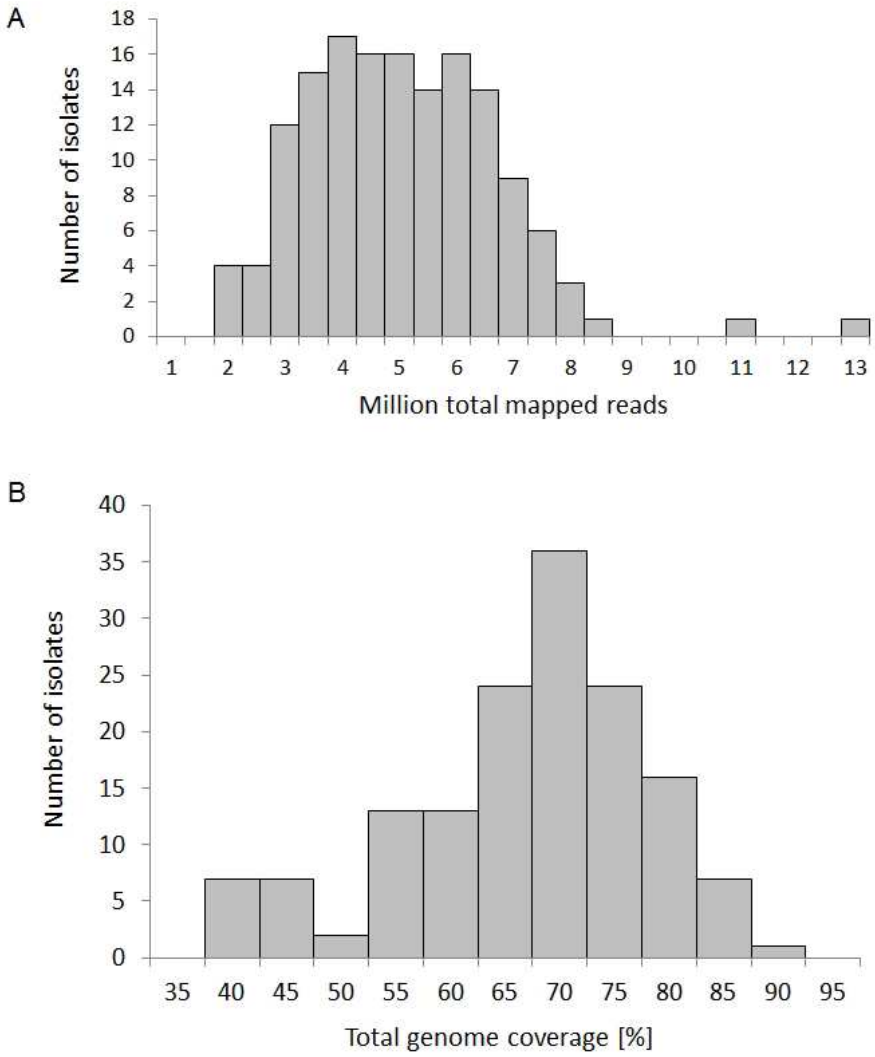

Figure 3.6 Overall RNA-seq data depth.

A: Coverage distribution of the *P. aeruginosa* clinical isolates mapped to the PA14 reference genome. The total number of mapped reads varied between two and 13 million, with an average of five million per sample. B: Distribution of the whole genome coverage (nucleotide positions with ≥ 1 read) of the clinical isolates by transcriptome sequencing of *P. aeruginosa* clinical isolates ranged from 40 % - 90 %. On average, genome coverage of 67 % was reached.

Besides the total amounts of mapped reads and the respective genome coverage, the relative transcript abundance of individual coding (mRNA) and non-coding (rRNA, sRNA, and tRNA) was determined to evaluate the impact of the library preparation method on small RNA species, and identify the rRNA removal and mRNA enrichment efficiency (Figure 3.7).

For rRNA removal, the clinical isolates were treated with a combination of MICROBExpress (before library preparation) and duplex-specific nuclease treatment (DSN; after library preparation), which yielded in up to 75 % mRNA per sample. However, rRNA removal efficiency strongly varied (between less than 10 % and more than 70 % mRNA content) depending on the individual sample and partly on the sequencing pools as a whole. Final mapped mRNA-rRNA ratios could not be predicted accurately

from concentration decrease after hybridization or DSN, or Bioanalyzer ratio calculation (data not shown).

Abundance of tRNA and sRNA was below 1 % and 8 %, respectively, throughout all samples.

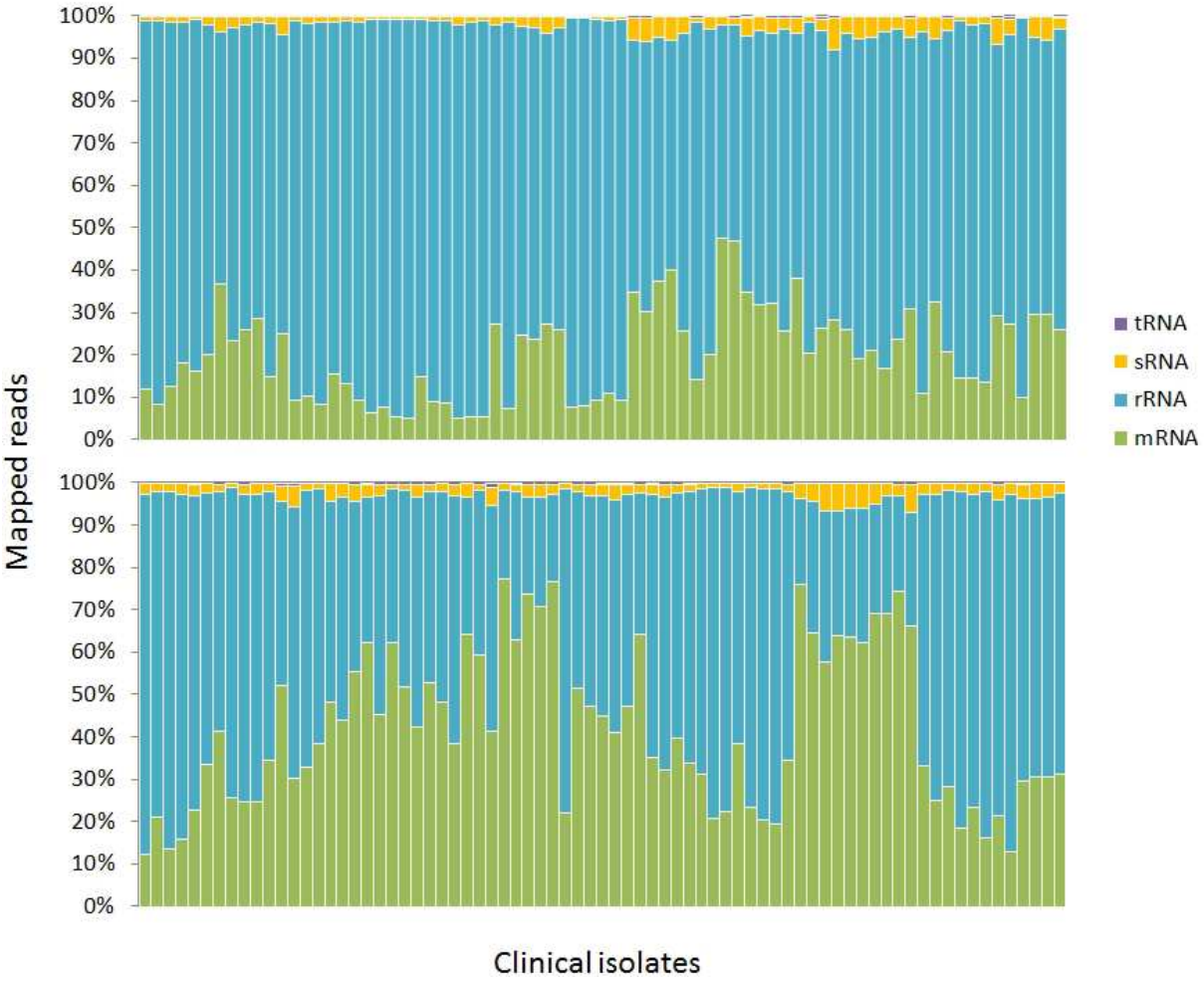

Figure 3.7 Distribution of mRNA, rRNA, sRNA and tRNA reads.

Percentages for mRNA, rRNA, sRNA, and tRNA mapped reads to the PA14 reference genome were calculated from the amount of the reads per gene (rpgs) from each category divided by the total number of rpgs per strain. Clinical isolates are depicted from left to right and top to bottom in order of sample preparation and sequencing. Average values for the first 75 samples (top) were 20.1 % (mRNA), 77.1 % (rRNA), 2.6 % (sRNA), and 0.1 % (tRNA), while average values for the last 74 samples (bottom) were 41.7 % (mRNA), 54.9 % (rRNA), 2.8 % (sRNA), and 0.2 % (tRNA), respectively.

3.2.2 Phylotyping by 214 genes identified a clonal outbreak

With the data obtained from RNA-sequencing, our first aim was to have a look at the phylogenetic relatedness of the isolates. This was supposed to provide more insight into taxonomical distributions and furthermore, ensure an unbiased study group for subsequent genetic analysis.

For obtaining information about phylogenetic distribution and clonal relatedness, strategies such as variable number tandem repeat (VNTR) and multilocus sequence typing (MLST) assays are widely used [221,222]. Although both methods are useful for strain typing, they are only based on a very limited level of sequence resolution, as for example just eight open reading frames (ORFs) are considered for conventional MLST analysis. A newer, higher-throughput, complementary approach was introduced in 2007 with the development of a typing microarray capable of discriminating 58 binary single nucleotide polymorphisms (SNPs) in seven conserved ORFs, as well as identifying the presence of strain-specific horizontally acquired genomic islands and islets [223].

We wanted to provide even higher resolution and therefore performed phylogenetic analysis based on the sequence similarity of all commonly expressed core genes. Thus, the sequences of all genes with a coverage of at least 90 % in all clinical isolates and orthologs in five selected *P. aeruginosa* reference strains (PAO1, PA14, PACS2, LESB58 and PA7), in total 214 genes, were compared with each other. The phylogenetic relationship was constructed from a k-mer-based matrix of this comparison, including the reference strains and the 149 sequenced clinical isolates.

As shown in Figure 3.8, the generated phylogenetic tree separated into two main lineages, one including the PA14 reference strain and the other containing PACS2, LESB58 and PAO1. Additionally, there were some taxonomically more distant isolates (MHH6887, MHH13682, MHH13684, MHH9830, and B34) and the known outlier PA7. Although we also identified a few groups of more closely related isolates, overall, the samples exhibited a broad taxonomical heterogeneity. One particular cluster (highlighted in red), however, only consisted of samples isolated at the Hannover Medical School within a short time-period of only a few months. Further investigation of the expression profiles (Figure 3.9) confirmed that the specific isolates likewise exhibited a very similar gene expression pattern, with twelve of the fourteen clustering directly together. Combined with a retrospective analysis of the patients` data, the phylogenetic and expression-wise clustering indicated very close clonal relatedness.

Since our study intended to identify resistance markers on a global scale by unbiased statistical analysis and provide information about the distribution and abundance of antibiotic resistance determinants within a cross-sectional group, all but one isolate (MHH8607) of this clonal cluster were excluded from further analyses (135 remaining isolates).

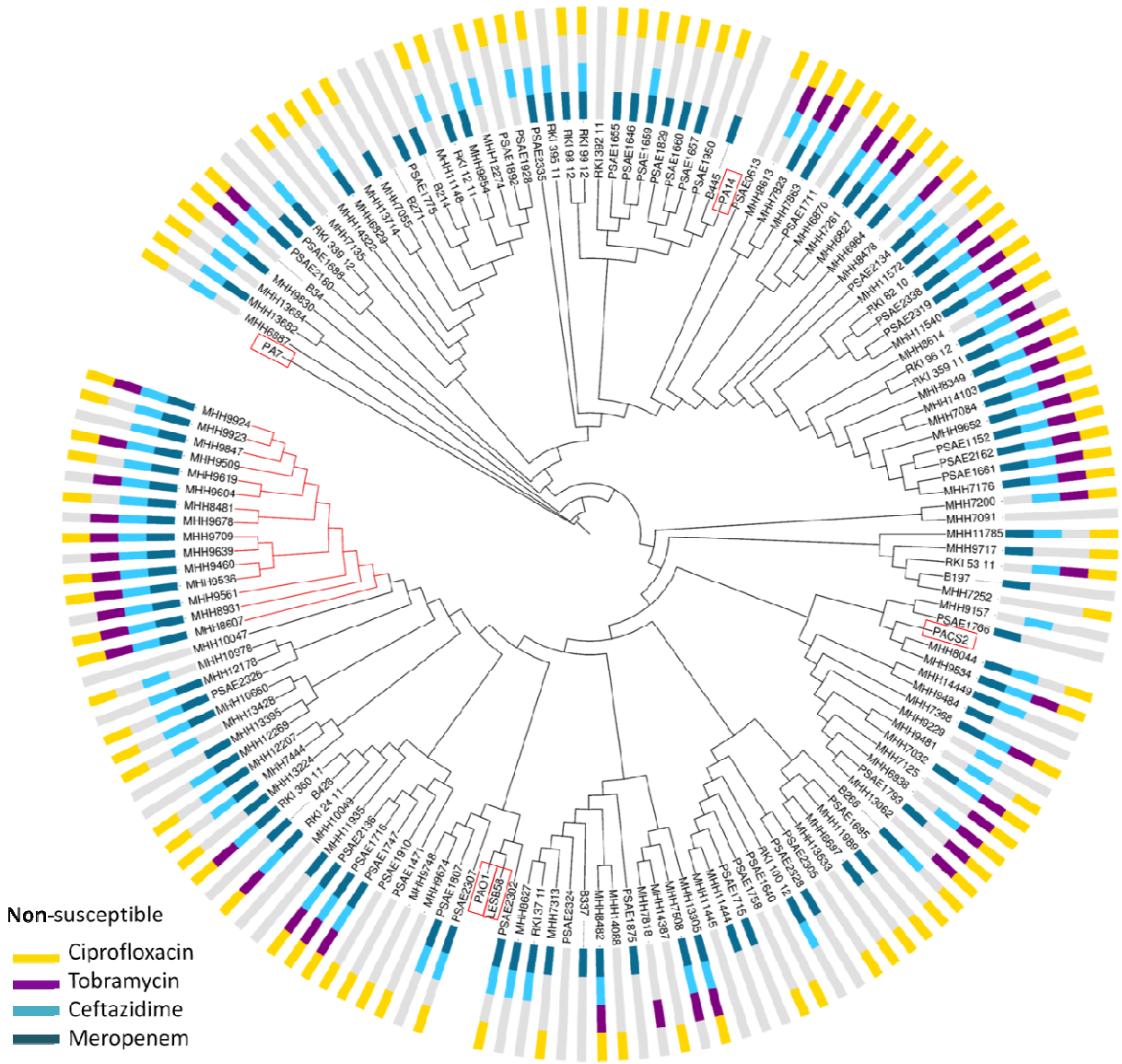

Figure 3.8 Phylogenetic clustering and antimicrobial resistance profile of all sequenced clinical isolates.

The phylogenetic tree of all sequenced clinical isolates and five reference strains (PA14, PAO1, LESB58, PACS2, PA7) was constructed with neighbor-joining algorithm and the reference strain PA7 defined as outgroup. Basis for the analysis of phylogenetic distances was a distance matrix calculated from k-mers of all genes with a coverage of at least 90 % in all clinical strains and respective orthologs in the reference strains (total 214 genes). Reference strains were framed in red, while red tree branches indicate strains belonging to one likely clonal cluster. The non-susceptibility (resistance or intermediate-resistance) of the isolates towards the important anti-pseudomonal drugs ciprofloxacin, tobramycin, ceftazidime and meropenem was indicated by respectively colored bars. The antibiotic resistance dataset was integrated using iTOL [203].

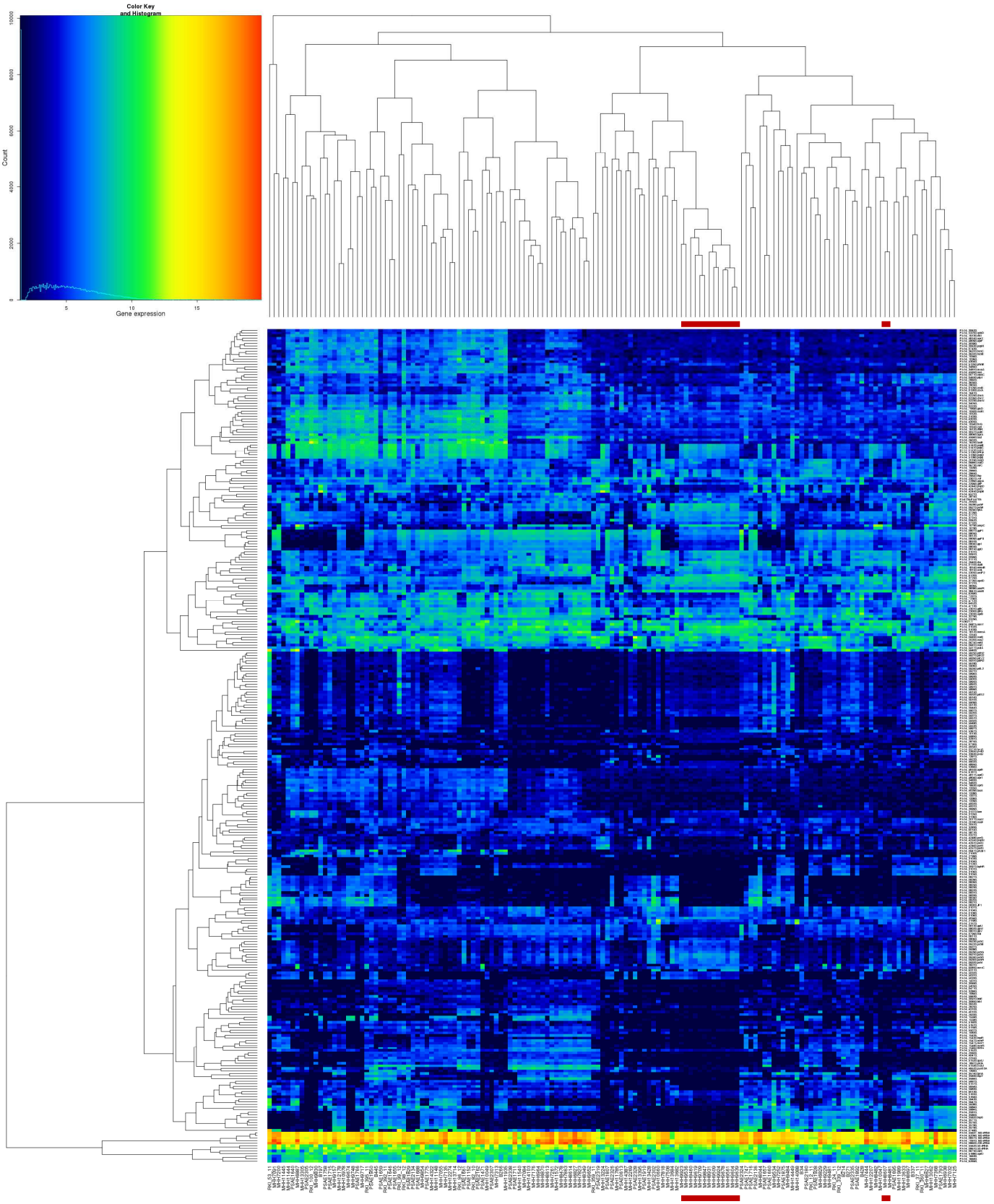

Figure 3.9 Gene expression clustering of clinical isolates.

The heatmap shows the gene expression profiles of all sequenced isolates. Included were all differentially regulated genes with an interquartile range (iqr) = 2 calculated from nrpk values. Hierarchically clustering was performed with the Hclust algorithm in R. Isolates belonging to one likely clonal cluster are marked in red.

These 135 clinical isolates were then analyzed for their I) acquired genetic elements, II) gene expression profiles, and III) sequence mutations (including SNPs, stops, and insertions/deletions). While the information on gene expression and gene sequence can be obtained from mapping to the reference genome, the search for acquired genetic elements has to be based on alternative strategies.

3.2.3 Nature and distribution of acquired β-lactamases

P. aeruginosa is well known for its ability to acquire resistance via horizontal transfer of genetic elements like plasmids, transposons (especially associated with integrons), and acquired β-lactamases which largely contribute to a rapid spread of β-lactam resistance among clinical isolates [140]. To search for the presence of such acquired resistance-conferring genes, particularly β-lactamases, in our collection of clinical isolates, we applied two different approaches. The first was to generate a collection of contigs from *de novo* transcriptome assembly, which were then aligned to a comprehensive resistance gene library containing a collection of 658 prokaryotic, transposable resistance genes, including 514 β-lactamases. The second approach was to generate an artificial genome based on the alignment of the mentioned resistance gene library. RNA-sequencing reads were subsequently mapped to this artificial genome and the sequence coverage of every gene was determined.

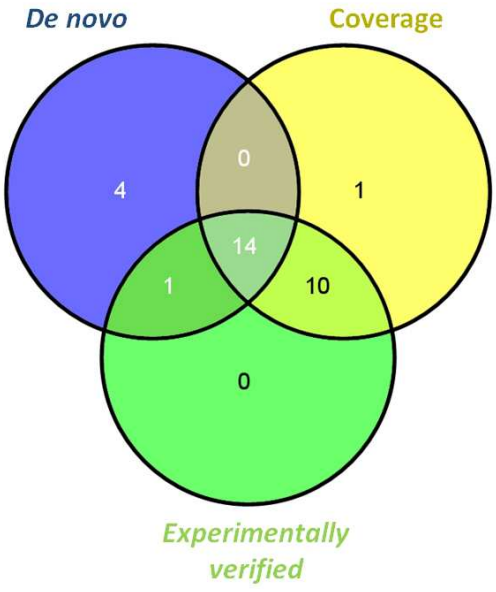

Figure 3.10 Direct comparison of bioinformatical β-lactamase detection approaches.

A total of 19 β-lactamases in 17 strains was detected using *de novo* transcriptome assembly and blast comparison, while a mapping-based approach identified 25 β-lactamases with sequence coverage of more than 90 %. Both approached showed a 46 % overlap with each other and an 83 % overlap with the supposed "actual" spectrum of acquired β-lactamases as validated by additional Sanger sequencing or phenotypic comparison. Venn diagram was created with VENNY [224].

While both methods detected a largely overlapping set of acquired β-lactamases (83 %), the gene coverage-based approach exhibited higher sensitivity and a lower false discovery rate (Figure 3.10). The false discovery rate was assigned by comparing the computational results with additional experimental data. The presence of acquired genes was exemplary confirmed by PCR and Sanger-sequencing, revealing a high accuracy of the transcriptomic approach. Additionally, we tested all MEM-CAZ resistant isolates for enzymatic carbapenemase activity, which matched the bioinformatic prediction (Figure 3.11). Eventually a combination of both approaches was used to unravel the complete acquired β-lactamase repertoire of all sequenced clinical isolates.

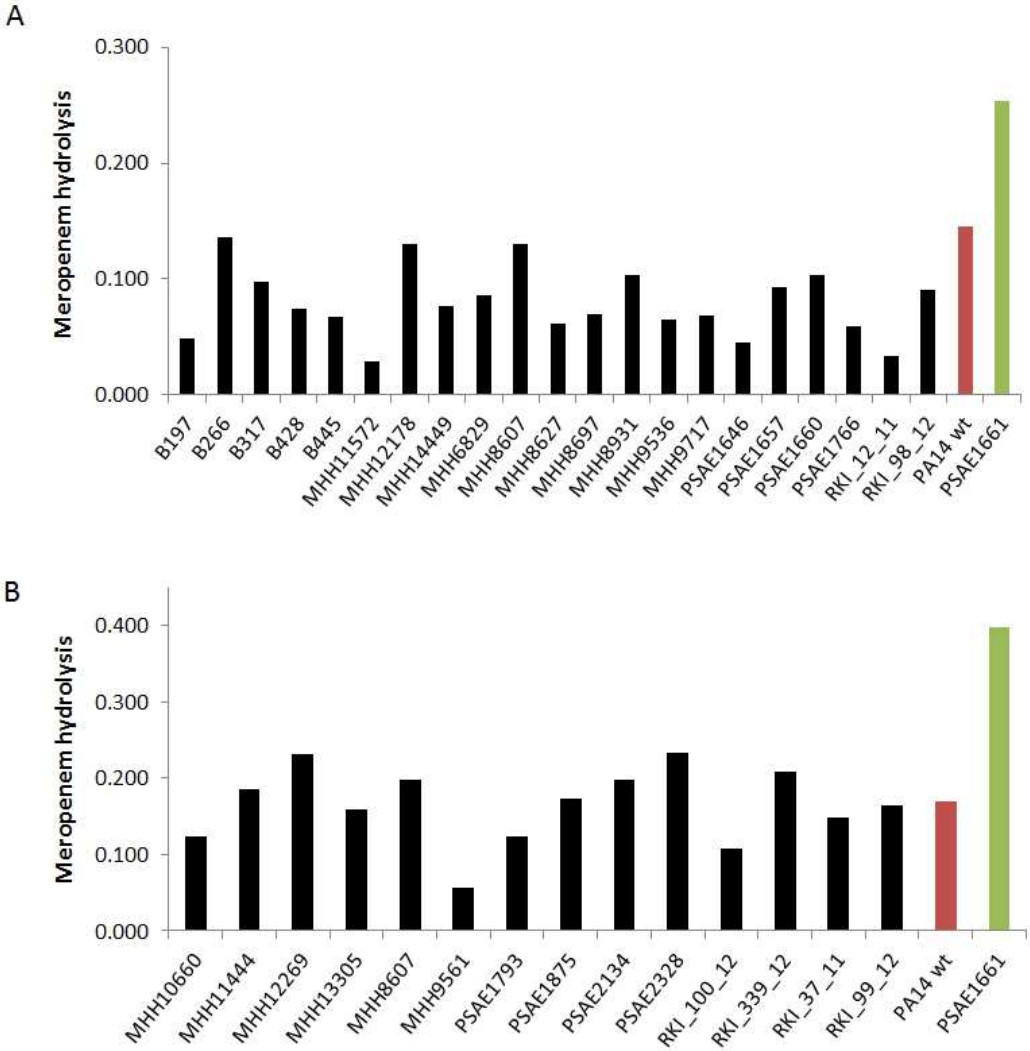

Figure 3.11 Carbapenemase activity of meropenem resistant strains.

Carbapenemase activity of all MEM-CAZ resistant clinical isolates in which bioinformatical approaches had not detected any presence of a corresponding enzyme was assayed by monitoring meropenem substrate hydrolysis spectrophotometrically at 297 and 300 nm. Depicted are the results from one representative experiment out of at least two biological replicates. PA14 wt was used as negative control, while the VIM-1 expressing PSAE1661 served as positive control. Of note, values in (A) were obtained from basic carbapenemase activity test, values in (B) from carbapenemase activity rescue. See methods section for details.

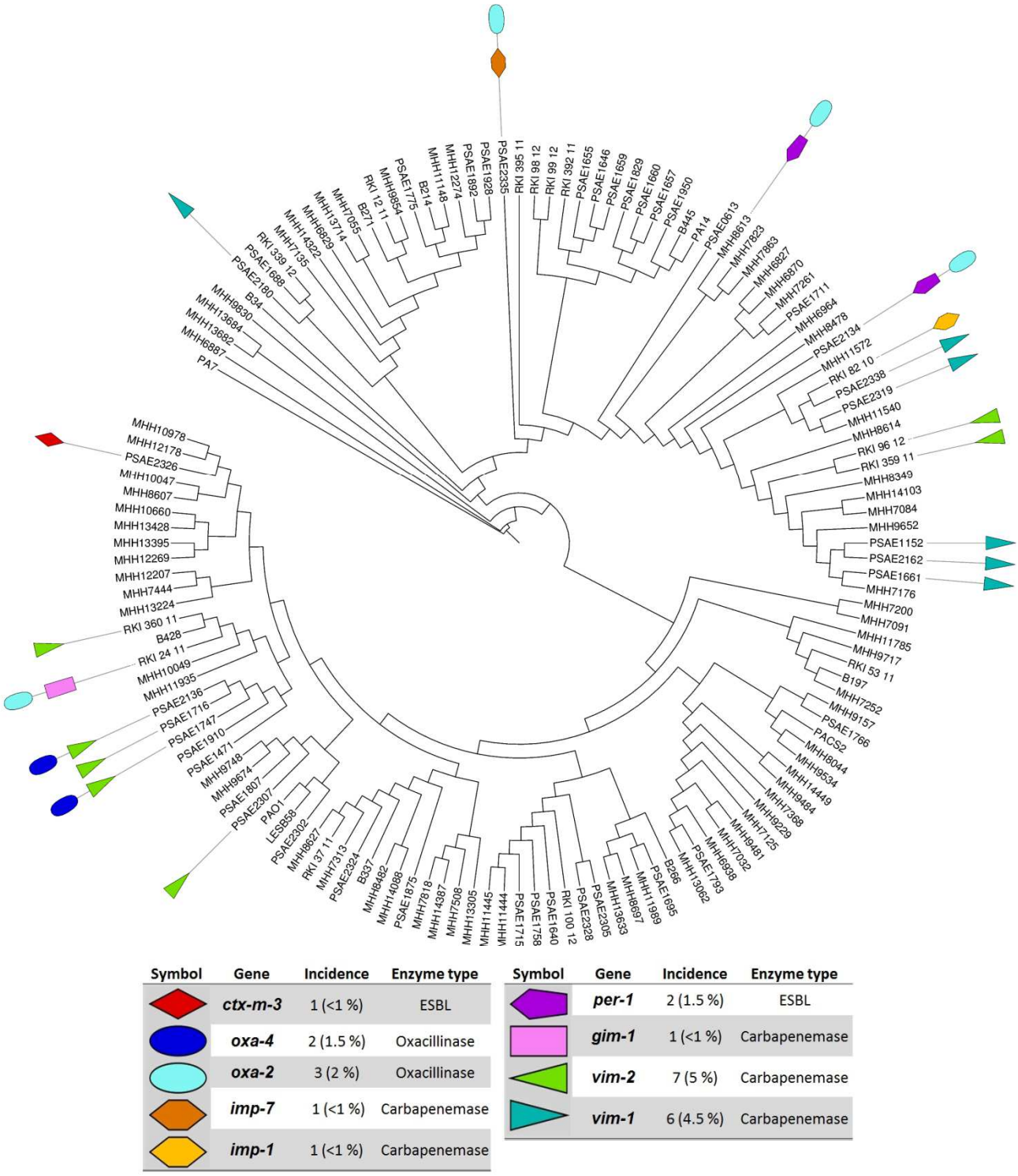

Symbol	Gene	Incidence	Enzyme type
	ctx-m-3	1 (<1 %)	ESBL
	oxa-4	2 (1.5 %)	Oxacillinase
	oxa-2	3 (2 %)	Oxacillinase
	imp-7	1 (<1 %)	Carbapenemase
	imp-1	1 (<1 %)	Carbapenemase

Symbol	Gene	Incidence	Enzyme type
	per-1	2 (1.5 %)	ESBL
	gim-1	1 (<1 %)	Carbapenemase
	vim-2	7 (5 %)	Carbapenemase
	vim-1	6 (4.5 %)	Carbapenemase

Figure 3.12 Distribution of β-lactamases among clonally unrelated clinical isolates.

The phylogenetic tree was constructed from all clonally unrelated clinical isolates (135 strains) using the same approach as previously described for generating the phylogenetic tree in Figure 3.9. A β-lactamase resistance enzyme dataset was integrated using iTOL. In total, nine different kinds of β-lactamases belonging to four enzymatic groups were detected in 19 isolates. β-lactamase distribution was widespread among isolates from diverse geographical origins and phylogenetic background. Six isolates contained two respective enzymes, however, in these cases one of the enzymes was an oxacillinase.

Various acquired β-lactamases (including broad- and extended-spectrum serine- (ESBL) and metallo-beta-lactamases (MBL)) were detected singular or in combinations in the individual clinical isolates (Figure 3.12). In total, we identified nine different β-lactamases (OXA-2 and 4, VIM-1 and 2, GIM-2, IMP-1 and 7, PER-1, and CTX-M-3) in overall 19 isolates (14 %) of which six contained two respective enzymes (4.4 %). In any of these cases, one enzyme was a MBL or ESBL, while the second enzyme belonged to the class D oxacillinases. Interestingly, only one isolate from the Hannover Medical School contained acquired β-lactamases.

Fourteen out of 45 meropenem (MIC ≥ 16 µg/ml) and 17 out of 61 ceftazidime (MIC ≥ 32 µg/ml) resistant isolates expressed a β-lactamase encoding gene. Additionally, two isolates with VIM-2 carbapenemases showed a MEM intermediate resistance phenotype. In general, the presence of β-lactamases was wide-spread and correlated in all cases with elevated MIC values against carbapenems and/or cephalosporins in dependence on the particular enzyme type.

Despite the occurrence of acquired β-lactamases, we also analyzed the presence of different types of integrase genes. To date, three classes of antibiotic-resistance mediating integrons have been described, based on the amino acid sequence of their IntI integrase gene (*intI1-3*) (29). No type 2 and 3 integrase genes were found, while type 1 integrase genes were detected in 49 clinical isolates. Integrase detection was defined positive, when either 90 % gene coverage or a combination of at least 70 % coverage together with *de novo* assembly and blast detection was observed. Interestingly, in all but two isolates with acquired β-lactamases integrase genes were expressed.

3.2.4 A systematic approach for comprehensive gene sequence and expression data analysis

With the scope of data whole transcriptome sequencing offers, the aim of this thesis was, besides the analysis of acquired genetic elements, not only to study individual core gene expression or previously discovered mutational hot spots, but to have a comprehensive, unbiased view at intrinsic gene regulation and sequence alterations as a whole and thereby investigate the global changes leading to a particular resistance phenotype. However, comprehensive and systematic analysis of such enormous amounts of data is challenging.

Overall, RNA-sequencing identified 1411 genes up- and 496 genes down-regulated at a median of at least two-fold over all clinical isolates compared to the PA14 wt. 2,349,331 SNPs were detected of which 19,358 led to amino acid exchanges (5575 genes) and 938 to intragenic stops (330 genes) (Figure 3.13).

Thus, we had to come up with an approach to facilitate the search for relevant genetic alterations and distinguish them from resistance phenotype irrelevant modifications.

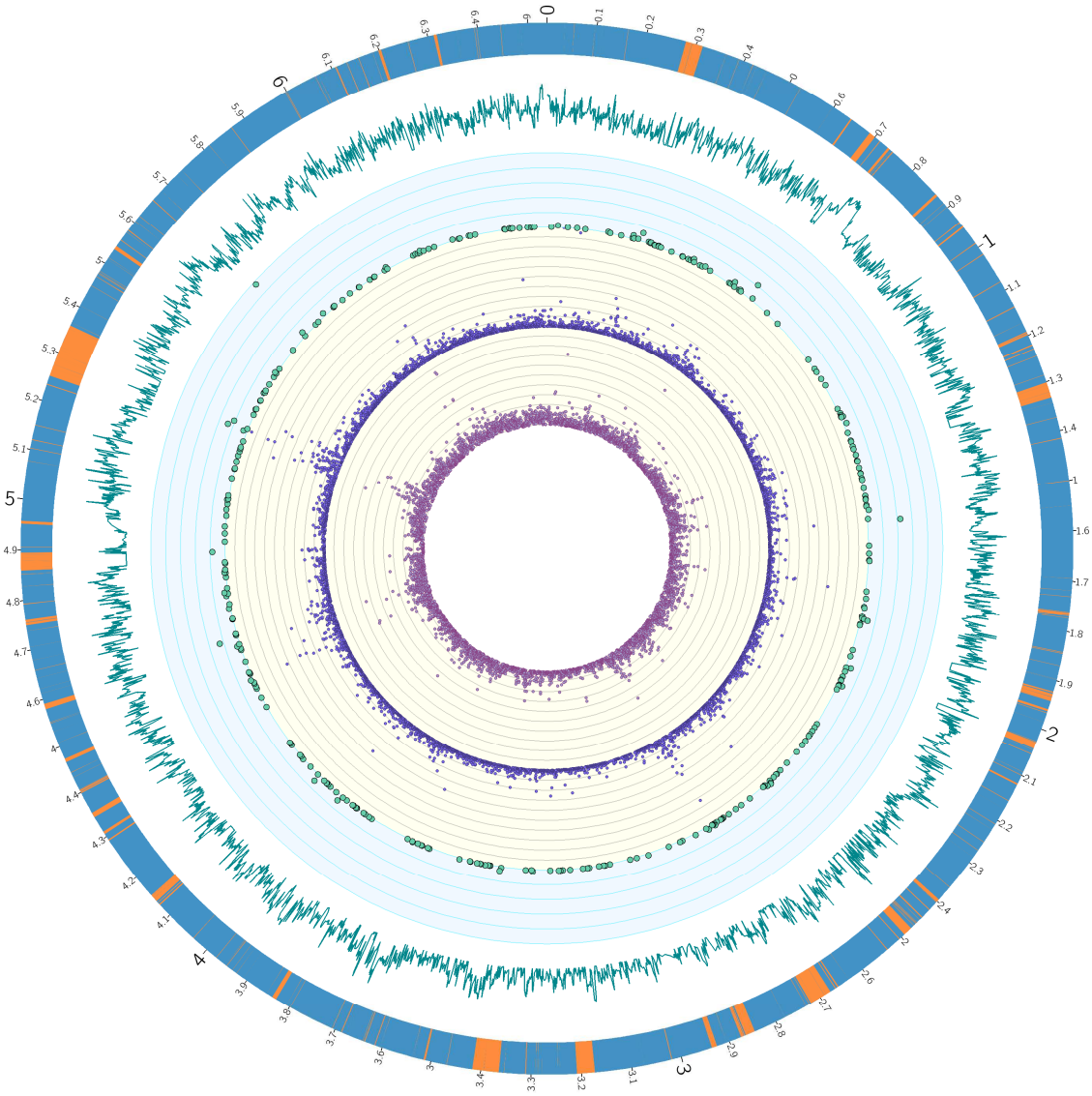

Figure 3.13 Global distribution of gene expression profiles, SNPs and intragenic stops.

Rings from outside to inside represent 1) *P. aeruginosa* pangenome using the core of PA14, as defined by Mathee and colleagues [217]. The core elements are depicted in light blue, the accessory elements in orange. 2) Median gene expression visualized from $\log_2$nrpk values (logarithmized reads per gene, normalized by gene lengths and DESeq size factor), colored in turquoise. 3) Intragenic stops summarized over all clinical isolates colored in dark green. 4) Non-synonymous SNPs over all clinical isolates, normalized by gene length depicted in dark blue. 5) Synonymous SNPs over all clinical isolates, normalized by gene length colored in purple. Data visualization was done using Circos [225].

3.2.4.1 Data storage and management within a web-based database facilitated genotype-phenotype correlations

Systematic and comprehensive analysis of RNA-seq data is challenging and makes data mining a topical issue. To cope with this challenge, we developed an online accessible database, the Bactome (https://bactome.helmholtz-hzi.de), which was programmed by Klaus Hornischer (Helmholtz Centre for Infection Research). Bactome comprises the gene expression levels, sequence composition, genomic location and annotation of the genes of all taxonomically different 135 clinical isolates, as well as further information on the origin, phenotype and resistance profile of each strain (Figure 3.14).

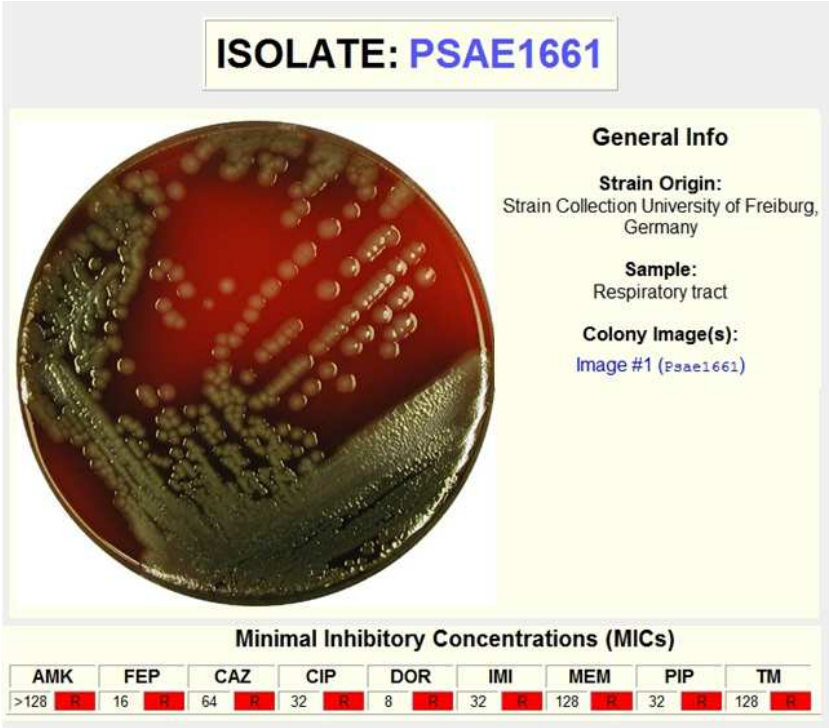

Figure 3.14 Display of additional strain specific information in Bactome.

Exemplified for the isolate PSAE 1661, Bactome comprises, next RNA-seq data, detailed information on the colony morphology, sample origin, including infection site, and the antibiotic resistance profile for each of the clinical isolates to facilitate phenotype-specific grouping as for example according to a particular antibiotic resistance phenotype.

Furthermore, using the information provided by the RNA-seq data in combination with R scripts, the database may perform a number of custom adjustable, statistical analyses in order to search for parallel evolved adaptive genetic variations that are distinct from unlinked neutrally evolving ones.

As a basis for the statistical comparison, the clinical isolates were compared in groups according to common phenotypic features, with one group exhibiting (positive) and the other opposing (negative) the particular phenotype, as for example resistance or susceptibility toward a particular antibiotic. The database then offers four options for comparative analysis: “SNPs position-wise”, “SNPs gene-wise”, “Stop codons”, and “Gene expression” (Figure 3.15).

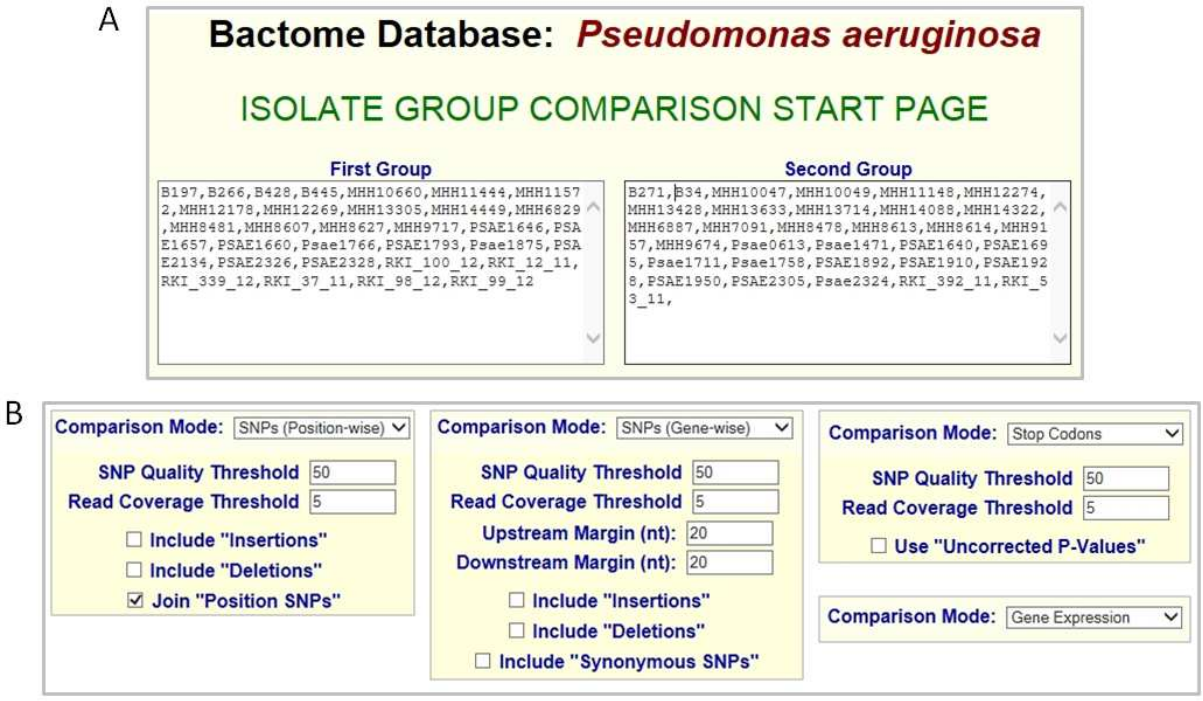

Figure 3.15 Custom adjustable group comparisons in Bactome facilitate the detection of genetic enrichments for pre-selected phenotypes.

A: As a basis for the statistical comparison, the clinical isolates need to be grouped according to whether they are positive or negative for a particular phenotypic feature. B: Next, Bactome offers 4 comparison modes to search for the accumulation of corresponding genetic markers. The groups can be analyzed for SNP clustering, either at distinct positions or within genes, unnaturally frequent intragenic stop codon formation or significant differential gene expression. Each comparison mode thereby comprises individual setup options, which include the additional incorporation of insertions and deletions, the choice between synonymous and non-synonymous SNPs, the analysis of upstream and downstream regions of genes, and the joining of non-synonymous SNP positions despite differing effects. Furthermore, stringency may be adjusted by varying minimal read coverage and SNP quality threshold (see text for further details).

The “SNPs position-wise” mode compares each nucleotide position of every strain in both groups to the PA14 reference and generates a matrix for all non-synonymous SNPs. For the “SNPs gene-wise” mode, the same is done, but merging all SNPs within one gene sequence, and with the option to include synonymous SNP to identify genes with high mutation rates despite possibly conserved

amino acid sequence. Besides, the gene-wise analysis can be extended to upstream and downstream sequences of each gene by defining the desired margins. Both comparisons contain the option of including insertion and deletions in the analysis, additionally to SNP mutations. Furthermore, a SNP quality threshold can be defined, as well as a minimal read coverage threshold to adjust stringency. A third option, the "Join Position SNPs" can be used in the position-wise mode, which, instead of handling them separately, joins non-synonymous SNPs occurring at the same nucleotide position but leading to different amino acid exchanges. This enables to detect mutational hot spots within a gene, without the necessity to have the same mutational mechanism involved.

In the "Stop codons" selection, intragenic stop codons are detected for every gene in every strain. For this purpose, a matrix is generated from comparing protein sequences corresponding to each gene for truncation. The respective protein sequences are created by introducing the previously detected SNPs (relative to the PA14 reference sequence) into the gene sequence of the PA14 reference strain and converting the nucleotide to the amino acid code.

Once the matrices have been generated, the accumulation of SNPs and intragenic stops in particular genes within one of the two defined groups of clinical isolates is calculated by Fisher's exact test.

To identify significant differential gene expression between the two groups, Student's T-test is performed on the normalized reads for every gene (nrpk), independent of the PA14 wt gene expression. Additionally, median expressions for every gene is calculated for both groups, together with the standard deviations and median differences between the groups, and any genes with a median of zero are excluded from the output list of significantly differentially regulated genes.

In addition to complete data output files, graphically displayed information is available for the top 30 hits obtained from each comparison. The kind of display of the information varies depending on the selected comparison mode (Figure 3.16). For SNPs and stops, bar charts indicate the distribution of the mutations within the groups and specify the amounts of detected mutations and wild type positions together with the number of strains for which the information could not be determined (e.g. due to insufficient read coverage at the selected position). Furthermore, a click on the gene name opens an integrative browser in which the median gene expression over all isolates for the selected gene is shown. Zooming in, one receives further information about the appearance and frequency of mutations within this gene, regarding all clinical isolates. The gene expression mode on the contrary displays the median gene expression calculated for the first (red) and second (blue) group by the transcript abundance for each nucleotide position within the selected gene.

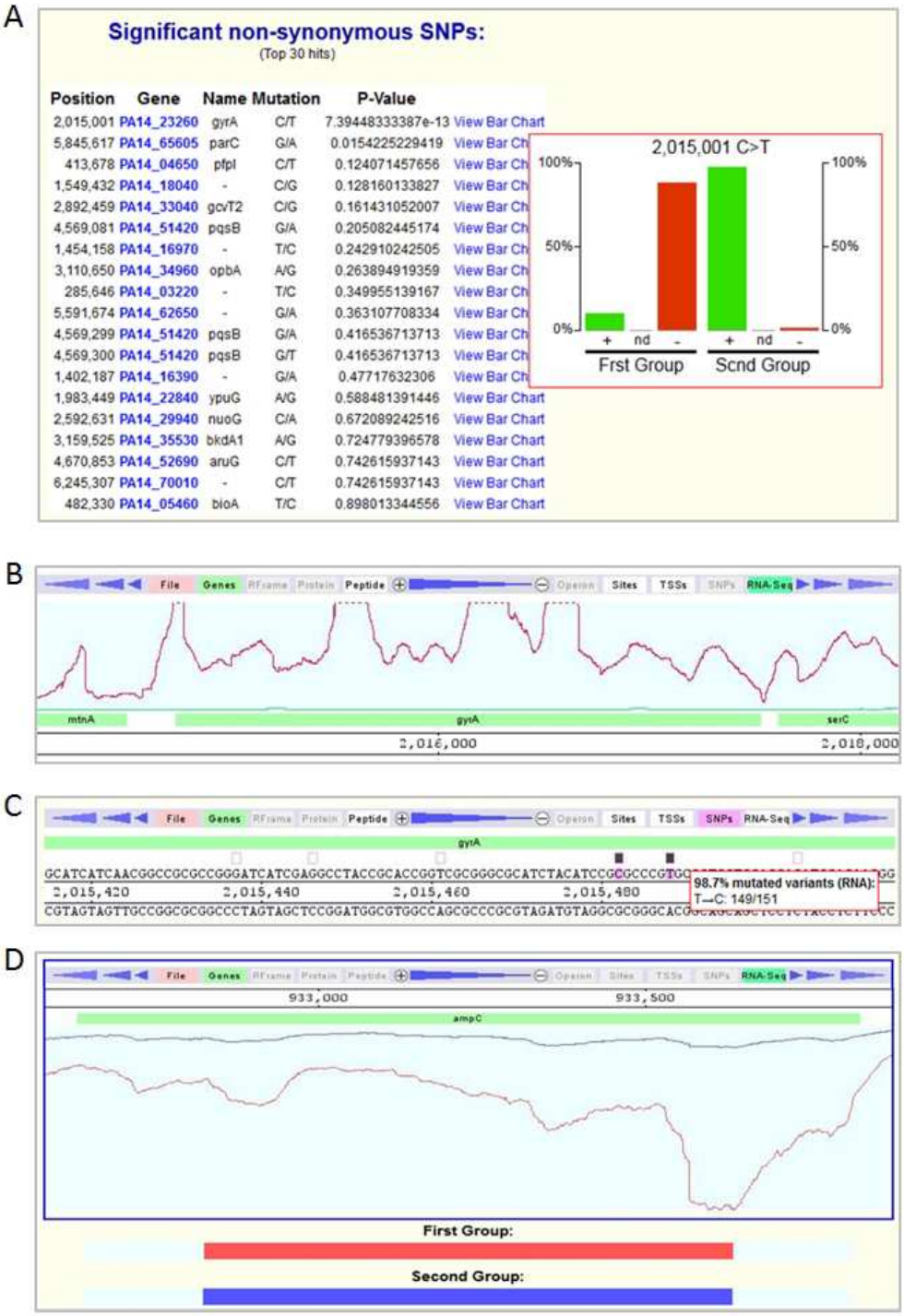

Figure 3.16 Graphical display of group comparison results in Bactome.

For the top 30 hits obtained from every group comparison, an additional graphical illustration of the results is available via Bactome. A: SNP and stop comparisons generate bar charts to depict the distribution of mutations with the amounts of strains in each group for which the mutation could be identified (+), not identified (-) or not determined due to low read coverage (nd). Clicking on the gene name opens an integrative browser which displays the median expression of the gene over all clinical isolates (B), or zoomed in, the occurrence and frequency of mutations over all clinical isolates (C). In gene expression comparison mode, this is replaced by a graph depicting the median gene expression for the first (red) and second (blue) group of the selected isolates.

In all cases, the adjusted p-values (padj; Benjamini-Hochberg (bh) corrected) are given to indicate significance of the findings. However, nonsense mutations that lead to premature translational stops are rare events across the genome. A summary of all intragenic stop sites of the sequenced clinical isolates is depicted in Figure 3.17. The majority of 5562 analyzed genes did not contain intragenic stops in any of the 135 clinical isolates and less than ten genes were stop-mutated in more than two isolates. Hence, it was not surprising that we did not identify any statistically significant accumulation of stops using adjusted p-values.

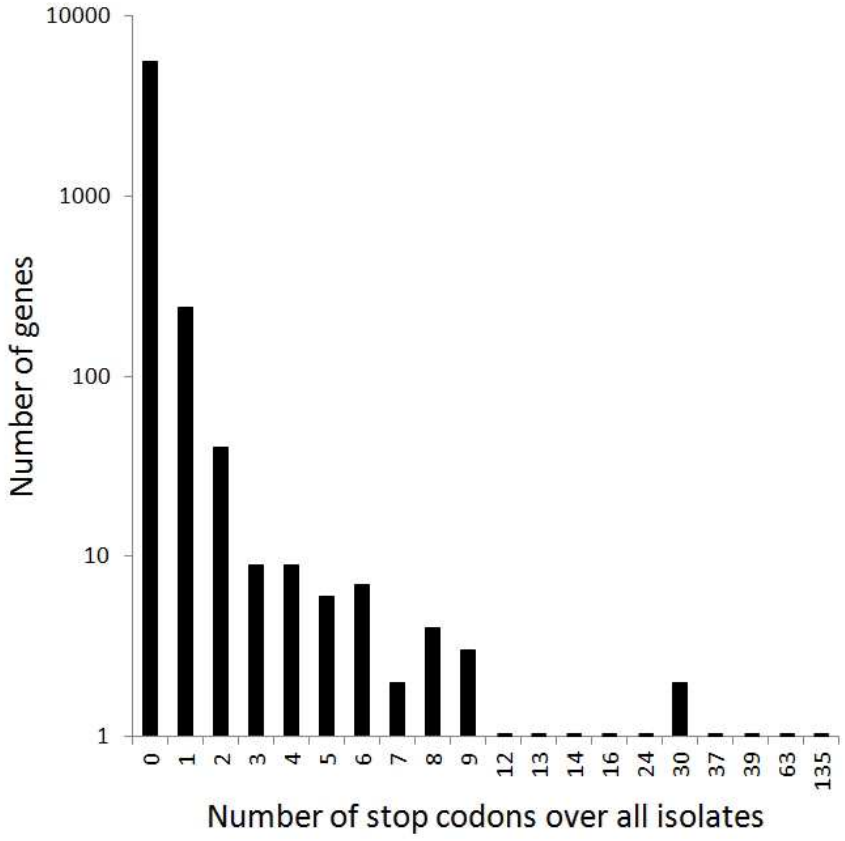

Figure 3.17 Transcriptome wide distribution of intragenic stop codons among clinical isolates.

Nonsense mutations are rare events. While the majority of 5562 analyzed genes did not contain any intragenic stops, less than 10 genes were mutated in three or more clinical isolates, and only one gene (*fdnG*) was mutated in all 135 isolates. In total, 330 nonsense mutations were identified over all isolates, corresponding to 0.04 % of the transcribed genes.

Despite the limitations of conventional statistics, we were nevertheless interested in investigating the possible role of nonsense mutations in the display of particular phenotypes. Thus, we decided to include the option of choosing the uncorrected p-values for the stop comparison mode to receive as well genes which would not be considered “significant” anymore after bh-correction. However, these uncorrected p-values should be interpreted as “significance score” in this case. To minimize false

positive results, additional permutation was performed for each dataset. This was also applied on the SNP and gene expression comparisons to gain more insight into the specificity and reliability of the chosen padj cut-offs. For the purpose of permutation, the expression values of each gene and SNP information of each position in the genome, respectively, were randomly rearranged within each strain. The resulting new matrices were then used as input for the respective statistical group comparisons. The minimal p-value obtained from ten permutations was considered as significance cut-off for the detected genes of the dataset, if it was lower than the usually used cut-off of 0.05.
For each group comparison, the option to choose between using the original matrices or permutated ones for the statistical calculation was implemented as selectable feature in Bactome.

3.2.5 Identifying intrinsic β-lactam resistance markers via unbiased phenotype-genotype correlation studies

With the possibilities of Bactome data management and the embedded tools for statistical analysis, we could now start a comprehensive search for core genetic variations that are connected to antibiotic resistance phenotypes. For this purpose, the 135 clinical isolates were grouped into “non-susceptible” and “susceptible” (according to CLSI guidelines [15]) towards the β-lactam antibiotics ceftazidime (CAZ) and meropenem (MEM), respectively. In order to focus on intrinsic resistance mechanisms, those isolates that expressed acquired resistance-conferring genes were excluded from the list of “non-susceptible” isolates, which resulted in 57 CAZ and 73 MEM non-susceptible isolates that were investigated for parallel evolved genetic variation regarding I) the enrichment of SNPs at a distinct position, II) the enrichment of SNPs within a particular gene, III) the enrichment of intragenic stop codons and IV) differentials in gene expression levels.

3.2.5.1 Global gene expression analysis emphasizes the importance of *ampC* expression in CAZ resistance and suggests the selection of cross-resistances

Whereas no significantly SNP enriched positions or genes could be detected, the group comparison of non-susceptible (n=57) versus susceptible (n=59) CAZ isolates revealed a list of four genes with accumulations of nonsense mutations and two significantly differentially regulated genes, both of which were up-regulated in the CAZ non-susceptible group (Table 3.3).
As the most significantly regulated gene, the chromosomally encoded β-lactamase *ampC* was identified with a p-value of 1.12E-07 (in contrast, the lowest p-value obtained after permutation was as high as 1.19E-01). This finding was not unexpected, since overexpression of *ampC* is known to be the most important intrinsic CAZ resistance mechanism. However, it emphasizes that determination of *ampC* expression could be used as a very suitable marker for molecular resistance detection in this

case. The second lowest p-value was obtained by PA14_10780, a gene directly downstream of *ampC*, producing an unknown, hypothetical protein. Most likely PA14_10780 itself does not actively contribute to CAZ resistance, but is merely up-regulated due to the preceding *ampC* overexpression.

Table 3.3 Group comparison for CAZ susceptible and non-susceptible isolates.

While the expression of two genes was significantly differentially regulated in the non-susceptible group of isolates (expression comparison mode) and four genes exhibited an accumulation of nonsense mutations (stop comparison mode), respectively, no significant enrichments were seen for position-wise and gene-wise SNP comparison mode with parameters minimal SNP score threshold 50 and minimal read coverage 1.

Antibiotic	Isolates [n]		Expression comparison [a]		Stop comparison [b]	
	Susceptible	Non-susceptible	Gene	Enrichment (padj)	Gene	Enrichment (pval)
CAZ	59	57 (19)*	*ampC*	4.85 (1.12E-07)	PA14_21520	12 (5.57E-03)
			PA14_10780	2.32 (2.94E-03)	*oprD*	2.3 (7.17E-03)
					mexB	11 (1.22E-02)
					PA14_03180	11 (1.29E-02)

* Isolates with acquired resistance enzymes which were excluded from the statistical group comparison

Enrichment = fold enrichment in the non-susceptible group

[a] Expression was analyzed as logarithmic, normalized reads per kilobase (lnrpk) values for every gene, giving the median, corresponding standard deviation (SD) and median difference between the two groups for each gene together with the adjusted p-value (padj) obtained from T-test. Genes were filtered for padj < 0.05 and median differences > 1, and genes with any median = 0 or SD > median were excluded.

[b] Nucleotide positions of all transcripts were analyzed for nonsense mutations and significance was determined by Fisher test, including all SNPs with a SAMtools quality score of at least 50. Shown are all hits with an uncorrected p-value of < 0.05.

In addition to two hypothetical genes, the porin gene *oprD,* and *mexB*, coding for a component of the MexAB-OprM efflux pump, were much more frequently stop mutated in the CAZ non-susceptible group. For all genes, p-values ranged between 1.29E-02 and 5.57E-03, while the lowest p-value calculated from ten permutated datasets was 1.15E-01, which confirmed a low potential of false positive hits within our list. However, the results were surprising, as MexAB-OprM has been described to enhance β-lactam efflux and thus promote non-susceptibility. One reason could be that efflux pumps play a role in initial, first step antibiotic tolerance rather than mediating high level antibiotic resistance. Thus, as soon as additional, more effective resistance mechanisms are employed, efflux overexpression might no longer provide advantages for the bacteria.

The second surprising finding within the list was the porin gene *oprD*, whose absence is primarily associated with carbapenem resistance, as CAZ cell entry via *oprD* is only marginal (see section 3.2.7). This result emphasizes the tight interconnections of cross resistance evolution in clinical isolates.

Interestingly, when we compared CAZ susceptible with only resistant variants (excluding intermediate resistant isolates), we additionally found a significant differential expression of *mexE*, a component of the MexEF-OprN multidrug efflux pump (Table 3.4). Curiously, overexpression of the MexEF-OprN pump has not been associated with CAZ resistance so far, but with an increased MIC of the fluoroquinolones CIP and levofloxacin (LVX) and a slightly increased MIC of MEM (via a MexT dependent repression of *oprD*) [66,226,227]. However, the transcriptional regulator AmpR has been described to be involved in the regulation of both, *ampC* and *mexEF-oprN,* as well as further genes involved in efflux, virulence and secretion [105,228,229]. Thus, we had a separate look at *ampR* expression and could indeed find the gene to be transcribed less in the resistant as opposed to the susceptible group of isolates, albeit only 1.48-fold (p-value 0.004). Since AmpR does not only regulate the expression of *ampC* but also of the efflux pump *mexEF-oprN*, this finding stresses once more the easy development of cross-resistances among clinical isolates that might be selected through antibiotic treatment pressure, highlighting the need for more targeted diagnostics and drug use.

Table 3.4 Group comparison for CAZ susceptible and resistant isolates for significant gene regulation.

Expression data are shown as logarithmic, normalized reads per kilobase (lnrpk) values for every gene, giving the median, corresponding standard deviation (SD) and median difference between the two groups for each gene, together with the adjusted p-value (padj) obtained from T-test. Genes were filtered for padj < 0.05, median differences value < 1, and genes with any median = 0 were excluded.

Gene	Padj	CAZ resistant		CAZ susceptible		Difference
		Median	SD	Median	SD	
ampC	3.59E-08	7.69	2.51	2.60	2.35	5.09
PA14_10780	2.52E-03	6.13	2.49	3.69	2.01	2.44
PA14_61270	8.64E-03	4.92	0.98	3.60	1.51	1.32
PA14_52490	1.12E-02	5.50	1.46	4.21	1.97	1.29
PA14_56090	1.94E-02	6.48	0.96	5.43	1.08	1.05
PA14_40660	3.42E-02	2.74	1.70	1.44	1.34	1.30
PA14_28210	3.74E-02	5.20	1.03	3.76	1.46	1.45
mexE	4.21E-02	2.85	1.89	1.39	1.72	1.45
PA14_31730	4.33E-02	4.72	1.46	3.34	1.23	1.37
pvdD	4.98E-02	0.42	0.95	2.04	1.14	-1.62

3.2.5.2 *ampC* expression as a molecular marker for CAZ resistance

As *ampC* was the only global expression marker found in the CAZ non-susceptible group, we were further interested in evaluating the potential of this gene as a future molecular marker for CAZ resistance. As shown in Figure 3.18, there was a clear correlation (r=0.638) between increased *ampC* gene expression and elevated CAZ MIC values ranging from 0.5 to 64 µg/ml. Only in rare cases, when extraordinary high resistance levels of MIC values above 64 µg/ml had been observed, additional mechanisms seemed to play a role. Furthermore, the majority of CAZ resistant (35/36) and intermediate-resistant (8/13) isolates exhibited high (>3 $\log_2$FC) *ampC* expression values, while most (49/56) susceptible variants in turn showed only slight or no constitutive overexpression. Only seven isolates (5 %) exhibited strongly increased *ampC* expression (> 5 $\log_2$FC) compared to reference strain PA14, but nevertheless showed a CAZ susceptible phenotype. Interestingly, all of them harbored mutations within the *ampC* gene. Particularly significant hereby were deletions of one to 10 nucleotides, additionally confirmed by Sanger sequencing, which led to frameshifts and thus most likely abolished functional protein production.

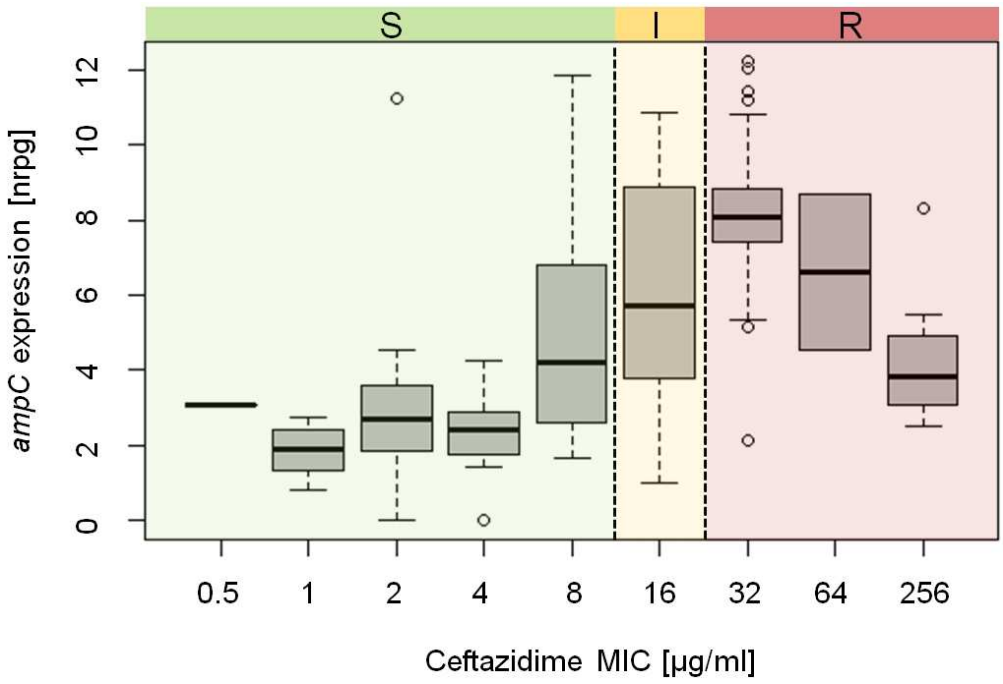

Figure 3.18 Correlation of *ampC* expression and CAZ MIC among clinical isolates.

Correlation was calculated from the *ampC* gene reads normalized by total reads per strain (nrpgs) in R from a total of 116 isolates (19 isolates which harbored acquired resistance conferring enzymes towards CAZ were excluded from the original panel). Box plots indicate 0.25 and 0.75 quartiles and the median (bold line). The sample minima and maxima are shown as whiskers with outliers depicted as open circles. Antibiotic susceptibility was classified in susceptible (S), intermediate (I), and resistant (R), according to CLSI guidelines.

In order to use *ampC* overexpression as a resistance marker, a defined threshold had to be determined to distinguish between CAZ susceptible and non-susceptible strains. For the calculation of this threshold, a receiver operating characteristic (ROC) curve was used (Figure 3.19). The correlation specifying area under the curve (AUC) was 0.889, when isolates with acquired CAZ resistance conferring enzymes and non-functional *ampC* had been excluded. Although it was not possible to define one particular gene expression threshold which strictly separated susceptible and non-susceptible strains, we could detect 63 % non-susceptibility (true positives) without including any false positives at an *ampC* expression threshold of 5.0 (log_2FC). At an *ampC* expression threshold of 3.9 (log_2FC), even identification of 75 % non-susceptibility was achieved while remaining with a tolerable amount of less than 5 % likewise detected susceptible strains (false positives).

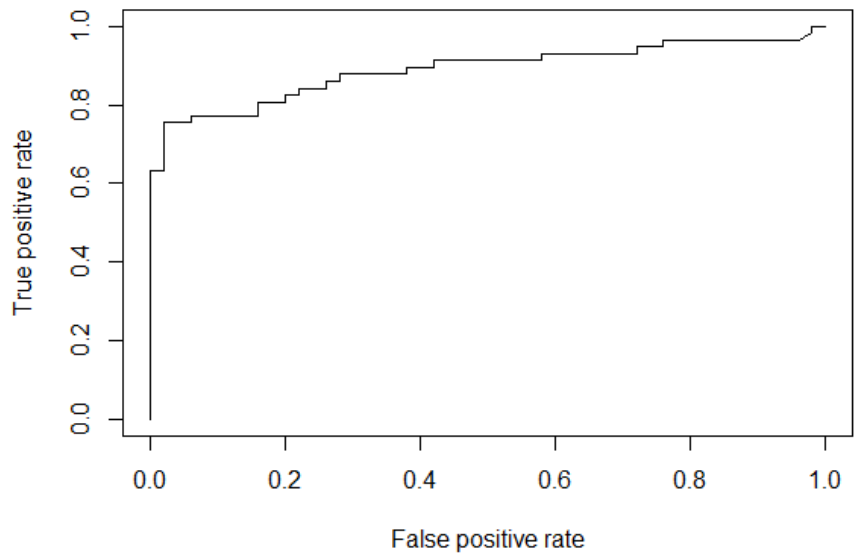

Figure 3.19 ROC correlation of *ampC* expression and CAZ resistance phenotype.

Calculation of the receiver operating characteristic (ROC) curve for the correlation of *ampC* expression (log_2FC) and CAZ susceptibility or non-susceptibility was performed from 107 isolates (isolates with acquired CAZ resistance conferring enzymes and strains with presumably non-functional AmpC due to severe mutational gene disruption were excluded). Correlation was determined by calculating the area under the curve (AUC): 0.889. We could detect 63 % non-susceptibility (true positives) not including any false positives at an *ampC* expression threshold of 5.0 (log_2FC). 75 % non-susceptibility was achieved at an *ampC* expression threshold of 3.9 (log_2FC), while remaining with less than 5 % likewise detected susceptible strains (false positives). On the other hand, an *ampC* expression threshold of 1.2 (log_2FC) allowed detection of > 90 % true positives but also included a range of 42 % false positives.

3.2.5.3 Global screen for nonsense mutations highlights the link of MEM resistance to functional OprD

When we compared groups of MEM susceptible and non-susceptible isolates with each other to find significant genetic alterations, we detected *oprD*, which was both down-regulated in the non-susceptible group and frequently nonsense mutated with p-values of 4.19E-02 and 1.40E-01, respectively. Furthermore, the gene *gbuA* exhibited slightly increased expression in the non-susceptible group (p-value 2.65E-02; Table 3.3). Though, it has to be noted that p-values from ten permutation of this dataset reached 4.00E-02 for significant differential gene expression and 1.43E-01 for enrichment of nonsense mutations. Thus, all obtained values were just on the border of the defined significance thresholds.

Table 3.5 Group comparison for MEM susceptible and non-susceptible isolates.

The statistical comparison between groups of MEM susceptible and non-susceptible isolates identified only one gene enriched for nonsense mutations in the non-susceptible group and two significant differentially expressed genes. SNP comparison mode (both, gene-wise and position-wise) did not show any significant hits with parameters minimal SNP score threshold 50 and minimal read coverage 1.

Antibiotic	Isolates [n]		Expression comparison [a]		Stop comparison [b]	
	Susceptible	Non-susceptible	Gene	Enrichment (padj)	Gene	Enrichment (pval)
MEM	46	73 (16)*	*gbuA*	1.22 (2.65E-02)	*oprD*	1.45 (1.40E-01)
			oprD	- 1.79 (4.19E-02)		

* Isolates with acquired resistance enzymes which were excluded from the statistical group comparison

Enrichment = fold enrichment in the non-susceptible group

[a] Expression was analyzed as logarithmic, normalized reads per kilobase (lnrpk) values for every gene, giving the median, corresponding standard deviation (SD) and median difference between the two groups for each gene together with the adjusted p-value (padj) obtained from T-test. Genes were filtered for padj < 0.05, median differences > 1 and genes with any median = 0 or SD > median were excluded.

[b] Nucleotide positions of all transcripts were analyzed for nonsense mutations and significance was determined by Fisher test, including all SNPs with a SAMtools quality score of at least 50.

However, a false positive detection is at least in the case of *oprD* rather unlikely as the *P. aeruginosa* outer membrane protein OprD is a 443 amino acid long porin, specific for the uptake of basic amino acids, small peptides and analogues such as the carbapenem antibiotics imipenem and meropenem [80]. Consequently, a decreased expression of functional OprD is expected to confer carbapenem resistance [81,90,96]. The significance of *gbuA*, coding for a guanidinobutyrase which is involved in the conversion of alanine to succinate, still requires further investigation. However, as OprD and

GbuA are both regulated in connection to arginine availability [86,99,230], a coincidental correlation is possible.

Figure 3.20 A depicts the distribution of premature translation termination mutations in *oprD*. These mutations occurred generally throughout the sequence, as opposed to single amino acid exchanges, which were mostly restricted to either the periplasmic hinge or the surface associated loops (Figure 3.20 B, C).

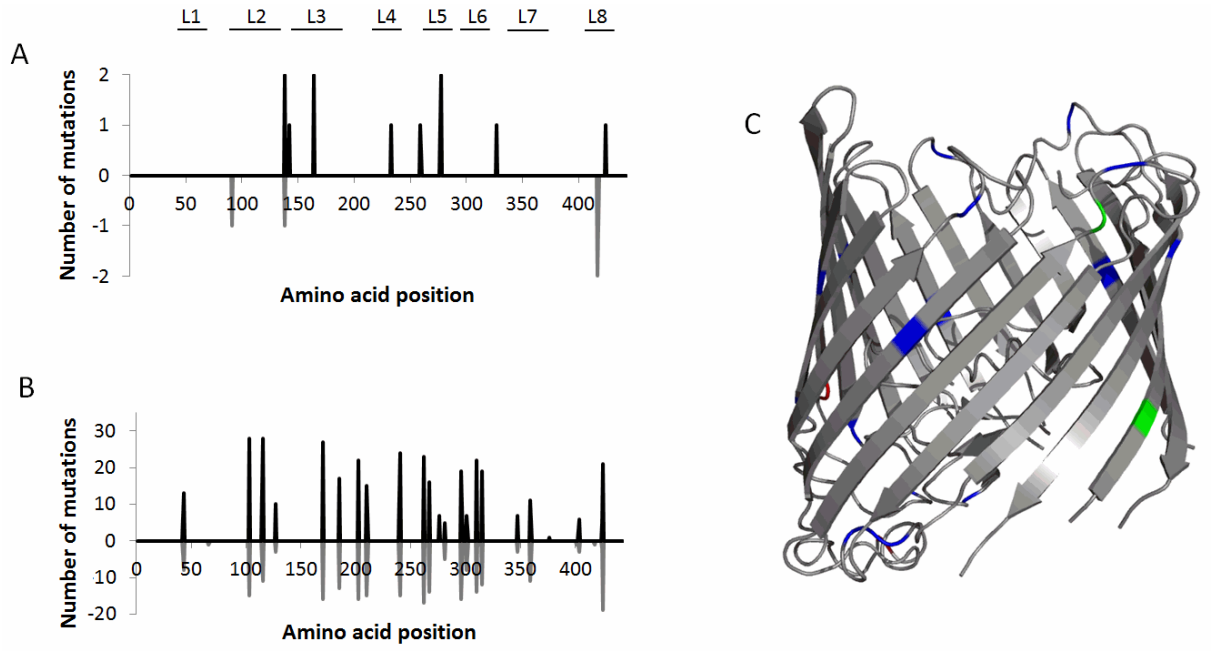

Figure 3.20 OprD sequence modifications by non-synonymous SNPs.

A: Nonsense mutation sites indicating premature translational stops. B: Total amounts of SNPs leading to single amino acid exchanges. The x-axis highlights the positions of the modified amino acids relative to protein length. Mutations in MEM resistant (n = 46) isolates are depicted above the x-axis (black), amino acid exchanges in MEM susceptible (n = 32) strains below the x-axis (grey). The positions of the eight external loops are labeled L1 to L8 (according to Huang *et al.* [92]). C: SNPs (excluding stop sites) mapped to the tridimensional structure of PAO1 OprD based on the model by Biswas *et al*. [93]. SNPs exclusively found in the MEM susceptible isolates are labeled in green, those found in the MEM resistant in red and those found in both in blue.

Furthermore, there was no systematic accumulation of SNPs depending on the resistance phenotype. MEM resistant and susceptible isolates exhibited almost identical mutation patterns due to natural sequence variations among susceptible *P. aeruginosa* variants (e.g. PAO1, LESB58). Altogether, 25 different positions with frequent single amino acid exchanges were identified. While the number of SNPs was equally distributed among the different MEM resistance phenotypes, the amount of strains with stop codons in *oprD* significantly decreased from resistant (11) and intermediate (23) to

susceptible (4) variants, with no more than one stop site per strain. Interestingly though, there was an unexpected accumulation of the Q327* mutation in 14 intermediate resistant strains from the Hannover Medical School.

Combining sequence and expression information, there was a clear correlation (τ=0.434) between the presence of nonsense mutations in *oprD* and/or a strong transcriptional repression (< -3 log_2FC) and elevated MEM MIC values. Eight out of 31 (26 %) MEM resistant and 17 out of 42 (40 %) intermediate resistant isolates harbored nonsense mutations within *oprD*, while 18 (58 %) MEM resistant and 16 (38 %) intermediate resistant isolates showed strong gene repression. Both mechanisms overlapped in seven (22 %) and three (7 %) cases for resistant and intermediate resistant isolates, respectively.

To evaluate how gene inactivation and repression correlated to protein expression, we performed immunoblot analysis with an OprD specific antibody and compared the actual protein levels of a total of 63 isolates of different MEM resistance phenotypes with the expression and sequence information obtained from RNA-sequencing. Remarkably, all tested nonsense mutations led to an abolishment of efficient translation (Figure 3.21).

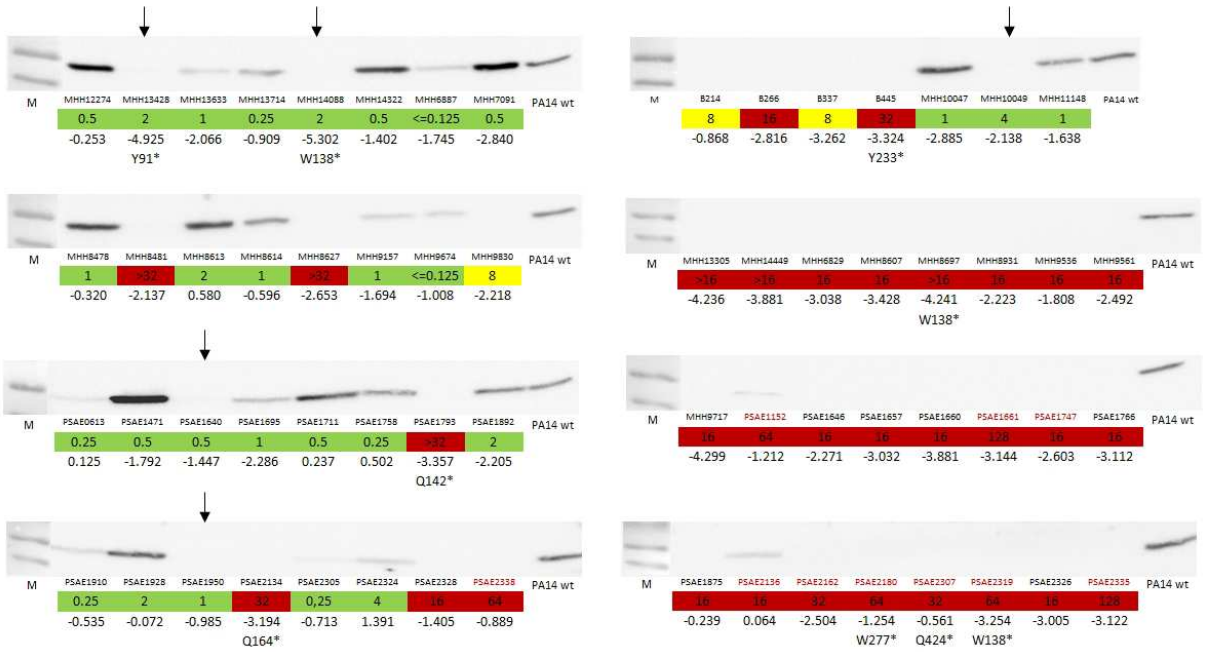

Figure 3.21 Correlation of *oprD* expression and OprD protein abundance with resistance against meropenem.

OprD protein levels were detected by Western blot analysis with a polyclonal anti-OprD antibody in 63 clinical isolates exhibiting various MIC values (in µg/ml) (MEM-resistant = red, intermediate = yellow, susceptible = green), *oprD* expression (shown as log_2 fold change) and amino acid stop mutations (e.g. Q165*) are depicted underneath. Additionally acquired β-lactamases leading to MEM resistance are highlighted in red font of the isolate name. Arrows indicate susceptible strains with a complete lack of OprD protein. M = PageRuler prestained protein ladder.

Furthermore, Western blot analysis revealed no or only very faint protein bands in any of the tested intermediate (n=3) or resistant (n=32) strains.

Whenever there was a faint band remaining, the respective isolate possessed additional, acquired resistance enzymes (PSAE 1152, *vim-1*; PSAE 2136, *vim-2*). The tested susceptible strains (n=28) on the other hand contained clearly visible amounts of OprD. However, there was an exception of a few isolates that were MEM susceptible despite the finding that no OprD protein was detectable.

Interestingly, there was only partial correlation between the *oprD* mRNA levels and protein production. In several cases, the amount of OprD protein was higher than in the PA14 reference strain, despite transcriptional down-regulation. On the other hand, numerous isolates with a complete lack of functional protein did not show significant transcriptional repression or sequence modification. One reason could be that OprD is subject to frequent, possibly MexT mediated, posttranscriptional regulation, as has been described before in PAO1 [106].

Moreover, we were particularly surprised to find four clearly susceptible (MIC 0.5-4 µg/ml) isolates with apparent premature translational stops (Y91*, W138*, W417*). We additionally visualized outer membrane proteins of these four isolates on Coomassie stained SDS gels, which is a less specific, but more sensitive approach (Figure 3.22).

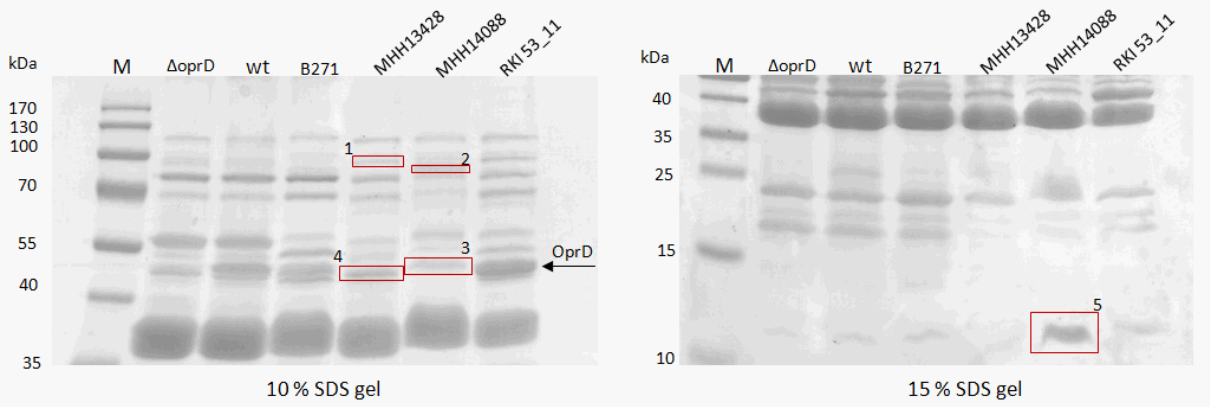

Figure 3.22 Outer membrane analysis of MEM susceptible isolates with *oprD* nonsense mutation.

Outer membranes of five susceptible clinical isolates with premature translational stops Y91* (MHH13428), W138* (MHH14088) and W417* (B271, RKI_53_11), the PA14 wt and PA14Δ*oprD* mutant were extracted, solubilized in SDS sample buffer and loaded to SDS-polyacrylamide gels (10 % or 15 %, respectively). MHH13428 and MHH14088 clearly did not produce functional OprD protein (standard (M) = PageRuler prestained protein ladder; OprD at 49 kDa). Protein bands cut for mass spectrometric identification are framed in red.

While the two isolates with W417* mutations exhibited faint protein bands at 49 kDa, which may be OprD, MHH13428 and MHH14088 clearly did not contain any matching protein band. This very

interesting observation has been made before by a Spanish multicenter study analyzing carbapenem intermediate and susceptible patients' isolates of *P. aeruginosa* from bacteremia [97]. To receive further information on how MEM might enter the bacterial cell on alternative ways, if it does not use OprD, the composition of selected protein bands cut from the coomassie stained SDS gel was analyzed by mass spectrometry. As there was no commonly differentially expressed protein band among the OprD deficient, MEM susceptible isolates, five unusually overexpressed sections compared to the PA14 wt were chosen (marked in red).

Table 3.6 Mass spectrometric identification of differentially expressed proteins in OprD negative, MEM susceptible clinical isolates.

Shown are the best identification hits for every protein band after comparison to PA14 and PAO1 specific SwissProt database entries.

Sample	Accesion no.	Proteinfunction	Name	Locus tag
1	116050339	Ferripyoverdine receptor	FpvA	PA14_33680
2	116052985; 15600030	Putative outer membrane protein (possibly Fe transport)	-	PA14_63960; PA4837
3	116050756; 15597956	Outer membrane porin, OprD family	OprQ / OprE3	PA14_28400; PA2760
4	116050756; 15597956	Outer membrane porin, OprD family	OprQ / OprE3	PA14_28400; PA2760
5	15598049	Outer membrane lipoprotein OprI precursor	OprI	PA2853

As shown in Table 3.6, mass spectrometric analyses identified the extracted bands as containing the ferripyoverdine receptor FpvA (1), a putative outer membrane protein which is possibly involved in iron transport (2), and the lipoprotein OprI (5). More interestingly however, the porin OprQ was detected in both isolates, which belongs to the OprD outer membrane porin family. However, the *oprQ* gene did not show increased expression in these isolates compared to the PA14 wt, posing the possibility that the OprQ protein band may have only been concealed by OprD in the OprD positive isolates. Thus, while OprQ might hint at alternative carbapenem entry, though this remains to be validated experimentally, clearly larger numbers of clinical isolates will be necessary to completely understand the regulatory and compensatory mechanism that may counter-balance the lack of OprD and contribute to the regained antibiotic susceptibility.

3.2.6 Penicillin binding proteins show high sequence variability, but their role in β-lactam resistance remains unclear

Although modifications in penicillin binding proteins (PBPs) are well known β-lactam resistance mechanisms in Gram-positive bacteria [52], their role in the resistance of Gram-negatives is still

largely unclear. However, is has been demonstrated that inactivation or lack of particular PBPs can indirectly affect β-lactam resistance via up-regulation of intrinsic β-lactamases [155,231,232].
We therefore wanted to investigate the role of PBPs in *ampC* expression regulation and searched for mutational patterns connected to β-lactam resistance.

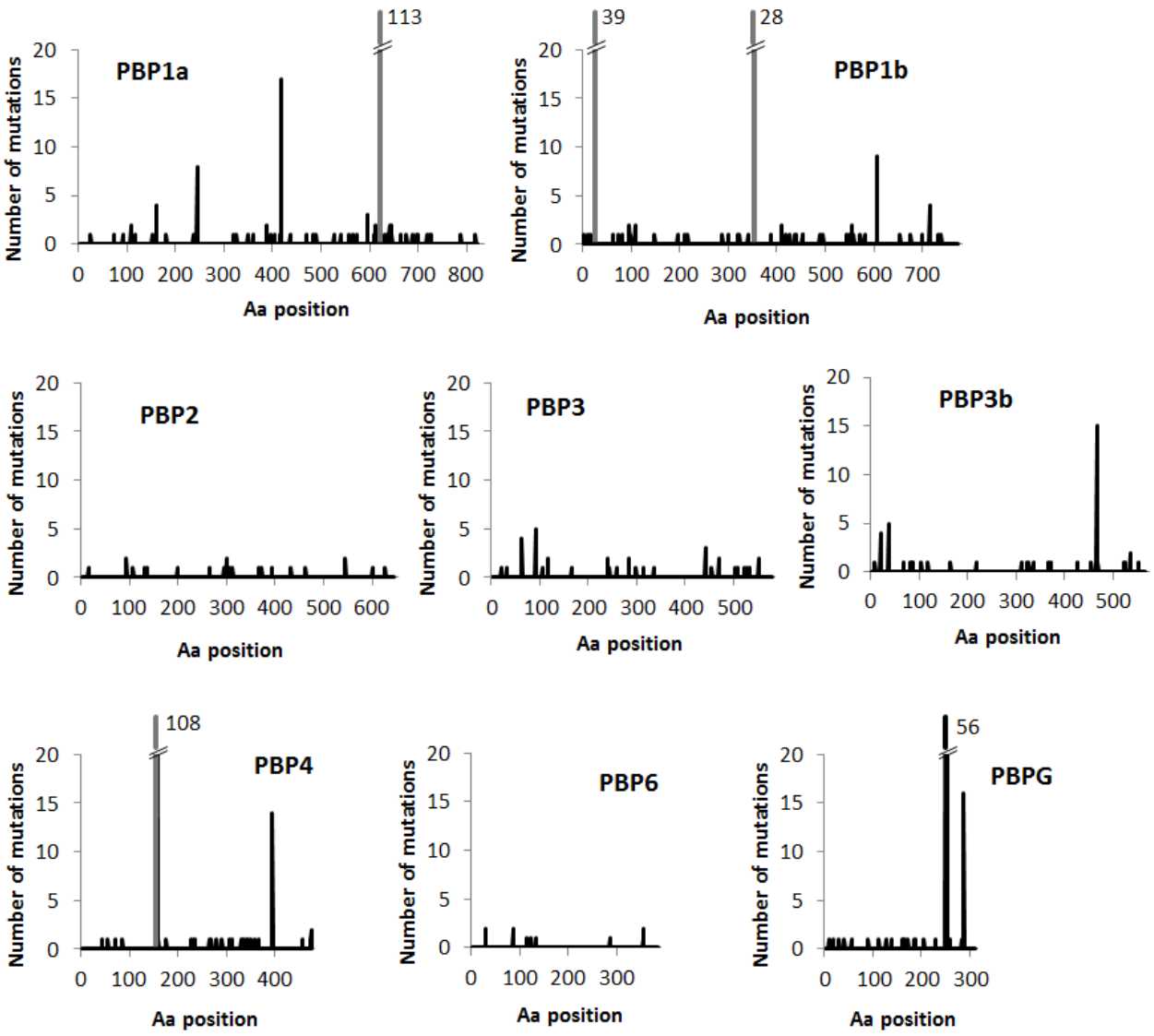

Figure 3.23 PBP sequence modification by SNPs leading to single amino acid exchanges.

The x-axis (relative to protein length) highlights the positions of the modified amino acids (Aa). Sequence variations between the reference strain PA14 and the common laboratory strain PAO1 (equally susceptible to β-lactam treatment) are depicted in grey.

29 strains exhibited major sequence disruptions (insertions and/or deletions) in any of the investigated PBPs. Interestingly, out of those, 20 isolates of wide geographical distribution contained the same three nucleotide deletion in the gene *ponA*, coding for a PBP1a with a missing proline at

amino acid position 616. The remaining nine strains revealed frameshifts in *pbpA* (PBP2), *dacB* (PBP4), *dacC* (PBP6), *mrcB* (PBP1a), *ftsI* (PBP3) and *pbpG*, respectively. However, possibly due to compensatory mechanisms, there was no correlation between loss of function of a particular PBP and increased *ampC* expression among our subset of clinical isolates (data not shown).

Despite only very few severe sequence modifications, we found a large variety of non-synonymous SNPs in any of the strains and PBPs, leading to a range of 2 % (PBP6) to 9 % (PBPG) of altered amino acids in total for the respective protein. SNPs were mostly equally distributed within the genes with a few exceptional accumulations at specific positions in PBP1A, PBP1B, PBP4 and PBPG (Figure 3.23). However, these positions with high mutation rates (> 20 isolates) indicated natural sequence variations among β-lactam susceptible *P. aeruginosa* variants. Additionally, PBP sequences of resistant and susceptible isolates were mutated equally frequently.

Thus, PBPs seem to play either no or only a very minor role in the emergence of antibiotic resistance in Gram-negatives.

3.2.7 The majority of β-lactam non-susceptible clinical isolates harbor dominant genetic resistance determinants

β-lactam resistance in *P. aeruginosa* is mediated mostly by three different mechanisms: reduced influx due to porin loss (OprD), degradation by intrinsic β-lactamases (AmpC), and expression of different types of acquired β-lactamases. The extent of contribution of efflux pump up-regulation is still controversy discussed and varies greatly depending on the substrate. As shown by knock-out mutants of the corresponding efflux repressors in Table 3.7, only overexpression of *mexAB-oprM* clearly influenced CAZ and MEM susceptibility in the PA14 strain background.

Table 3.7 β-lactam resistance profile of efflux and porin mutants.

	MIC [µg/ml]*				
Strain	CAZ		MEM		Efflux system[a]
PA14 wt	1	(S)	0.19	(S)	
PA14Δ*nfxB*	1	(S)	0.19	(S)	*mexCD-oprJ*
PA14Δ*mexR*	4	(S)	1	(S)	*mexAB-oprM*
PA14Δ*mexS*	1	(S)	0.38	(S)	*mexEF-oprN*
PA14Δ*mexZ*	1	(S)	0.19	(S)	*mexXY*
PA14Δ*oprD*	1.5	(S)	4	(S)	
PA14Δ*oprD*Δ*mexR*	4	(S)	>32	(R)	

* Classification of resistance and susceptibility according to CLSI guidelines is indicated in brackets.
[a] Efflux systems which were overexpressed due to the knock-out of the corresponding repressor.
MIC values were determined by E-test.

Nevertheless, MIC values for this mutant still ranged within low susceptibility classification. Surprisingly, a *mexR-oprD* double knock-out led to high MEM resistance (MIC > 32 µg/ml), although both mechanisms alone only moderately decreased MEM susceptibility (MIC values of 4 µg/ml lacking OprD and 1 µg/ml overexpressing *mexAB-oprM*, respectively). However, a combination of lack of OprD and enhanced expression of MexAB-OprM was found in less than 50 % of the MEM non-susceptible isolates, despite its resulting high MIC increase. One explanation is probably the simultaneously decreasing fitness of these double mutants in infection models compared to the wild type strains [233].

Of note, there was no direct correlation between *mexAB-oprM* expression and CAZ or MEM MIC values (data not shown).

As shown in Figure 3.24, we found a partial overlap of intrinsic and acquired resistance mechanisms (9 % and 12 % for CAZ and MEM resistance mechanisms, respectively) within our panel of clinical isolates. Though this indicated that either one does not diminish acquisition of the other, most isolates exhibited intrinsic resistance mechanism.

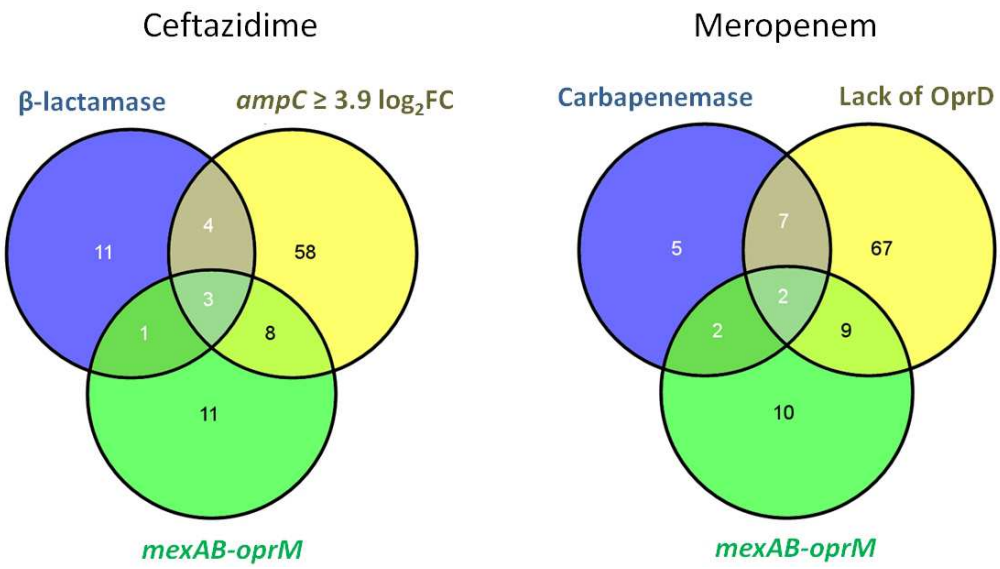

Figure 3.24 Overlapping acquired and intrinsic mechanisms conferring ceftazidime and meropenem resistance.

Lack of OprD was defined as strains with either nonsense mutations in *oprD*, expression repression ≤ - 2.5 log_2FC, no visible protein band in Western blot analysis or combinations thereof. *MexAB-oprM* overexpression was defined as ≥ 2 log_2FC. Venn diagrams were created with VENNY [224].

As *mexAB-oprM* efflux pump overexpression alone did not strongly affect β-lactam resistance, we concentrated on individual mechanisms with a more pronounced effect for a direct correlation approach of genetic markers with resistance phenotypes.

Overall, we were able to predict the resistance phenotypes of 82 % of CAZ and 87 % of MEM non-susceptible clinical isolates by dominant genetic markers detected via RNA-sequencing (Figure 3.25). In 18 % and 25 % of the MEM and CAZ resistant isolates, respectively, the acquisition of resistance mediating enzymes was observed. Of the remaining CAZ non-susceptible strains, more than 75 % showed constitutive *ampC* overexpression ($log_2FC \geq 3.9$). The overexpression cut-off was defined by calculation of the receiver operating characteristic (ROC) curve for the correlation of *ampC* expression and CAZ susceptibility with a false discovery rate of 5 %.

Among the remaining 73 MEM non-susceptible isolates, which did not express additional acquired enzymes leading to carbapenem resistance, further 61 showed significant decrease in OprD based on strong gene repression as well as lack of protein due to nonsense mutations.

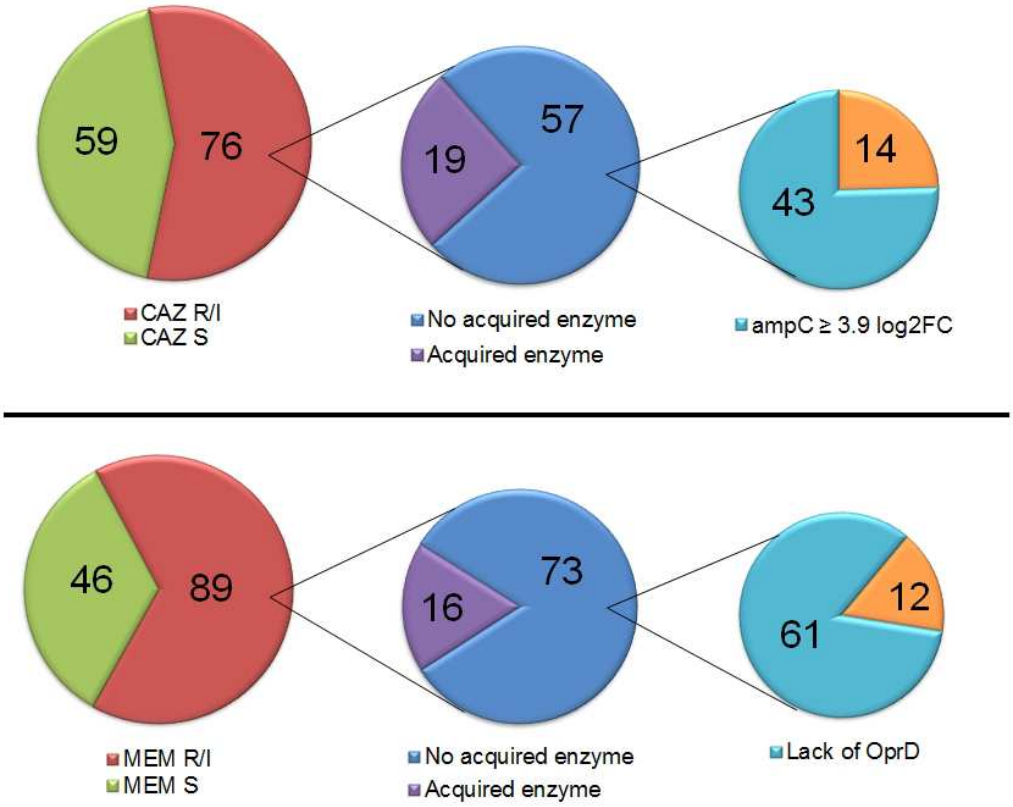

Figure 3.25 Contribution of diverse intrinsic and acquired resistance mechanisms to the β-lactam resistance phenotype in clinical isolates.

Lack of OprD was defined by nonsense mutations in *oprD*, expression repression ≤ -2.5 log_2FC, lack of visible protein band in Western blot analysis or combinations thereof.

However, of the residual 14 CAZ non-susceptible strains, six exhibited an *ampC* expression level below the defined threshold of 3.9 log_2FC, but still greater than 2 log_2FC and further three isolates were only intermediate-resistant, just on the boarder to susceptibility. Of the residual 12 MEM non-

susceptible strains, all except three showed *oprD* down-regulation (at least -0.8 log_2FC) in combination with *mexAB-oprM* overexpression. Thus, apart from strict thresholds, it is likely that for only five CAZ and three MEM non-susceptible variants *de facto* no genetic resistance determining marker could be identified (4.8 %).

3.3 Impact of sub-inhibitory antibiotic concentrations on bacterial cells

In addition to primary antibiotic targets, also a variety of secondary mechanisms has already been described as important contributors to antibiotic tolerance [156-161]. These mechanisms can be either unique for a particular class of antibiotics or part of a common response towards structurally diverse compounds [157,159]. As drug concentrations during treatment can vary across a patient's body, and microorganisms frequently encounter low level antibiotics gradients in their environments, in particular the response of bacteria upon low level antibiotic exposure and the identification of thereby induced mechanisms aiding in the evolution of resistances were of interest for this study. For this purpose, five structurally different compounds including the quinolone ciprofloxacin (CIP), the aminoglycoside tobramycin (TOB), and the β-lactams meropenem (MEM, carbapenem), ceftazidime (CAZ, cephalosporin) and piperacillin (PIP, penicillin) were chosen as representative bactericidal antibiotics and administered in low level concentrations to investigate bacterial responses.

3.3.1 Sub-inhibitory antibiotic treatment enhanced ROS production

For the observation of low level effects, we choose to use the highest sub inhibitory concentrations for which no severe cell damage was observed compared to an untreated control. In liquid culture containing nutrient rich medium (LB), the PA14 wt strain did not show a growth deficiency when challenged with antibiotic concentrations of one tenth of the MIC values (determined by broth dilution), when it was plated for live cell counts during up to three hours post treatment (Figure 3.26).

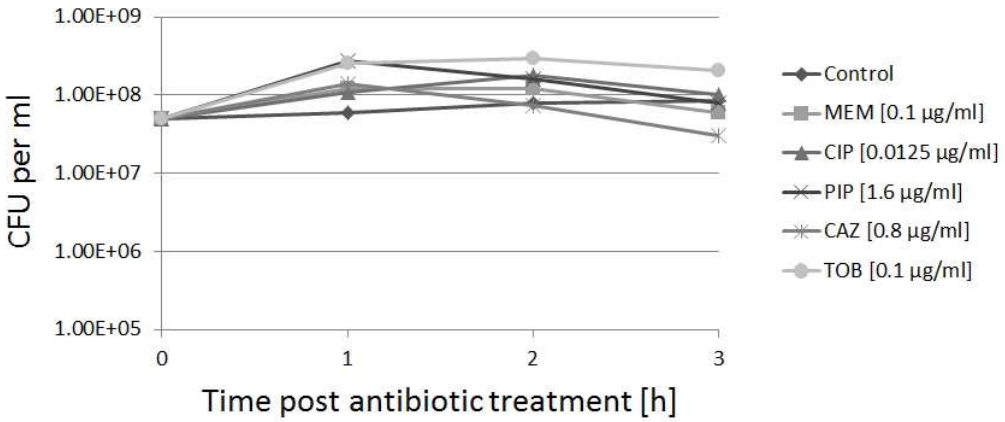

Figure 3.26 Growth of sub-inhibitory antibiotic treated PA14 wt in LB.

PA14 wt was grown in LB broth until an OD_{600} of 0.5 before cultures were challenged with different antibiotics (MEM, CIP, PIP, CAZ, and TOB) in concentrations of 1/10 of MIC values. Bacteria were plated at indicated time points on LB-agar plates to calculate the amount of colony forming units (CFU) per ml.

While the low concentrations of antibiotics did not seem to impact directly on cell proliferation rates, we still observed an increase in reactive oxygen species (ROS) production within the cells as determined by staining with a hydroxyl radical sensitive dye and flow cytometric analysis (Figure 3.27). The amount of fluorescent cells ranged between one and five percent, with the exception of CIP treated samples at the three hour time point, where the fluorescent cells comprised 17 % of the total population. For PIP, CAZ and TOB exposed cells, reactive oxygen stress was highest two hours after drug addition, while in the case of MEM and CIP highest values were reached after three hours.

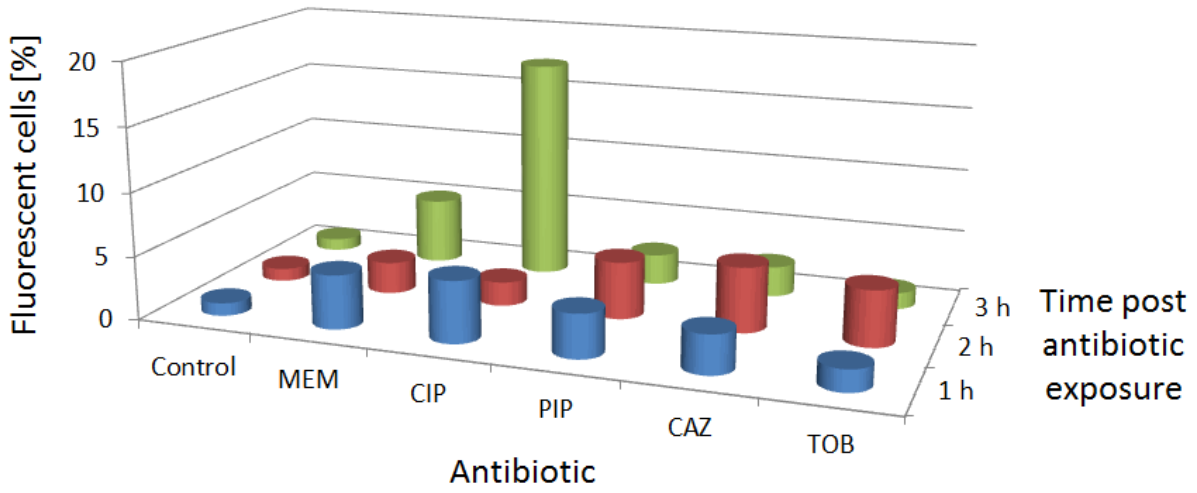

Figure 3.27 Enhanced production of reactive oxygen species by sub-inhibitory antibiotic treatment.

PA14 wt cells were grown in LB broth and treated with sub-inhibitory concentrations of different antibiotics. Production of reactive oxygen species (ROS) was assayed at time points one, two and three hours post antibiotic treatment by staining with the hydroxyl radical sensitive fluorescent dye H2DCFDA and subsequent flow cytometric analysis. Representative results from one experiment out of at least two are shown.

It is known that lethal concentrations of bactericidal antibiotics, particularly quinolones, may induce oxidative stress responses [164]. However, it was surprising to observe the same effect at very low, sub-inhibitory antibiotic concentrations. Thus, we were interested in exploring the underlying transcriptional modifications, and investigate whether they differ from or are similar to those previously described for lethal concentrations in other organisms [164]. Furthermore, it was interesting to see whether we would find a differential expression of any genes previously predicted to contribute to resistance from *P. aeruginosa* transposon mutant screens [234].

3.3.2 Transcriptional responses upon sub-inhibitory antibiotic stress

In order to investigate gene regulation as a function of sub-inhibitory antibiotic stress, transcriptional profiling was used. For this purpose, PA14 wt cells were cultivated in LB broth until early logarithmic

growths phase (OD_{600} of 0.5) and challenged with the respective low level concentrations of antibiotics. The samples were harvested for cDNA-library preparation at time points one, two and three hours post antibiotic treatment, and sequencing was performed in single-end mode. For reliable data analysis, the experiment was performed in duplicates.

When analyzing the RNA-seq data, we first noticed that there was no distinct clustering of the corresponding biological duplicates in principal component analysis (Figure 3.28). Clustering rather occurred in groups, depending on the sample harvesting time point and individual experiment replica. This indicated only very slight transcriptional effects due to sub-MIC antibiotic treatment compared to growth phase dependent gene expression regulation, and resembled the results of a previous report, where no differential gene expression could be detected at all in sub-MIC antibiotic treated *E. coli* [164].

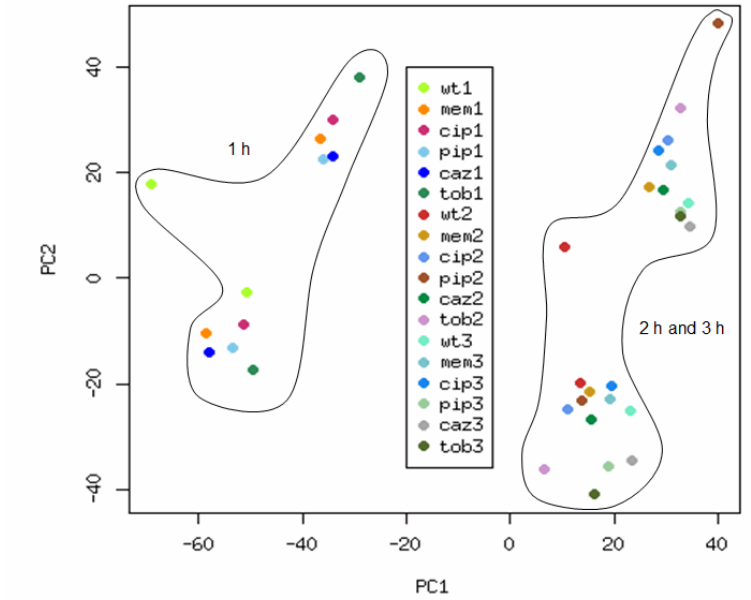

Figure 3.28 Principal component analysis based on gene expression of sub-inhibitory antibiotic treated PA14 wt samples

Clustering was performed according to similarities in gene expression based on rpg values. Harvesting time points of the samples are indicated.

For this reason, data analysis to identify differentially regulated genes was performed in two steps. First, differential expression was analyzed separately for each of the two individual experiments. All genes which were regulated overlapping for each condition in both approaches with a bh-corrected p-value of less than 0.05 were selected to comprise the antibiotic dependent transcriptional response. For the calculation of exact expression fold changes of these genes, however, the biological replicas were treated as duplicates in a second DESeq analysis. From this analysis, the fold changes of all previously identified genes were taken without considering the corresponding p-values from duplicate analysis.

In total, 105 genes were differentially regulated in both replicates. While only five differentially expressed genes could be detected for sub-MIC PIP treated cells, regulation was more pronounced for MEM (19 genes), CAZ (12 genes), TOB (21 genes), and CIP (71 genes). A detailed list of all differentially regulated genes is presented in Table 3.8.

Table 3.8 Gene expression changes upon sub-inhibitory antibiotic treatment.

Antibiotic	Locus tag	Gene	Diff. Expression [log_2FC]		
			1 h	2 h	3 h
MEM	PA14_06080	*creD*	2,611	6,659	5,840
	PA14_06090		2,170	6,345	3,923
	PA14_06750	*nirS*	-0,066	1,408	2,342
	PA14_06810	*norC*	0,888	0,254	2,819
	PA14_06830	*norB*	1,359	0,964	3,242
	PA14_06840		1,551	1,052	3,222
	PA14_08200		0,933	-1,553	-0,804
	PA14_13770	*narK2*	-0,468	0,565	1,608
	PA14_13780	*narG*	0,453	0,341	0,541
	PA14_14540		0,381	-2,616	-2,996
	PA14_20200	*nosZ*	0,781	1,499	2,464
	PA14_20230	*nosR*	0,637	1,469	3,521
	PA14_29640	*fhp*	0,536	1,410	0,763
	PA14_29660		0,636	1,383	0,421
	PA14_37210		-1,623	-3,215	-3,233
	PA14_42450	*popB*	0,638	1,406	3,015
	PA14_46740		-0,752	0,433	1,262
	PA14_50460	*flgD*	0,208	-0,456	-2,675
	PA14_50480	*flgB*	-0,081	-0,448	-3,539
CAZ	PA14_06750	*nirS*	-0,535	0,844	2,056
	PA14_06810	*norC*	0,200	0,529	2,243
	PA14_06830	*norB*	0,402	0,918	3,069
	PA14_06875	*rsmY*	2,864	1,409	1,434
	PA14_13280	*moeA1*	1,104	2,277	0,281
	PA14_13750	*narK1*	-0,090	1,517	0,889
	PA14_13770	*narK2*	-0,611	-0,418	1,669
	PA14_20200	*nosZ*	0,177	0,879	2,232
	PA14_20230	*nosR*	0,226	1,347	3,034
	PA14_25620		0,166	-0,214	0,181
	PA14_29640	*fhp*	0,082	1,298	0,684
	PA14_51850		0,093	0,541	0,040
TOB	PA14_06750	*nirS*	1,122	0,430	2,583
	PA14_06810	*norC*	1,704	0,063	2,956
	PA14_06830	*norB*	2,200	0,487	3,727
	PA14_06840		2,629	0,325	2,600

Antibiotic	Locus tag	Gene	Diff. Expression [log_2FC]		
			1 h	2 h	3 h
CIP	PA14_07980		1,693	3,321	3,547
	PA14_07990		1,610	3,262	3,725
	PA14_08000		1,506	2,933	3,798
	PA14_08010		1,846	4,185	4,087
	PA14_08020		1,565	3,790	4,139
	PA14_08030		1,654	3,511	4,394
	PA14_08040		2,261	3,864	4,397
	PA14_08050		1,733	3,408	4,176
	PA14_08060		1,322	3,427	4,046
	PA14_08070		1,649	3,204	4,012
	PA14_08090		1,599	3,279	4,126
	PA14_08100		0,978	2,731	4,022
	PA14_08110		2,183	3,211	3,958
	PA14_08120		1,233	3,051	4,392
	PA14_08130		1,679	3,324	3,996
	PA14_08140		2,147	3,895	4,193
	PA14_08150		1,667	3,291	4,176
	PA14_08160		1,699	4,366	4,263
	PA14_08180		2,434	3,416	4,736
	PA14_08190		1,973	4,274	4,822
	PA14_08200		2,510	3,336	4,685
	PA14_08210		1,614	3,641	4,152
	PA14_08220		1,736	4,263	4,460
	PA14_08230		2,160	3,614	4,057
	PA14_08240		1,509	3,468	4,305
	PA14_08250		2,241	3,489	3,908
	PA14_08260		1,714	3,707	4,035
	PA14_08270		1,804	3,757	4,476
	PA14_08280		1,739	3,920	4,711
	PA14_08300		1,564	3,600	4,462
	PA14_08310		1,240	3,022	3,757
	PA14_08320		0,734	2,871	3,630
	PA14_08330		0,867	2,425	3,186
	PA14_13940		-0,036	1,456	2,435
	PA14_14540		1,245	2,989	3,900

	PA14_06875	*rsmY*	2,223	1,136	0,767
	PA14_07560	*rpsU*	-2,566	-0,952	-1,687
	PA14_13770	*narK2*	0,946	-1,236	1,314
	PA14_13780	*narG*	1,580	0,220	-0,144
	PA14_20190	*nosD*	3,021	0,518	2,658
	PA14_20200	*nosZ*	2,344	0,569	2,946
	PA14_20230	*nosR*	1,474	0,431	3,819
	PA14_25670	*acpP*	0,704	0,266	-0,904
	PA14_29640	*fhp*	0,792	0,991	0,857
	PA14_29660		0,708	0,971	0,286
	PA14_39070		1,258	0,060	-2,250
	PA14_46740		-0,156	0,589	0,054
	PA14_49410		0,916	1,019	-0,677
	PA14_50740		0,753	-0,063	-0,193
	PA14_61000		2,251	0,765	2,788
	PA14_61380		0,649	0,315	-1,359
	PA14_70640	*rubA1*	1,404	0,051	-1,934
PIP	PA14_06680	*nirH*	0,477	3,658	0,569
	PA14_06875	*rsmY*	1,197	2,305	1,063
	PA14_08200		1,197	-1,289	-0,479
	PA14_29800		-0,127	-1,315	-2,614
	PA14_52320		-1,848	1,533	-3,114
CIP	PA14_00810		2,148	2,056	3,812
	PA14_01010		-0,120	0,695	2,537
	PA14_01030		0,378	0,587	2,387
	PA14_04180		0,044	0,312	3,390
	PA14_06830	*norB*	2,440	1,089	3,413
	PA14_07950	*prtN*	1,549	3,194	3,752
	PA14_07970		1,685	3,314	3,360
	PA14_14550		1,521	3,070	3,883
	PA14_14590	*queA*	-0,926	1,683	2,316
	PA14_17530	*recA*	1,802	2,593	2,902
	PA14_19530		-1,613	0,873	4,604
	PA14_19940		0,897	4,762	2,606
	PA14_23680	*ibpA*	0,865	1,137	2,450
	PA14_25150		1,688	2,322	3,270
	PA14_25160	*lexA*	2,007	2,956	3,555
	PA14_49510	*pyoS3I*	0,192	1,782	2,578
	PA14_49520	*pyoS3A*	0,684	2,359	3,297
	PA14_52330		2,294	2,799	2,812
	PA14_52480		0,517	2,701	3,247
	PA14_52490		0,632	2,561	3,337
	PA14_52500		1,155	4,183	4,193
	PA14_52510		-0,616	2,826	3,989
	PA14_52520		1,278	2,451	2,949
	PA14_53680		1,042	999,000	3,439
	PA14_53810		0,136	2,042	3,581
	PA14_53820		0,738	3,096	3,752
	PA14_55610		2,604	3,716	2,885
	PA14_57010	*groEL*	-0,114	1,109	2,236
	PA14_57020	*groES*	-0,089	0,637	2,191
	PA14_59220		1,709	3,962	4,607
	PA14_60630		0,236	0,785	3,633
	PA14_62970	*dnaK*	0,138	1,265	2,812
	PA14_62990	*grpE*	-0,033	0,948	2,268
	PA14_63010	*recN*	2,284	3,123	3,508
	PA14_66790	*hslU*	0,346	1,328	2,292
	PA14_69130	*glpT*	-1,639	-1,186	-0,638

Figure 3.29 depicts overlapping gene regulation for the different antibiotics. Interestingly, the majority of genes were regulated compound specifically upon CIP treatment, while TOB, CAZ, PIP, and MEM treated bacteria exhibited largely overlapping differential gene expression.

Besides large clusters of hypothetical genes, low levels of CIP mostly induced the expression of specific DNA repair mechanisms and SOS response (*prtN, recA, recN, dnaK, lexA, pyoS3,* PA14_00810), in combination with heat shock proteins and chaperons (*ibpA, hslU, grpE, groEL, groES*). This matched results of general quinolone stress responses in diverse bacteria with the particular induction of the SOS response and DNA repair mechanisms [234,235].

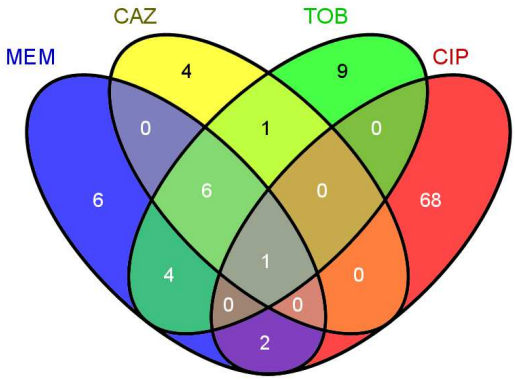

Figure 3.29 Antibiotic dependent transcriptional overlaps.

A total of 105 genes were differentially regulated in both duplicates upon sub-MIC antibiotic exposure (not considering the individual time points). PIP treated cells displayed 3 uniquely expressed genes and two overlapping ones (PA14_08200, MEM; *rsmY*, CAZ, TOB,).

Despite the large amount of CIP specific expression alteration, only few genes were regulated similarly distinct for the remaining antibiotics, as 30S ribosomal subunit coding *rpsU* (TOB) or membrane alteration protein coding *creD* (MEM). *creD* overexpression has been described to be highly inducible by classical *ampC* inducers and to be involved in β-lactam resistance, most likely through enhanced intrinsic β-lactamase activity [236]. *creD* overexpression may therefore rather indicate facilitated cross-resistance development, as MEM itself is a strong AmpC inducer, but cannot be hydrolyzed by this enzyme, in contrast to cephalosporins and other β-lactam antibiotics [141].

Although *rpsU* has not been connected with aminoglycoside resistance yet, respective transposon mutants could previously be associated with reduced susceptibility towards lipopeptide and glycopeptide antibiotics [237]. Elucidating its role in tobramycin stress adaptation, however, requires further investigation.

Overlapping gene regulation could be found for the regulatory RNA *rsmY* which was down-regulated in several different antibiotic treated samples (CAZ, TOB, and PIP). *rsmY* is known to regulate the GacA/GacS two-component system, which has previously been demonstrated to be involved in the a variety of different antibiotic resistances, including β-lactam and aminoglycoside non-susceptibility [238].

Remarkably, all tested antibiotics, independent of their functional classes, also induced expression of nitrate metabolism operons, including *nir, nor, nar,* and *nos* genes, with a particular increase in oxidoreductases. This indicates the induction of denitrification pathways, as shown in Figure 3.30.

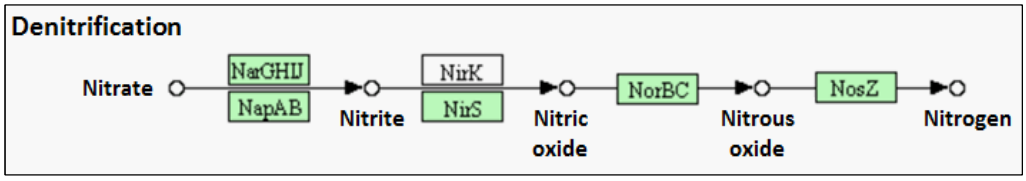

Figure 3.30 Denitrification in *Pseudomonas aeruginosa*.

Denitrification pathway of *P. aeruginosa* PAO1, including involved genes and chemical substrates according to the Kyoto Encyclopedia of Genes and Genomes (KEGG) [239].

P. aeruginosa usually prefers oxygen as terminal electron acceptor under aerobic conditions. However, a decrease in oxygen consumption had been detected previously in kanamycin treated *E. coli* [165], which made us curious about the metabolic reason for a possible induction of denitrification associated genes.

Interestingly, Kohanski and colleagues had previously described a common mechanism of antibiotic induced cell death by bactericidal agents, which included an interference with energy metabolism and the tricarboxylic acid (TCA) cycle [164]. Though, in their hypothesis, enhanced respiration was the underlying reason. Thus, we wondered what precise effects sub-inhibitory concentrations of antibiotic might have on energy metabolism pathways.

3.3.3 Metabolic changes induced by sub-inhibitory antibiotic stress

To investigate metabolic changes induced by sub-inhibitory antibiotic stress, we monitored the biosynthesis of a number of different amino acids, which originate from different metabolic pathways. This was done by feeding the bacterial cells in minimal medium with isotope labeled carbon sources, while challenging them with the respective antibiotics, followed by gas chromatography coupled mass spectrometry (GC-MS) analysis of the samples.

Pseudomonas can utilize acetate in the form of acetyl-CoA directly as substrate in the TCA cycle, or alternatively assimilate glucose, which is first converted to pyruvate in the Entner-Doudoroff (ED) pathway, before it enters the TCA cycle [240]. Finally, both substances are used as carbon sources for the biosynthesis of amino acids. Thus, to get insight into the occurring metabolic changes and their locations, the conversion of both substrates, glucose and acetate, was comparatively monitored.

As depicted in Figure 3.31, neither the use of isotope labelled glucose nor acetate led to growth deficiencies in minimal medium when the samples were treated with the respective low level antibiotic concentrations. The corresponding ^{13}C incorporation in newly synthesized amino acids is featured in Figure 3.32.

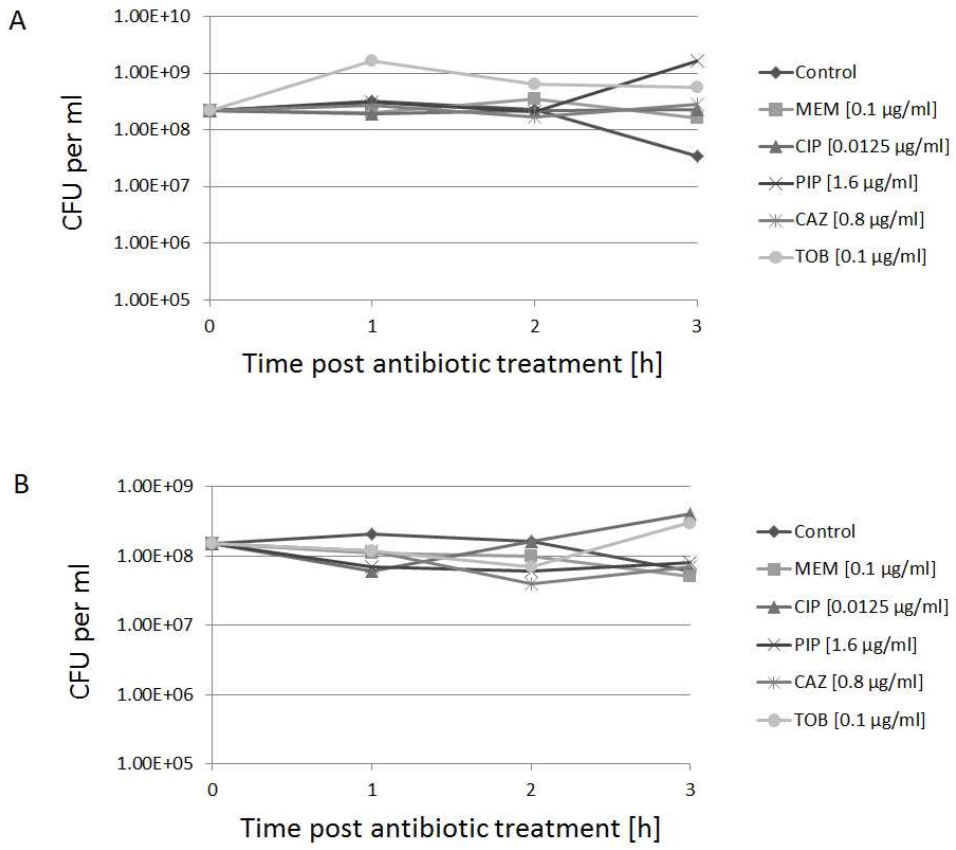

Figure 3.31 Growth of sub-inhibitory antibiotic treated PA14 wt in minimal medium.

Cells were grown in BM2 minimal medium to an OD_{600} of 0.8 and treated with either isotope labeled glucose (A) or acetate (B), followed by addition of indicated antibiotics. Bacteria were plated 1, 2, and 3 hours post antibiotic treatment on LB-agar plates to calculate the amount of colony forming units (CFU) per ml.

Interestingly, all administered antibiotics slightly increased the integration of glucose derived ^{13}C into the twelve surveyed amino acids over time, suggesting a general enhancement of metabolic processes. However, much more striking was a significant, strong increase in the detection of isotope labeled serine after three hours of growth in ^{13}C glucose, which was equally pronounced for all antibiotics. Serine is produced from 3-phosphoglycerate, which makes it the first amino acid directly generated from glucose (PseudoCyc, [241]). Our findings therefore suggest significantly increased activity of the glycolytic pathway.

In contrast to the relatively long retardation time for glucose incorporation, samples supplied with isotope labeled acetate exhibited distinct metabolic patterns considerably faster (after one hour). One likely reason is that acetate derived carbon enters metabolic pathways faster as it can be used directly for the TCA cycle, which also makes it a preferred carbon source for *P. aeruginosa*.

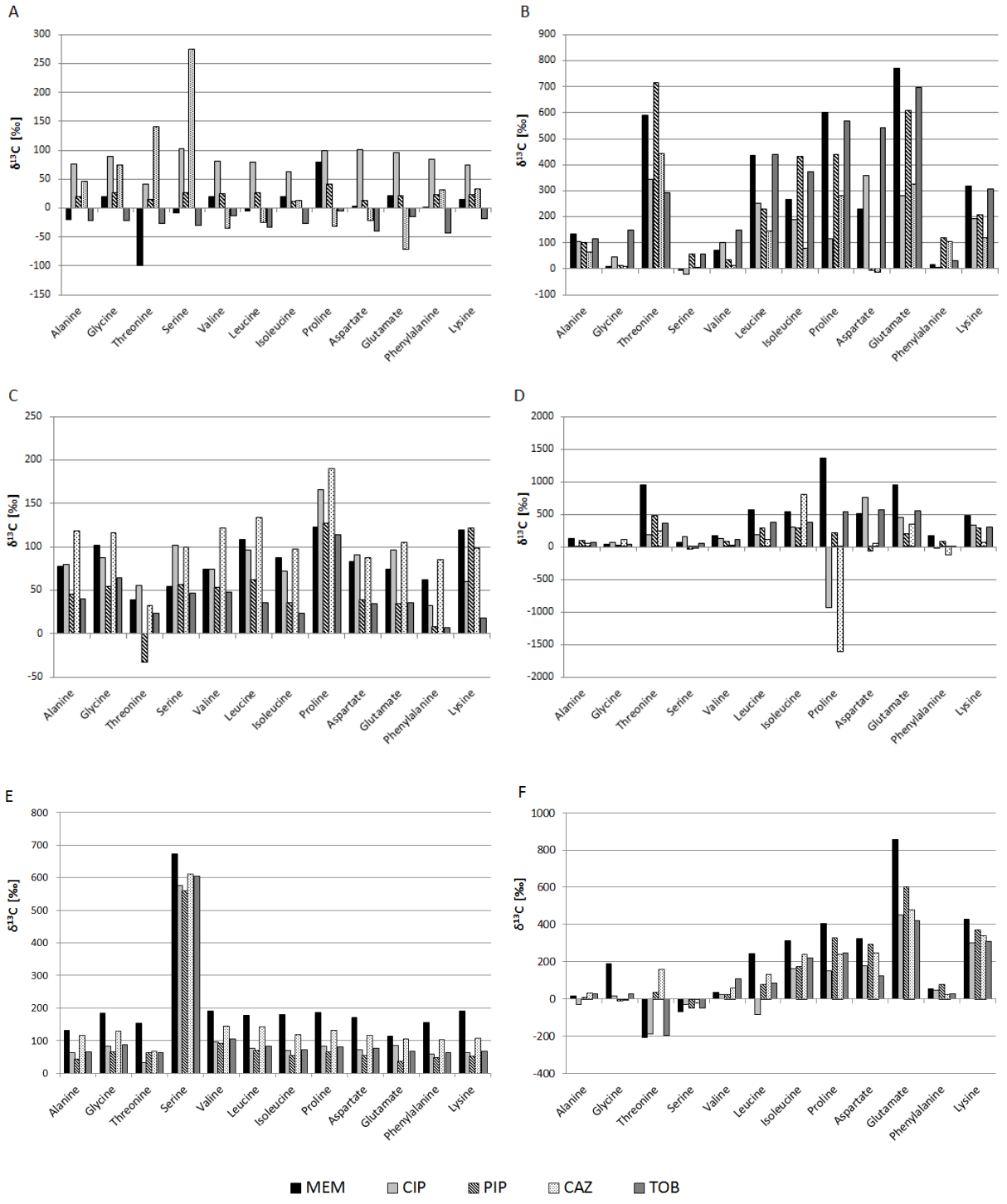

Figure 3.32 Alterations in amino acid synthesis of sub-inhibitory antibiotic treated bacterial cells.

Amino acid synthesis was monitored with GC-MS using isotope labeled glucose (A, C, E), or acetate (B, D, F). Sample were grown in BM2 minimal medium to an OD_{600} of 0.8, until cultures were supplemented with the labeled carbon sources and challenged with sub-inhibitory concentrations of antibiotics (MEM (0.1 µg/ml), CIP (0.0125 µg/ml), PIP (1.6 µg/ml), CAZ (0.8 µg/ml), TOB (0.1 µg/ml)). Samples were harvested at time point 1 h (A, B), 2 h (C, D), and 3 h (E, F) post antibiotic treatment.

^{13}C incorporation is shown relative to untreated PA14 wt control samples.

Most interestingly, however, we noticed a significantly enhanced biosynthesis of particular, acetate derived amino acids for all antibiotic treatments. These amino acids were either directly derived from TCA cycle dependent metabolic pathways, as threonine, proline, aspartate, glutamate and lysine or were indirectly TCA cycle dependent as leucine and isoleucine, which require glutamate and acetyl-CoA.

These findings suggest that even sub-inhibitory concentrations of antibiotics already induce common stress responses which are I) largely independent of their specific cellular targets and II) apparently involve an overstimulation of the TCA cycle, as also suggested previously for lethal antibiotic concentrations. The strong increase in glucose derived serine could further implicate that also NAD^+ and $NADP^+$ dependent pathways independent of the TCA cycle, as such involved in the conversion of glucose, might be subject to hyperactivation. However, validating this hypothesis requires further investigation.

4 Discussion

4.1 The increasing threat of bacterial antibiotic resistance

The frequency of antibiotic resistance in bacterial pathogens is steadily increasing around the world, resulting in a growing threat to public health [242]. On the one hand, adequate treatment is diminishing due to the low discovery rate of novel compounds [188]. On the other hand, the lack of optimal and prompt diagnostics leads to widespread and empirical use of antibiotics, which further promotes the expansion of resistance and the occurrence of multi- or even pandrug-resistant phenotypes [243].

4.1.1 Antibiotic treatment leads to resistance selection

One main problem is the selection of resistant variants with genetic mutations that provide fitness advantages upon antibiotic exposure and help these mutants to easily outgrow the respective susceptible “wild type”-part of the population. A Europe-wide multicenter study has demonstrated that countries with a higher consumption of antimicrobials in hospitals also show higher frequencies of developing methicillin resistant *Staphylococcus aureus* (MRSA) [244]. Direct consumption-resistance correlations could also be seen for carbapenemase or extended spectrum β-lactamase (ESBL) producing Gram-negatives [245,246], and single and multi-resistant *P. aeruginosa* [247-249] in individual institutions. Additionally, there are significant connections between drug-use and initial colonization with resistant organisms [250,251].

Although the presence of antibiotic agents is a factor to promote resistance, their subsequent absence does not automatically lead to susceptibility reversion. For instance, non-reverting resistances to the often used trimethoprim/sulphonamide combination therapy have been described in *E. coli*, despite significantly decreased use of these antibiotics in the respective communities [252,253]. This occurs, when the resistance does not harbor a significant fitness cost [254].

4.1.2 Antibiotic concentration reservoirs promote adaptation

A second significant problem, in addition to resistance selection, is over time adaptation of the bacteria when they are confronted with antibiotic concentration reservoirs. The amounts of antimicrobial compounds which bacteria encounter can vary greatly, depending on their respective environments. Both in individual humans (within a patient’s body) and at the level of the whole

human population (within the environment of communities), we frequently find varying, gradual antibiotic pressure.

In aquatic and soil habitats, some antibiotics as a number of β-lactams and aminoglycosides which are derived from natural sources (e.g. other bacteria or fungi) may increase in quantities dependent on their producers. However, the greatest portion of antimicrobial substances is released into the environment due to man-made industrial pollution from hospitals or pharmaceutical industries [255]. Despite growing knowledge and concerns on the subject of resistance evolution, antibiotic prescription generally showed an increasing trend in the European Union comparing the years 1999-2008 [256]. In 2008 the inpatient Defined Daily Doses (DDD) of antibiotics for systemic bacterial infection treatment was between one and 3.5, the outpatient antibiotics consumption even ranged between 10 and 45 DDD per 1000 inhabitants in the participating countries [256], with the majority prescribed for the treatment of respiratory tract infections [257].

Due to pharmacokinetic aspects, these antibiotics create high density temporal and spatial gradients within the human body as they vary in their diffusion rates into various tissues, local inactivation, responses to the host's microbiota or pathogenic flora, and metabolic inactivation [258]. Furthermore, the different administered compounds show a wide range in the degree to which they are degraded in humans. Some are metabolized by 90 %, while others are metabolized by only 10 % or even less [259]. Based on nationwide consumption rates it was found that 70 % of the total amounts of antibiotics used in Germany are excreted unchanged as active compounds [255]. Thus, it is not surprising that several broad spectrum antibiotics, in particular ciprofloxacin, have been found in high concentrations reaching up to mg per ml ranges in connection with sewage outlets from hospitals or pharmaceutical industries [260]. In another study, β-lactams were detected in the ng per ml range in hospital effluent and in the influent of a municipal sewage treatment plant [261]. Degradation and dissipation of these products in the environment differ greatly, often leading to mixed antibiotic gradients over time [262].

Thus, we are presently left with an increasingly alarming future perspective when it comes to combating bacterial infections. One way to cope with this problem is to improve diagnostics to enable more targeted and prompt treatment. This would positively affect the course of the disease of the individual patient, and at the same time help to advance hygiene measures to minimize the emergence and spread of resistant bacteria.

4.2 Limitations of culture-based diagnostics

Presently, antibiotic resistance is determined based on minimal inhibitory concentrations (MICs), which are the lowest concentrations of an antimicrobial that will inhibit the visible growth of a

microorganism after overnight incubation [263]. These MIC values in combination with the pharmacodynamic parameters of the drug (e.g. cytotoxicity) are the foundation for the definition of clinical breakpoints, which guide clinicians in their treatment by dividing isolates into “susceptible” or “resistant” [264]. However, methods depending on culture-based techniques which include *in vitro* growth inhibition tests have several disadvantages and limitations.

Cultivation is time-consuming

The currently performed growth dependent MIC determination requires a considerable amount of time. Patient swabs need to be plated and incubated for more than 12 hours to gain pure, single bacterial colonies. Next, a second round of incubation is necessary to test for antibiotic growth inhibition, which takes another 16 to 20 hours for *P. aeruginosa*, but may even exceed 24 hours for other bacterial species [265]. For slow-growing bacteria, as e.g. *Mycobacterium tuberculosis*, the whole process may even take months [187]. This considerable time delay until a suitable antibiotic therapy can be determined may be critical for the outcome of an infection. Furthermore, approximately 10 % of all infectious bacterial pathogens are believed to be non-culturable, limiting their phenotypic evaluation altogether [187].

MIC determination and breakpoint definition require high standardization

MIC threshold detection and breakpoint determination results are sensitive and vary not only depending on the initial inoculum and growths conditions (medium, incubation time and temperature), which have been standardized by the European Committee on Antimicrobial Susceptibility Testing (EUCAST) and the Clinical and Laboratory Standards Institute (CLSI), but also differ depending on the used detection devices. Recently, a Spanish study comparatively evaluated accurate susceptibility testing and interpretation by sending 13 pre-characterized *P. aeruginosa* strains to 54 participating centers. Very major errors (false negative characterization) occurred in up to 22 % of the cases for β-lactam antibiotics [266]. Additionally, breakpoint definition and testing parameter guidelines from the two main institutions, EUCAST and CLSI, differ for many antibiotics and thus lack direct comparability [265,267]. This may render a particular strain resistant in one laboratory, while the same one is still considered susceptible in another [268], and thereby substantially affect adequate treatment and prompt infection eradication.

Single colony MIC values are not optimal for population resistance determination

Furthermore, it is known that even within a susceptible wild-type population, a small fraction of cells ($< 10^{-9}$) is not affected when challenged with an antimicrobial agent, allowing their selection during

clinical treatment [254]. However, MIC measurements of single colonies do not consider this, often pharmacodynamics-dependent, resistance selection window between the MIC of the susceptible population and the MIC of the resistant variants. To improve risk management for the evolution of resistant populations, it has therefore been suggested to introduce a mutant prevention concentration instead (MPC), based on the upper boundary of the selection window [269]. Data provided by several studies already emphasized the sometimes remarkable discrepancies between MIC and MPC values [270-272]. However, this approach requires significantly larger inoculums and labor intense concentration gradient plating, questioning its feasibility in daily clinical routine.

Proto-resistance mutations are not taken into account

Last but not least, growth dependent susceptibility testing is only able to detect the *present* phenotypic state of a bacterium. However, besides target alterations that lead directly to antibiotic resistance, also mutations which merely promote resistance evolution occur. These so called proto-resistance mutations alone do not significantly affect antibiotic susceptibility, but facilitate resistance evolution and quick MIC increases upon antibiotic pressure [273]. One such example is the *gyrA* mutation T83I. While this mutation does not obligatory confer ciprofloxacin (CIP) resistance in *P. aeruginosa* clinical isolates (MIC values ranging from 2 to 8 µg/ml), double mutants harboring the additional S87L variation in *parC* always exhibit high level CIP resistance (MIC = 32 µg/ml) [69]. Thus, optimal antibiotic therapy should ideally refrain from using CIP for the treatment of such strains to minimize the risks for rapid high level resistance evolution and spread.

One way to overcome the problems and limitations connected to cultivation-based antibiotic resistance profiling (phenotype observation) could be the use of molecular methods for the direct screening of genetic determinants (genotype observation) instead.

4.3 Transcriptome sequencing of drug resistant clinical isolates

Within our pilot study, we fully sequenced the transcriptomes of 149 clinical *P. aeruginosa* isolates to search for genetic markers which are suitable for fast and reliable resistance phenotype determination to advance clinical microbiology. Our focus was hereby set on RNA instead of DNA sequencing, as this strategy allows for the combined data acquisition of gene sequence information and - at the same time - gene expression patterns.

4.3.1 Inexpensive whole transcriptome sequencing provided reasonable single nucleotide coverage throughout the whole *P. aeruginosa* genome

The first goal for our broad transcriptome study was to find a way of sequencing a maximum number of clinical isolates with minimal costs. The Illumina GenomeAnalyzer-IIx (GAIIx) provided up to two times 40 million reads in paired-end mode (75-150 bp length). This was a sufficient capacity for the simultaneous sequencing of several cDNA libraries of different strains and thereby allowed to lower sequencing costs by multiplexing. At the time of the start of this project, no commercially available, strand-specific method for transcriptome sequencing existed, which was suitable for multiplexing of several samples on one Illumina sequencing lane. Perkins and colleagues had published a strand-specific method for analyzing *Salmonella typhi*, but using random primers for cDNA synthesis [274], which may introduce a sequence bias to transcriptional profiles. Therefore, a custom protocol was developed for high-throughput application and especially optimized for the sequencing of *P. aeruginosa,* including the use of adapter-specific primers for reverse transcription [275]. One particular challenge during protocol optimization was the effective enrichment of mRNA, which comprises only about 1-5 % of the total bacterial RNA, as opposed to the > 90 % portion of rRNA [212]. Consequently, the more rRNA is removed, the more samples can be multiplexed for sequencing. For this purpose, different hybridization-based and enzymatic rRNA removal approaches were compared for their effectiveness. In *P. aeruginosa,* enzymatic degradation of the rRNA using terminator-5'-phosphate-dependent exonuclease (TEX) proved to be ineffective due to incomplete rRNA removal (only 5-10 %) and simultaneous mRNA damage (Figure 3.3). As this enzyme is specific for RNAs containing a 5'-monophosphate (rRNA), with no exonuclease activity on RNAs with 5'-triphosphates (mRNA), also partially degraded mRNAs seem to be subject to digestion. This influenced in our experiments expression patterns and abolished start site detection. Similar effects had been observed in meta-transcriptomic studies with other organisms [214], rendering this enzyme rather inapplicable for these kinds of transcriptomic studies.

Better results could be obtained with the hybridization-dependent commercially available MICROBExpress Kit in combination with *Pseudomonas* sp. specific capture-oligomers for the

depletion of 16S and 23S rRNA. According to the manufacturer, an rRNA reduction of more than 95 % could be achieved for *E. coli*. We were able to remove rRNA by up to 40 % in the *P. aeruginosa* PA14 strain (Figure 3.3 A). Furthermore, this method did not significantly affect native mRNA expression profiles (Figure 3.3 B), which had also been confirmed by other studies [183,213,214]. Thus, it did not interfere with transcriptional start site detection. MICROBExpress proved to be the most effective of all tested hybridization approaches (Table 3.1) and the depletion range matched a previous report in *E. coli*, where 38 % rRNA decrease was observed [194]. For maximal reduction, it was combined with additional rRNA removal by duplex-specific nucleases in the clinical strains. This method had previously been shown to efficiently reduce rRNA in *E. coli* without interfering with native transcription patterns [194,276]. A combination of MICROBExpress (before library preparation) and DSN (after library preparation) finally yielded in up to 75 % mRNA per sample. However, rRNA removal efficiency strongly varied (between less than 10 % and more than 70 % mRNA content) depending on the individual sample and partly on the sequencing pools as a whole (Figure 3.7). This could be due to the method of hybridization-based rRNA removal, which is only able to deplete completely intact rRNA. With the different physiology of clinical isolates, however, partial RNA fragmentation/degradation might be a problem for some (particularly mucoid) samples, despite the use of protective agents. Additionally, the initial rRNA/mRNA ratios of isolates with very diverse metabolic activity and growth phenotype may vary and thus partially account for the observed differences.

A maximum of twelve individual strains were pooled for clinical isolate sequencing. This resulted in 1.8 to 13.8 million reads per sample, of which on average five million reads aligned to the PA14 genome (Figure 3.6A). Thereby, we obtained up to 90 % total genome coverage (Figure 3.6B), with up to 80 % of nucleotide positions covered with three or more reads. According to previous studies, this amount was sufficient for high quality expression analysis of bacterial transcriptomes [277] and, due to the high percentage of total genome coverage, additionally allowed for the successful detection and investigation of mutations within the expressed regions. The high amount of total genome coverage is partly due to the nature of bacterial chromosomes, which display a dense alignment of expression sites in their operon structure. However, *P. aeruginosa* additionally shows the particular feature of a broad, constitutive subliminal gene expression throughout the chromosome, which has also been observed by others before [278]. This special characteristic renders the organism particularly suitable for transcriptome-based sequence determination. Moreover, advances in sequencing depth (Illumina HiSeq 2500) presently provide five to seven fold increased read amounts [279]. This enables even higher multiplexing of samples, which further significantly reduces sequencing costs and at the same time allows for consistent > 93 % total genome coverage in *P. aeruginosa* (our unpublished data). This indicates presumably the upper boarder of

accomplishable total genome coverage, as we observed saturation at around 90 % coverage despite more than twice increased read quantities for some samples (Figure 3.5). Furthermore, it was previously shown that only approximately 90 % of the *P. aeruginosa* genome belongs to strongly conserved, 'core' genetic elements [219,220]. Thus, the remaining 10 % may be flexible between different clinical isolates and possibly contribute to varying overall sequence coverage when mapped to the PA14 reference strain.

Thus, RNA-sequencing could for the purposes of this and related studies virtually replace conventional DNA-sequencing with the additional advantage of delivering expression information.

4.3.2 In depth taxonomical profiling could distinguish between actual clonal outbreaks and sequence type related strains

With the data obtained from RNA-sequencing, we could identify 214 genes, which were highly expressed in all clinical isolates. Sequence comparisons of these commonly expressed genes allowed performing in depth taxonomical profiling of the clinical strains (Figure 3.8) with much higher resolution than conventional strategies such as variable number of tandem repeats (VNTR) or multilocus sequence typing (MLST) [221,222]. We could clearly identify a particular clonal outbreak at the Hannover Medical School, as the corresponding isolates exhibited very similar sequence and expression profiles. Furthermore, we observed that two phylogenetic clusters which we identified as most likely representing high-risk MLST sequence types ST235 (clustering around PSAE0613) and ST175 (clustering around MHH7368), still displayed considerable sequence variability, as well as gene expression differences (compare Figure 3.9). These findings suggests that the presently used methods to determine clonal relationships based on only few open reading frame sequences (MLST) may not be sufficient for proper phylogenetic analysis and could lead to misinterpretations.

These limitations of currently used MLST schemes have as well already been acknowledged in other areas, as for instance on differentiating *Bacillus* on the species level [280], and new differentiation strategies based on greater numbers of open reading frame sequences have been proposed [281].

With sequencing costs decreasing, the acquisition of sufficient large numbers of gene sequences is best done by whole genome sequencing (WGS) or whole transcriptome sequencing (WTS) [187].

4.3.3 The acquired β-lactam resistome

β-lactam resistance in *P. aeruginosa* can be divided into two parts: intrinsic mutational changes and the horizontal acquisition of new genes. The detection of each mechanism requires a different analytical approach. Acquired resistance mediating enzymes were identified by a combination of *de novo* assembly and gene coverage investigation. Their acquisition was observed in 18 % and 25 % of

the non-clonal MEM and CAZ resistant isolates, respectively. Generally, the presence and nature of acquired β-lactamases varied greatly, which matches the known diversity between different populations, with country specific epidemiological patterns [114]. A nationwide investigation in France regarding the occurrences of extended-spectrum β-lactamases (ESBLs) and metallo-β-lactamases (MBLs) identified 9.5 % of CAZ resistant *P. aeruginosa* to harbor one of these enzymes [282]. In a German study, 19.9 % of all carbapenem resistant *P. aeruginosa* isolates harbored carbapenemases, most frequently VIM-2 [283]. A surveillance study including 14 European and Mediterranean countries on carbapenem non-susceptible *P. aeruginosa* identified 25.6 % being positive for MBLs [284].

We discovered nine different β-lactamases (OXA-2 and 4, VIM-1 and 2, GIM-2, IMP-1 and 7, PER-1, and CTX-M-3) in overall 19 isolates (14 %) of which six contained two respective enzymes (4.4 %) (Figure 3.12). In any of these cases, one enzyme was a MBL or ESBL, while the second enzyme belonged to the class D oxacillinases. Furthermore, the presence of an acquired β-lactamase always led to resistance towards the corresponding antibiotic.

The detection of carbapenemase producing organisms is an important matter for the choice of appropriate therapeutic schemes and the implementation of infection control measures. However, presently, phenotypic identification poses a number of difficulties as it cannot simply be based on the resistance profile, and specific testing has not been well standardized yet and often lacks accuracy [129]. For example does the detection of acquired MBLs in *P. aeruginosa* often rely on disk diffusion assays, which lack, depending on the test used, either reliable sensitivity (31 % to 88 %) or specificity (28 % to 81 %) [285], demonstrating the need for molecular detection systems in this field to improve surveillance and avoid resistance spread. One already widely used method for some β-lactamases is the detection by multiplex-PCR [286]. However, this method cannot distinguish between the mere presence and actual expression of the corresponding genes.

We could show that RNA-sequencing provides clearly improved conditions for the detection of acquired β-lactamases, with a high sensitivity (96 %) and a low false discovery rate of only 0.67 % for carbapenemases (Figure 3.10).

4.3.4 Unbiased global correlation studies as an approach to detect novel phenotype specific genetic markers

The greatest benefit of global approaches as WGS or WTS is based on their comprehensive data.

Thus, instead of individually screening for known resistance markers, we aimed to use this data to investigate the enrichment of particular genetic changes in CAZ and MEM non-susceptible isolates. This was done by database supported statistical analyses, which compared the sequence information and transcript abundance of all genes in all isolates with each other. This approach substantially

facilitates the detection of frequent, resistance-phenotype specific modification and allows as well the identification of previously unknown factors.

Identification of enriched genetic determinants in CAZ non-susceptible isolates

With the above mentioned approach, we identified the intrinsic β-lactamase *ampC* and a directly adjacent gene as significantly more expressed in the CAZ non-susceptible group of isolates (Table 3.3). AmpC overexpression is known to reflect an important intrinsic β-lactam resistance mechanism in *P. aeruginosa* [287]. Interestingly, we also found *oprD* and *mexB* to contain more frequently nonsense mutations in the CAZ non-susceptible group. The MexAB-OprM pump usually promotes β-lactam non-susceptibility through enhanced drug efflux [58]. However, it has also been shown that this pump is dispensable or maybe even disadvantageous in adaptation to the CF lung environment [288]. Therefore, the successive mutational inactivation of the pump to compensate preceding overexpression may comprise a fitness advantage in the host, once alternative and more efficient β-lactam resistance mechanisms have developed. Of note, all of the CAZ resistant isolates with *mexB* mutations, except one, showed constitutive *ampC* overexpression. Furthermore, the absence of functional OprD is not primarily associated with ceftazidime resistance, as CAZ cell entry is equally distributed between a number of porins, including OprC, OprD, and OprE [289]. Therefore the frequent nonsense mutations in this gene in the CAZ non-susceptible group emphasize the tight interconnections of cross resistance evolution in clinical isolates. This could also be seen when comparing CAZ resistant and susceptible isolates and thereby detecting the enhanced expression of *mexE* (Table 3.4) in the resistant group of isolates. While overexpression of the MexEF-OprN efflux pump is not directly associated with CAZ resistance [66,226], its regulation is influenced by the transcriptional regulator AmpR, which is also the main regulator controlling *ampC* transcription [290,291].

MEM non-susceptible isolates showed specific genetic enrichments

When screening for genetic enrichments in the MEM non-susceptible group, we identified *oprD* as the only gene which frequently showed nonsense mutations and expression repression in these isolates (Table 3.5). It is already known that a lack of OprD significantly contributes to carbapenem resistance in *P. aeruginosa* [81,90,96], as this outer membrane protein is a porin, which can be used for cell entry by carbapenem antibiotics as imipenem and meropenem [80].

Analyzing the *oprD* sequences of all isolates in more detail, we observed a number of mutations leading to premature translation termination, which were located throughout the open reading frame (Figure 3.20). Single amino acid exchanges on the other hand occurred preferentially in the

surface-associated loop regions. Mutations in these regions mostly do not interfere with the barrel structure of the porin, but still allow high variability to influence host pathogen interactions and aid in immune evasion [98]. It is described that some mutations in the loop regions may also alter carbapenem binding properties and thereby influence drug uptake, as particularly loop two, for instance, is required for imipenem interaction [88,94]. However, we could not detect any particular enrichment of such mutations, as MEM resistant and susceptible isolates exhibited almost identical SNP patterns (Figure 3.20 B).

Although we were able to trace back most carbapenem resistance phenotypes to either carbapenemase expression or diminished functional OprD, we were surprised to also find a few meropenem susceptible strains, which exhibited a complete lack of OprD protein (due to premature stop codons within the *oprD* sequence) (Figure 3.21 and 3.22). This finding has also been observed previously in *P. aeruginosa* clinical isolates, however, no clear explanation could be found yet [97]. So far it is only known that porins OprC, OprE and OprF are most likely not involved in MEM transport [289]. We therefore performed mass spectrometric analysis on proteins enriched in the outer membranes of these isolates to search for compensatory effects, and identified the porin OprQ as a candidate in two analyzed strains (Figure 3.22 and Table 3.6). OprQ might hint at an alternative way of meropenem entry in clinical isolates, although a *P. aeruginosa* PAO1 *oprQ* interposon mutant strain did not show changes in carbapenem susceptibility [292]. This emphasizes the need for further studies to completely understand the complex regulatory and compensatory mechanism (as counterbalancing the lack of OprD) of antibiotic resistance.

4.3.5 Evaluating RNA-sequencing for direct resistance prediction

Our RNA-sequencing data allowed not only for global phenotype-genotype comparisons, but was also sufficient to screen each strain individually for all known genetic β-lactam resistance markers and perform direct correlations to the respective strain's antibiotic susceptibility profile. Thereby we were able to identify the causative genetic variations responsible for non-susceptibility in 82 % and 87 % of the clinical isolates for CAZ and MEM, respectively, when strict expression cut-offs were used (Figure 3.25). Even up to 95.2 % was achieved with less stringent restriction.

Recently, there have been several whole-genome sequencing approaches which identified bacterial adaptive genetic evolution, including antibiotic resistance determinants, which were consistent with the predicted antibiotic resistance phenotype [293-295]. Furthermore, Gordon and colleagues evaluated the accuracy of WGS prediction compared to exhibited resistance phenotypes in *Staphylococcus aureus* in detail and calculated overall error rates of 0.5-0.7 % for selected antibiotics [296]. In addition to the detection of target mutations, RNA-sequencing is actually able to provide gene expression data. This enabled us to focus not only on antibiotic resistance due to target site

mutations (as known for quinolones), but also mechanisms applied for the defense against other clinically important antibiotics, which are more dependent on enzymatic substrate degradation (e.g. β-lactams or aminoglycosides). However, opposed to target site mutations, gene expression covers a dynamic range which complicates threshold prediction for one phenotype or the other (as shown in this study for *ampC*). Thus, while target alterations and the expression of acquired resistance genes can directly distinguish between susceptibility and non-susceptibility, constitutive overexpression or repression of intrinsically present genes obtained from WTS data may at the moment rather be used as additional information for the identification of antibiotic resistances, but not yet predict susceptibility with sufficient accuracy.

4.3.6 High-throughput target screening as a future clinical outlook

Despite the enormous progress in sequencing during the last years, clinical adoption of whole genome or transcriptome sequencing in resistance prediction is challenging, even if all genetic determinants are known. Although it is unlikely that WGS or WTS will be able to replace phenotypic resistance determination in the near future, the great potential of these applications is obvious. With the RNA-sequencing approaches, sequence information and transcript abundance of any expressed genome position are recorded and can be applied repeatedly for new phenotype-related analysis to address various questions. This may be used to determine individual genetic markers, which can be screened directly in the hospitals using alternative technologies.

One system demonstrating high potential for such applications is the Sequenom MassARRAY®. This device uses matrix assisted laser desorption/ionization time-of-flight mass spectrometry (MALDI TOF-MS) for high-throughput analysis of nucleotide sequence variations [297]. The principal method to detect them is thereby based on multiplexed single nucleotide primer extension to simultaneously discover up to 50 sequence polymorphisms [298]. This new approach has recently already been used in several human studies for large scale detection of specific DNA mutations [299-302] and MLST determination in the Gram-negative bacterium *Neisseria gonorrhoeae* with greater than 98 % accuracy [303].

However, antibiotic resistance results from complex interactions and can be based not only on specific single target alterations, but also on enzyme up-regulation due to an unpredictable high amount of different spontaneous mutations, as in the case of *ampC*. Thus, a combination of sequence and expression information will be necessary for resistance prediction. If the Sequenom method is used on cDNA instead of DNA, this could provide the required additional information and allow not only the detection of SNPs, but also gene expression by the evaluation of the relative abundance of a primer extension reaction based on the native sequence of a selected gene. Thus, this method could be used to monitor *ampC* overexpression as a molecular marker for the prediction

of CAZ resistance. MEM resistance, however, correlated to the abundance of OprD protein levels. The random appearance of loss of function mutations throughout the whole *oprD* sequence and lack of direct mRNA to protein level correlations limit the value of resistance phenotype prediction based on *oprD* transcription.

Therefore a better approach for molecular diagnostics might be the screening for specific protein abundances, as opposed to mRNA levels, in combination with DNA-based target mutation detection. Furthermore, mass spectrometry has already been used successfully in the detection and identification of β-lactamases based on the hydrolysis patterns of their different target compounds [304-307]. As several hundreds of different horizontally transferable β-lactamases are known, their detection could be greatly facilitated by screening directly for their hydrolytic activity.

Although there is still work to be done, a mass spectrometric approach may in the future be suitable for a combined analysis of molecular markers including DNA target mutations, protein abundances, and small molecule degradation. It would undoubtedly be of great benefit to have early resistance marker detection available for all clinically important antibiotics to maximize successful therapy outcome and minimize resistance selection and spread.

4.4 The impact of low-level antibiotic concentration reservoirs

It is indisputable that high antibiotic concentrations, as they are desired during therapeutic infection treatment, can select for resistant bacterial mutants and furthermore that widespread and empirical use of antibiotics promotes the expansion of resistance and the occurrence of multi- or even pandrug-resistant phenotypes [243]. However, pharmacodynamic models generally assume that the selection window for these mutants occurs between the minimal inhibitory concentration of the susceptible wild type (MIC_{susc}) and that of the corresponding resistant bacteria (MIC_{res}) [308,309]. Concentrations below MIC_{susc} will not inhibit growth and were therefore long assumed not to be selective. Recently, however, several studies elucidated that the process of selection required only minimal fitness advantages with minute differences in growth already being sufficient [156,310]. Resistant *E. coli* mutants were even able to outgrow susceptible ones at concentrations of one fifth of the MIC for ciprofloxacin and one twentieth of the MIC for tetracycline [311]. In another study, Gullberg and colleagues proved that concentrations significantly below MIC values were sufficient to select for ciprofloxacin resistant *E. coli* and streptomycin resistant *Salmonella typhimurium* [312].
Nevertheless, much of our current knowledge on the evolution of antibiotic resistances is based on mutant selection in lethal drug concentrations. The importance of low-level, sub-inhibitory drug amounts and respective bacterial adaptation mechanisms is still largely unclear.

4.4.1 Common transcriptional changes cope with oxidative stress

To investigate the particular aspect of low-level antibiotic influence, we challenged *P. aeruginosa* PA14 cells with sub-inhibitory concentrations of five different bactericidal antibiotics, the quinolone ciprofloxacin (CIP), the aminoglycoside tobramycin (TOB), and the β-lactams meropenem (MEM, carbapenem), ceftazidime (CAZ, cephalosporin) and piperacillin (PIP, penicillin). In our experiments, antibiotic concentrations as low as one tenth of the MIC values clearly affected the cells in several ways, despite no apparent growth deficiency compared to the untreated wild-type control.
We detected low level increases in oxidative stress by monitoring oxygen radical formation in all samples within the first hours after antibiotic exposure, with the by far strongest effect caused by CIP treatment after three hours (Figure 3.27). Certain reactive oxygen species (ROS), as hydroxyl radicals, have been described to be able to directly damage DNA and lead to the accumulation of mutations [313], and a recent study in *E. coli* clearly correlated an enhanced formation of ROS with an increased mutation rate [42]. This finding was suggested to originate mainly from induction of the SOS response (e.g. via RecA) by quinolones and β-lactams, or additional SOS independent DNA repair mechanisms in the case of ciprofloxacin [164,235]. Transcriptome analysis revealed that *P. aeruginosa* cells indeed activated SOS response mechanisms when treated with CIP, even at

concentrations of one tenth of the MIC values. As activation of the SOS genes occurs after DNA damage by the accumulation of single stranded DNA blocking the DNA polymerase at replication forks, it was not surprising to find this defense mechanism at low antibiotic concentrations only in the CIP treated samples, since the effect of β-lactam dependent, indirect DNA damage is generally less pronounced [164].

Remarkably, antibiotic specific gene regulation was only partly target-specific (membrane alteration genes for β-lactams, a possible ribosomal subunit response for aminoglycosides, DNA repair mechanisms for fluoroquinolones) with large overlaps between individual compound classes. *RsmY* regulation, for example, was affected in β-lactams and aminoglycosides. This small, regulatory RNA is under control of the GacS/GacA two-component system, which regulates a broad range of stress responsive genes, but is also involved in the expression of acute and chronic virulence determinants [314-316]. Furthermore, genes involved in denitrification (*nir, nor, nar*, and *nos*) were commonly regulated in all samples independent of the administered antibiotic. Complete denitrification consists of four sequential steps to reduce nitrate (NO_3^-) to nitrogen gas (N2) via nitrite (NO_2^-), nitric oxide (NO) and nitrous oxide (N_2O). Each step is catalyzed by individual metalloenzymes: nitrate reductase (NAR), nitrite reductase (NIR), nitric oxide reductase (NOR) and nitrous oxide reductase (N_2OR) [317]. In *P. aeruginosa,* this metabolic pathway is regulated by the transcriptional regulator Anr (for anaerobic regulation of arginine catabolism and nitrate reduction), an analogue of the *E. coli* Fnr, which belongs to the Fnr-Crp regulator family [318,319]. These regulators sense the level of intracellular oxygen and induce required gene regulation to adapt to varying oxygen levels [320]. As our experiment was performed under aerobic conditions, it is possible that the increased generation of oxygen radicals led to a shortage and fluctuations in the levels of intracellular oxygen gas (O_2) and thus induced Anr dependent transcriptional regulation.

4.4.2 Sub-inhibitory antibiotic exposure affects the respiratory chain and leads to fundamental metabolic changes

As Anr is a critical component aiding in the adaptation of the energy metabolism, we sought to investigate the overall metabolic impact of low-level antibiotic exposure by analyzing amino acid biosynthesis pathways. In *P. aeruginosa,* these biosynthesis pathways initially use either glucose or acetate as substrates for the generation of their products. Thus, the conversion of both substrates was comparatively monitored with the help of isotope ^{13}C carbon.

Interestingly, all administered antibiotics led to a metabolic activation with a slightly enhanced amino acid biosynthesis, though kinetics differed for glucose and acetate integration, respectively. This can most likely be explained by the underlying chemical processes, which allow the use of acetate directly as substrate for the tricarboxylic acid cycle (TCA), while glucose has to undergo pre-

processing, e.g. in the Entner-Doudoroff pathway (ED), before its products can be used further (PseudoCyc, [241]).

The most interesting finding, however, was that independent of the respective antibiotic targets all antibiotics featured the induction of similar metabolic patterns. The biosynthesis of amino acids generated from acetate which were either directly derived from the TCA cycle or indirectly TCA cycle-dependent was markedly enhanced due to antibiotic treatment. Furthermore, there was a strong increase in serine, the first amino acid generated from glucose, precisely 3-phosphoglycerate, after its conversion with the help of NAD^+ and $NADP^+$ reduction.

In 2007, Kohanski and colleagues had proposed a "common mechanism of bacterial killing" for all bactericidal antibiotics. Briefly, this mechanism was supposed to include augmented activity of the electron transport chain and a thereby stimulated generation of superoxides. These superoxides are capable of damaging iron-sulfur clusters within proteins and enable hydrogen peroxide to interact with the resulting free ferrous iron. Via the Fenton reaction, oxidation of this iron leads to the production of hydroxyl radicals. When the hydroxyl radical pool reaches critical concentrations, DNA, lipid and protein damage occur and ultimately lead to cell death [164]. A sequential study observed that, indeed, the cytotoxicity of quinolones and β-lactams seems to arise predominantly from lethal double stand DNA breaks due to guanine oxidation caused by a hydroxyl radical depended process [169].

Particularly the occurrence of the Fenton reaction upon lethal antibiotic treatment and the production of hydroxyl radicals which may damage cell components have been confirmed by several other studies in which mostly radical scavengers as thiourea or iron chelators as 2,2'-dipyridyl were used to promote bacterial survival of different Gram-positive and -negative species upon antibiotic encounter [321-326]. However, it is still discussed controversy whether ROS generation is indeed the major cause for antibiotic provoked cell death and where the required stimulation of the electron transport chain originates from.

Kohanski and colleagues had monitored the NAD^+/NADH ratio upon antibiotic killing in *E. coli* and their hypothesis included that the hyperstimulation of the electron transport chain is due to enhanced TCA cycle activity [164]. In this study, we could confirm this proposed mechanism and further show that the elevated NADH and NADPH levels arise from enhanced metabolic activity not only of the TCA cycle, but possibly also related glucose processing pathways. Additionally, low level sub-MIC concentrations of bactericidal antibiotics were sufficient to induce these metabolic changes.

This argues not only in favor of the hypothesis presented by Kohanski, but also against the recently published models presented by Keren and Liu about the impact of bactericidal antibiotics. Both suggested that bactericidal killing does not depend on reactive oxygen species [165,166]. Liu investigated oxygen consumption post kanamycin and norfloxacin treatment with a Clark-type

electrode and argued based on the decline over time that an enhanced respiratory chain activity could not be the source of electrons required for ROS generation. We, however, could clearly demonstrate that antibiotics promote TCA cycle activity by measuring the biosynthesis of respiratory chain derived metabolites, whose production was significantly increased, compared to similar metabolites generated by other pathways. Furthermore, the biosynthesis was equally increased upon contact with all tested classes of antibiotics, even at the administered low-level concentrations. A next step will be to unravel how this common metabolic feedback is achieved by different classes of chemical compounds, and to further investigate combined stress response activation signals.

4.4.3 A need for avoiding trace-antibiotic reservoirs and targeting bacterial stress responses

Strikingly, such common stress response inductions even when facing low level antibiotic concentrations open new possibilities for bacteria. Antibiotic resistance may not only arise by the selection of previously mutated strains but also by an enhanced mutation potential upon drug encounter, which facilitates resistance evolution [42,169,327]. There is also evidence that some bacteria as *E. coli* promote oxidative stress protective mechanisms to enhance antibiotic tolerance in neighboring cells by the secretion of indole when facing increasing antibiotic gradients [328]. Altogether, this implies a particular threat for the development of further adaptations and cross resistances. Previous studies could show that sub-MIC treatment of *E. coli* cells with the β-lactam ampicillin, promoted resistance not only to ampicillin, but also different structurally unrelated antibiotics as norfloxacin, kanamycin or chloramphenicol [42]. Furthermore, within these studies a range of resistances was observed, often exceeding the values of the initially used sub-MIC concentrations. Thus, low-level antibiotics may likely promote the evolution of clinically significant resistance and cross-resistance levels. Making the matters worse, we are so far not able to predict the minimal antibiotic thresholds required for such occurrences as e.g. in one case 1/230 of the wild-type MIC was sufficient to select for a ciprofloxacin resistant mutant in *E. coli* harboring the also clinically relevant *gyrA* S82L exchange [329].

While these findings on the one hand illustrate the considerable threat emanating from the release of antibiotics into our environment, they may also open up new possibilities for effective antibacterial therapy by potentiating bactericidal activity with the use of additional drug targets. Their modes of action could include inhibiting dsDNA repair mechanisms (e.g. Rec) or enzymes involved in the process of controlling hydroxyl radical generation as catalases-peroxidases which are responsible for hydrogen peroxide detoxification (before it may enter the Fenton reaction) [330].

This approach could also be of particular interest for the treatment of *P. aeruginosa*, as it was recently proposed, that the bacterium's enhanced antibiotic tolerance within biofilms might result to

a large extent from active starvation control (stringent response) and a connected reduction of oxidative stress, rather than passive growth arrest [331,332].

5 References

1. Anzai Y, Kim H, Park JY, Wakabayashi H, Oyaizu H (2000) Phylogenetic affiliation of the pseudomonads based on 16S rRNA sequence. Int J Syst Evol Microbiol 50 Pt 4: 1563-1589.
2. Palleroni NJ (2003) Prokaryote taxonomy of the 20th century and the impact of studies on the genus Pseudomonas: a personal view. Microbiology 149: 1-7.
3. Yamamoto S, Kasai H, Arnold DL, Jackson RW, Vivian A, et al. (2000) Phylogeny of the genus Pseudomonas: intrageneric structure reconstructed from the nucleotide sequences of gyrB and rpoD genes. Microbiology 146 (Pt 10): 2385-2394.
4. Cultures DLID-GCoMaC.
5. Goldberg JB (2000) Pseudomonas: global bacteria. Trends Microbiol 8: 55-57.
6. Williams HD, Zlosnik JE, Ryall B (2007) Oxygen, cyanide and energy generation in the cystic fibrosis pathogen Pseudomonas aeruginosa. Adv Microb Physiol 52: 1-71.
7. Van Alst NE, Picardo KF, Iglewski BH, Haidaris CG (2007) Nitrate sensing and metabolism modulate motility, biofilm formation, and virulence in Pseudomonas aeruginosa. Infect Immun 75: 3780-3790.
8. Vander Wauven C PA, Kley-Raymann M, Haas D. (1984) Pseudomonas aeruginosa mutants affected in anaerobic growth on arginine: evidence for a four-gene cluster encoding the arginine deiminase pathway. J Bacteriol 160: 928-934.
9. Eschbach M, Schreiber K, Trunk K, Buer J, Jahn D, et al. (2004) Long-term anaerobic survival of the opportunistic pathogen Pseudomonas aeruginosa via pyruvate fermentation. J Bacteriol 186: 4596-4604.
10. Haas D, Matsumoto H, Moretti P, Stalon V, Mercenier A (1984) Arginine degradation in Pseudomonas aeruginosa mutants blocked in two arginine catabolic pathways. Mol Gen Genet 193: 437-444.
11. Palleroni NJ (1993) Pseudomonas classification. A new case history in the taxonomy of gram-negative bacteria. Antonie Van Leeuwenhoek 64: 231-251.
12. Lessie TG, Phibbs PV, Jr. (1984) Alternative pathways of carbohydrate utilization in pseudomonads. Annu Rev Microbiol 38: 359-388.
13. Entner N, Doudoroff M (1952) Glucose and gluconic acid oxidation of Pseudomonas saccharophila. J Biol Chem 196: 853-862.
14. Green SK, Schroth MN, Cho JJ, Kominos SK, Vitanza-jack VB (1974) Agricultural plants and soil as a reservoir for Pseudomonas aeruginosa. Appl Microbiol 28: 987-991.
15. Rahme LG, Stevens EJ, Wolfort SF, Shao J, Tompkins RG, et al. (1995) Common virulence factors for bacterial pathogenicity in plants and animals. Science 268: 1899-1902.
16. Petersen AD, Walker RD, Bowman MM, Schott HC, 2nd, Rosser EJ, Jr. (2002) Frequency of isolation and antimicrobial susceptibility patterns of Staphylococcus intermedius and Pseudomonas aeruginosa isolates from canine skin and ear samples over a 6-year period (1992-1997). J Am Anim Hosp Assoc 38: 407-413.
17. Morrison AJ, Jr., Wenzel RP (1984) Epidemiology of infections due to Pseudomonas aeruginosa. Rev Infect Dis 6 Suppl 3: S627-642.
18. Lister PD, Wolter DJ, Hanson ND (2009) Antibacterial-resistant Pseudomonas aeruginosa: clinical impact and complex regulation of chromosomally encoded resistance mechanisms. Clin Microbiol Rev 22: 582-610.
19. NNIS (1998) National Nosocomial Infections Surveillance System report, data summary from October 1986-April 1998, issued June 1998. Am J Infect Control 26: 522-533.
20. Gaynes R, Edwards JR, National Nosocomial Infections Surveillance S (2005) Overview of nosocomial infections caused by gram-negative bacilli. Clin Infect Dis 41: 848-854.
21. U.S. Department of Health and human Services - Centers for Disease Control and Prevention (2013) Antibiotic Resistance Threats in the United States.

22. Lyczak JB, Cannon CL, Pier GB (2002) Lung infections associated with cystic fibrosis. Clin Microbiol Rev 15: 194-222.
23. Ratjen F, Doring G (2003) Cystic fibrosis. Lancet 361: 681-689.
24. Tümmler B, Kiewitz C (1999) Cystic fibrosis: an inherited susceptibility to bacterial respiratory infections. Mol Med Today 5: 351-358.
25. Visca P, Colotti G, Serino L, Verzili D, Orsi N, et al. (1992) Metal regulation of siderophore synthesis in Pseudomonas aeruginosa and functional effects of siderophore-metal complexes. Appl Environ Microbiol 58: 2886-2893.
26. Hauser AR (2009) The type III secretion system of Pseudomonas aeruginosa: infection by injection. Nat Rev Microbiol 7: 654-665.
27. Reszka KJ, Bilski PJ, Britigan BE (2010) Quenching of singlet oxygen by pyocyanin and related phenazines. Photochem Photobiol 86: 742-746.
28. Abdel-Mawgoud AM, Lepine F, Deziel E (2010) Rhamnolipids: diversity of structures, microbial origins and roles. Appl Microbiol Biotechnol 86: 1323-1336.
29. Burrows LL (2005) Weapons of mass retraction. Mol Microbiol 57: 878-888.
30. Magiorakos AP, Srinivasan A, Carey RB, Carmeli Y, Falagas ME, et al. (2012) Multidrug-resistant, extensively drug-resistant and pandrug-resistant bacteria: an international expert proposal for interim standard definitions for acquired resistance. Clin Microbiol Infect 18: 268-281.
31. Robert Koch Institut (2012) Hygienemaßnahmen bei Infektionen oder Besiedlung mit multiresistenten gramnegativen Stäbchen. In: Bundesgesundheitsblatt 55; Abteilung: Kommission für Krankenhaushygiene und Infektionsprävention, editor: Springer-Verlag. pp. 1311–1354.
32. Gasink LB, Fishman NO, Weiner MG, Nachamkin I, Bilker WB, et al. (2006) Fluoroquinolone-resistant Pseudomonas aeruginosa: assessment of risk factors and clinical impact. Am J Med 119: 526 e519-525.
33. Aloush V, Navon-Venezia S, Seigman-Igra Y, Cabili S, Carmeli Y (2006) Multidrug-resistant Pseudomonas aeruginosa: risk factors and clinical impact. Antimicrob Agents Chemother 50: 43-48.
34. Carmeli Y, Troillet N, Karchmer AW, Samore MH (1999) Health and economic outcomes of antibiotic resistance in Pseudomonas aeruginosa. Arch Intern Med 159: 1127-1132.
35. Tansarli GS, Karageorgopoulos DE, Kapaskelis A, Falagas ME (2013) Impact of antimicrobial multidrug resistance on inpatient care cost: an evaluation of the evidence. Expert Rev Anti Infect Ther 11: 321-331.
36. Forrest RD (1982) Early history of wound treatment. J R Soc Med 75: 198-205.
37. Foster W, Raoult A (1974) Early descriptions of antibiosis. J R Coll Gen Pract 24: 889-894.
38. Waksman SA (1947) What is an antibiotic or an antibiotic substance? Mycologia 39: 565-569.
39. Coates A, Hu Y, Bax R, Page C (2002) The future challenges facing the development of new antimicrobial drugs. Nat Rev Drug Discov 1: 895-910.
40. Schwentker FF, Gelman S, Long PH (1984) Landmark article April 24, 1937. The treatment of meningococcic meningitis with sulfanilamide. Preliminary report. By Francis F. Schwentker, Sidney Gelman, and Perrin H. Long. JAMA 251: 788-790.
41. Coates AR, Halls G, Hu Y (2011) Novel classes of antibiotics or more of the same? Br J Pharmacol 163: 184-194.
42. Kohanski MA, Dwyer DJ, Collins JJ (2010) How antibiotics kill bacteria: from targets to networks. Nat Rev Microbiol 8: 423-435.
43. Walsh C (2003) Antibiotics: Actions, Origins, Resistance: ASM Press.
44. Moore NM, Flaws ML (2011) Treatment strategies and recommendations for Pseudomonas aeruginosa infections. Clin Lab Sci 24: 52-56.
45. Mingeot-Leclercq MP, Glupczynski Y, Tulkens PM (1999) Aminoglycosides: activity and resistance. Antimicrob Agents Chemother 43: 727-737.
46. Drlica K, Hiasa H, Kerns R, Malik M, Mustaev A, et al. (2009) Quinolones: action and resistance updated. Curr Top Med Chem 9: 981-998.
47. Poole K (2004) Resistance to beta-lactam antibiotics. Cell Mol Life Sci 61: 2200-2223.

48. Worthington RJ, Melander C (2013) Overcoming resistance to beta-lactam antibiotics. J Org Chem 78: 4207-4213.
49. Bartlett JG (2003) Pocket Book of Infectious Disease Therapy. Baltimore: Lippincott Williams & Wilkins.
50. Holtje JV (1998) Growth of the stress-bearing and shape-maintaining murein sacculus of Escherichia coli. Microbiol Mol Biol Rev 62: 181-203.
51. Madigan MT, Martinko JM, Stahl DA, Clark DP (2011) Brock Biology of Microorganisms: Pearson.
52. Zapun A, Contreras-Martel C, Vernet T (2008) Penicillin-binding proteins and beta-lactam resistance. FEMS Microbiol Rev 32: 361-385.
53. Tipper DJ, Strominger JL (1965) Mechanism of action of penicillins: a proposal based on their structural similarity to acyl-D-alanyl-D-alanine. Proc Natl Acad Sci U S A 54: 1133-1141.
54. Fish DN, Piscitelli SC, Danziger LH (1995) Development of resistance during antimicrobial therapy: a review of antibiotic classes and patient characteristics in 173 studies. Pharmacotherapy 15: 279-291.
55. Dimatatac EL, Alejandria MM, Montalban C, Pineda C, Ang C, et al. (2003) Clinical outcomes and costs of care of antibiotic resistant Pseudomonas aeruginosa infections. Philipp J Microbiol Infect Dis 32: 159-167.
56. Morita Y, Tomida J, Kawamura Y (2014) Responses of Pseudomonas aeruginosa to antimicrobials. Front Microbiol 4: 422.
57. Yoshimura F, Nikaido H (1982) Permeability of Pseudomonas aeruginosa outer membrane to hydrophilic solutes. J Bacteriol 152: 636-642.
58. Schweizer HP (2003) Efflux as a mechanism of resistance to antimicrobials in Pseudomonas aeruginosa and related bacteria: unanswered questions. Genet Mol Res 2: 48-62.
59. Nikaido H (1994) Prevention of drug access to bacterial targets: permeability barriers and active efflux. Science 264: 382-388.
60. Poole K (2001) Multidrug efflux pumps and antimicrobial resistance in Pseudomonas aeruginosa and related organisms. J Mol Microbiol Biotechnol 3: 255-264.
61. Piddock LJ (2006) Multidrug-resistance efflux pumps - not just for resistance. Nat Rev Microbiol 4: 629-636.
62. Poole K (2005) Efflux-mediated antimicrobial resistance. J Antimicrob Chemother 56: 20-51.
63. Kohler T, van Delden C, Curty LK, Hamzehpour MM, Pechere JC (2001) Overexpression of the MexEF-OprN multidrug efflux system affects cell-to-cell signaling in Pseudomonas aeruginosa. J Bacteriol 183: 5213-5222.
64. Lomovskaya O, Lee A, Hoshino K, Ishida H, Mistry A, et al. (1999) Use of a genetic approach to evaluate the consequences of inhibition of efflux pumps in Pseudomonas aeruginosa. Antimicrob Agents Chemother 43: 1340-1346.
65. Jahandideh S (2013) Diversity in structural consequences of MexZ mutations in Pseudomonas aeruginosa. Chem Biol Drug Des 81: 600-606.
66. Sobel ML, Hocquet D, Cao L, Plesiat P, Poole K (2005) Mutations in PA3574 (nalD) lead to increased MexAB-OprM expression and multidrug resistance in laboratory and clinical isolates of Pseudomonas aeruginosa. Antimicrob Agents Chemother 49: 1782-1786.
67. Sobel ML, Neshat S, Poole K (2005) Mutations in PA2491 (mexS) promote MexT-dependent mexEF-oprN expression and multidrug resistance in a clinical strain of Pseudomonas aeruginosa. J Bacteriol 187: 1246-1253.
68. Elena SF, Lenski RE (2003) Evolution experiments with microorganisms: the dynamics and genetic bases of adaptation. Nat Rev Genet 4: 457-469.
69. Bruchmann S, Dötsch A, Nouri B, Chaberny IF, Häussler S (2013) Quantitative contributions of target alteration and decreased drug accumulation to Pseudomonas aeruginosa fluoroquinolone resistance. Antimicrob Agents Chemother 57: 1361-1368.
70. Masuda N, Gotoh N, Ohya S, Nishino T (1996) Quantitative correlation between susceptibility and OprJ production in NfxB mutants of Pseudomonas aeruginosa. Antimicrob Agents Chemother 40: 909-913.

71. Masuda N, Sakagawa E, Ohya S, Gotoh N, Tsujimoto H, et al. (2000) Substrate specificities of MexAB-OprM, MexCD-OprJ, and MexXY-oprM efflux pumps in Pseudomonas aeruginosa. Antimicrob Agents Chemother 44: 3322-3327.
72. Baum EZ, Crespo-Carbone SM, Morrow BJ, Davies TA, Foleno BD, et al. (2009) Effect of MexXY overexpression on ceftobiprole susceptibility in Pseudomonas aeruginosa. Antimicrob Agents Chemother 53: 2785-2790.
73. Srikumar R, Kon T, Gotoh N, Poole K (1998) Expression of Pseudomonas aeruginosa multidrug efflux pumps MexA-MexB-OprM and MexC-MexD-OprJ in a multidrug-sensitive Escherichia coli strain. Antimicrob Agents Chemother 42: 65-71.
74. Li XZ, Nikaido H, Poole K (1995) Role of mexA-mexB-oprM in antibiotic efflux in Pseudomonas aeruginosa. Antimicrob Agents Chemother 39: 1948-1953.
75. Hancock RE, Brinkman FS (2002) Function of pseudomonas porins in uptake and efflux. Annu Rev Microbiol 56: 17-38.
76. Yoshimura F, Nikaido H (1985) Diffusion of beta-lactam antibiotics through the porin channels of Escherichia coli K-12. Antimicrob Agents Chemother 27: 84-92.
77. Nikaido H (1989) Outer membrane barrier as a mechanism of antimicrobial resistance. Antimicrob Agents Chemother 33: 1831-1836.
78. Hancock RE (1987) Role of porins in outer membrane permeability. J Bacteriol 169: 929-933.
79. Stover CK, Pham XQ, Erwin AL, Mizoguchi SD, Warrener P, et al. (2000) Complete genome sequence of Pseudomonas aeruginosa PAO1, an opportunistic pathogen. Nature 406: 959-964.
80. Trias J, Nikaido H (1990) Outer membrane protein D2 catalyzes facilitated diffusion of carbapenems and penems through the outer membrane of Pseudomonas aeruginosa. Antimicrob Agents Chemother 34: 52-57.
81. Köhler T, Michea-Hamzehpour M, Epp SF, Pechere JC (1999) Carbapenem activities against Pseudomonas aeruginosa: respective contributions of OprD and efflux systems. Antimicrob Agents Chemother 43: 424-427.
82. Sakyo S, Tomita H, Tanimoto K, Fujimoto S, Ike Y (2006) Potency of carbapenems for the prevention of carbapenem-resistant mutants of Pseudomonas aeruginosa: the high potency of a new carbapenem doripenem. J Antibiot (Tokyo) 59: 220-228.
83. Naenna P, Noisumdaeng P, Pongpech P, Tribuddharat C (2010) Detection of outer membrane porin protein, an imipenem influx channel, in Pseudomonas aeruginosa clinical isolates. Southeast Asian J Trop Med Public Health 41: 614-624.
84. Trias J, Nikaido H (1990) Protein D2 channel of the Pseudomonas aeruginosa outer membrane has a binding site for basic amino acids and peptides. J Biol Chem 265: 15680-15684.
85. Muramatsu H, Horii T, Morita M, Hashimoto H, Kanno T, et al. (2003) Effect of basic amino acids on susceptibility to carbapenems in clinical Pseudomonas aeruginosa isolates. Int J Med Microbiol 293: 191-197.
86. Tamber S, Hancock RE (2006) Involvement of two related porins, OprD and OpdP, in the uptake of arginine by Pseudomonas aeruginosa. FEMS Microbiol Lett 260: 23-29.
87. Tamber S, Ochs MM, Hancock RE (2006) Role of the novel OprD family of porins in nutrient uptake in Pseudomonas aeruginosa. J Bacteriol 188: 45-54.
88. Li H, Luo YF, Williams BJ, Blackwell TS, Xie CM (2012) Structure and function of OprD protein in Pseudomonas aeruginosa: from antibiotic resistance to novel therapies. Int J Med Microbiol 302: 63-68.
89. Lynch MJ, Drusano GL, Mobley HL (1987) Emergence of resistance to imipenem in Pseudomonas aeruginosa. Antimicrob Agents Chemother 31: 1892-1896.
90. Wolter DJ, Hanson ND, Lister PD (2004) Insertional inactivation of oprD in clinical isolates of Pseudomonas aeruginosa leading to carbapenem resistance. FEMS Microbiol Lett 236: 137-143.
91. Ochs MM, Bains M, Hancock RE (2000) Role of putative loops 2 and 3 in imipenem passage through the specific porin OprD of Pseudomonas aeruginosa. Antimicrob Agents Chemother 44: 1983-1985.

92. Huang H, Jeanteur D, Pattus F, Hancock RE (1995) Membrane topology and site-specific mutagenesis of Pseudomonas aeruginosa porin OprD. Mol Microbiol 16: 931-941.
93. Biswas S, Mohammad MM, Patel DR, Movileanu L, van den Berg B (2007) Structural insight into OprD substrate specificity. Nat Struct Mol Biol 14: 1108-1109.
94. Huang H, Hancock RE (1996) The role of specific surface loop regions in determining the function of the imipenem-specific pore protein OprD of Pseudomonas aeruginosa. J Bacteriol 178: 3085-3090.
95. Epp SF, Kohler T, Plesiat P, Michea-Hamzehpour M, Frey J, et al. (2001) C-terminal region of Pseudomonas aeruginosa outer membrane porin OprD modulates susceptibility to meropenem. Antimicrob Agents Chemother 45: 1780-1787.
96. Pirnay JP, De Vos D, Mossialos D, Vanderkelen A, Cornelis P, et al. (2002) Analysis of the Pseudomonas aeruginosa oprD gene from clinical and environmental isolates. Environ Microbiol 4: 872-882.
97. Ocampo-Sosa AA, Cabot G, Rodriguez C, Roman E, Tubau F, et al. (2012) Alterations of OprD in carbapenem-intermediate and -susceptible strains of Pseudomonas aeruginosa isolated from patients with bacteremia in a Spanish multicenter study. Antimicrob Agents Chemother 56: 1703-1713.
98. Galdiero S, Falanga A, Cantisani M, Tarallo R, Della Pepa ME, et al. (2012) Microbe-host interactions: structure and role of Gram-negative bacterial porins. Curr Protein Pept Sci 13: 843-854.
99. Ochs MM, Lu CD, Hancock RE, Abdelal AT (1999) Amino acid-mediated induction of the basic amino acid-specific outer membrane porin OprD from Pseudomonas aeruginosa. J Bacteriol 181: 5426-5432.
100. Perron K, Caille O, Rossier C, Van Delden C, Dumas JL, et al. (2004) CzcR-CzcS, a two-component system involved in heavy metal and carbapenem resistance in Pseudomonas aeruginosa. J Biol Chem 279: 8761-8768.
101. Conejo MC, Garcia I, Martinez-Martinez L, Picabea L, Pascual A (2003) Zinc eluted from siliconized latex urinary catheters decreases OprD expression, causing carbapenem resistance in Pseudomonas aeruginosa. Antimicrob Agents Chemother 47: 2313-2315.
102. Caille O, Rossier C, Perron K (2007) A copper-activated two-component system interacts with zinc and imipenem resistance in Pseudomonas aeruginosa. J Bacteriol 189: 4561-4568.
103. Muller C, Plesiat P, Jeannot K (2011) A two-component regulatory system interconnects resistance to polymyxins, aminoglycosides, fluoroquinolones, and beta-lactams in Pseudomonas aeruginosa. Antimicrob Agents Chemother 55: 1211-1221.
104. Köhler T, Michea-Hamzehpour M, Henze U, Gotoh N, Curty LK, et al. (1997) Characterization of MexE-MexF-OprN, a positively regulated multidrug efflux system of Pseudomonas aeruginosa. Mol Microbiol 23: 345-354.
105. Ochs MM, McCusker MP, Bains M, Hancock RE (1999) Negative regulation of the Pseudomonas aeruginosa outer membrane porin OprD selective for imipenem and basic amino acids. Antimicrob Agents Chemother 43: 1085-1090.
106. Köhler T, Epp SF, Curty LK, Pechere JC (1999) Characterization of MexT, the regulator of the MexE-MexF-OprN multidrug efflux system of Pseudomonas aeruginosa. J Bacteriol 181: 6300-6305.
107. Nikolaidis I, Favini-Stabile S, Dessen A (2013) Resistance to antibiotics targeted to the bacterial cell wall. Protein Sci.
108. Majiduddin FK, Materon IC, Palzkill TG (2002) Molecular analysis of beta-lactamase structure and function. Int J Med Microbiol 292: 127-137.
109. Bush K, Jacoby GA (2010) Updated functional classification of beta-lactamases. Antimicrob Agents Chemother 54: 969-976.
110. Jacoby G, Bush K.
111. Perez-Llarena FJ, Kerff F, Zamorano L, Fernandez MC, Nunez ML, et al. (2013) Characterization of the new AmpC beta-lactamase FOX-8 reveals a single mutation, Phe313Leu, located in the R2 loop that affects ceftazidime hydrolysis. Antimicrob Agents Chemother 57: 5158-5161.

112. Bebrone C, Bogaerts P, Delbruck H, Bennink S, Kupper MB, et al. (2013) GES-18, a new carbapenem-hydrolyzing GES-Type beta-lactamase from Pseudomonas aeruginosa that contains Ile80 and Ser170 residues. Antimicrob Agents Chemother 57: 396-401.
113. Pollini S, Maradei S, Pecile P, Olivo G, Luzzaro F, et al. (2013) FIM-1, a new acquired metallo-beta-lactamase from a Pseudomonas aeruginosa clinical isolate from Italy. Antimicrob Agents Chemother 57: 410-416.
114. Cornaglia G, Giamarellou H, Rossolini GM (2011) Metallo-beta-lactamases: a last frontier for beta-lactams? Lancet Infect Dis 11: 381-393.
115. Ambler RP (1980) The structure of beta-lactamases. Philos Trans R Soc Lond B Biol Sci 289: 321-331.
116. Naas T, Nordmann P (1999) OXA-type beta-lactamases. Curr Pharm Des 5: 865-879.
117. Walsh TR, Toleman MA, Poirel L, Nordmann P (2005) Metallo-beta-lactamases: the quiet before the storm? Clin Microbiol Rev 18: 306-325.
118. Queenan AM, Bush K (2007) Carbapenemases: the versatile beta-lactamases. Clin Microbiol Rev 20: 440-458, table of contents.
119. Girlich D, Naas T, Leelaporn A, Poirel L, Fennewald M, et al. (2002) Nosocomial spread of the integron-located veb-1-like cassette encoding an extended-pectrum beta-lactamase in Pseudomonas aeruginosa in Thailand. Clin Infect Dis 34: 603-611.
120. Morfin-Otero R, Rodriguez-Noriega E, Deshpande LM, Sader HS, Castanheira M (2009) Dissemination of a bla(VIM-2)-carrying integron among Enterobacteriaceae species in Mexico: report from the SENTRY Antimicrobial Surveillance Program. Microb Drug Resist 15: 33-35.
121. Mendes RE, Bell JM, Turnidge JD, Castanheira M, Jones RN (2009) Emergence and widespread dissemination of OXA-23, -24/40 and -58 carbapenemases among Acinetobacter spp. in Asia-Pacific nations: report from the SENTRY Surveillance Program. J Antimicrob Chemother 63: 55-59.
122. Medeiros AA (1997) Evolution and dissemination of beta-lactamases accelerated by generations of beta-lactam antibiotics. Clin Infect Dis 24 Suppl 1: S19-45.
123. Poirel L, Nordmann P (2002) Acquired carbapenem-hydrolyzing beta-lactamases and their genetic support. Curr Pharm Biotechnol 3: 117-127.
124. Hall RM, Collis CM (1998) Antibiotic resistance in gram-negative bacteria: the role of gene cassettes and integrons. Drug Resist Updat 1: 109-119.
125. Partridge SR, Tsafnat G, Coiera E, Iredell JR (2009) Gene cassettes and cassette arrays in mobile resistance integrons. FEMS Microbiol Rev 33: 757-784.
126. Cambray G, Guerout AM, Mazel D (2010) Integrons. Annu Rev Genet 44: 141-166.
127. Stokes HW, Hall RM (1989) A novel family of potentially mobile DNA elements encoding site-specific gene-integration functions: integrons. Mol Microbiol 3: 1669-1683.
128. Collis CM, Hall RM (1992) Site-specific deletion and rearrangement of integron insert genes catalyzed by the integron DNA integrase. J Bacteriol 174: 1574-1585.
129. Miriagou V, Cornaglia G, Edelstein M, Galani I, Giske CG, et al. (2010) Acquired carbapenemases in Gram-negative bacterial pathogens: detection and surveillance issues. Clin Microbiol Infect 16: 112-122.
130. Akinci E, Vahaboglu H (2010) Minor extended-spectrum beta-lactamases. Expert Rev Anti Infect Ther 8: 1251-1258.
131. Poirel L, Weldhagen GF, De Champs C, Nordmann P (2002) A nosocomial outbreak of Pseudomonas aeruginosa isolates expressing the extended-spectrum beta-lactamase GES-2 in South Africa. J Antimicrob Chemother 49: 561-565.
132. Claeys G, Verschraegen G, de Baere T, Vaneechoutte M (2000) PER-1 beta-lactamase-producing Pseudomonas aeruginosa in an intensive care unit. J Antimicrob Chemother 45: 924-925.
133. Polotto M, Casella T, de Lucca Oliveira MG, Rubio FG, Nogueira ML, et al. (2012) Detection of P. aeruginosa harboring bla CTX-M-2, bla GES-1 and bla GES-5, bla IMP-1 and bla SPM-1 causing infections in Brazilian tertiary-care hospital. BMC Infect Dis 12: 176.

134. Danel F, Hall LM, Duke B, Gur D, Livermore DM (1999) OXA-17, a further extended-spectrum variant of OXA-10 beta-lactamase, isolated from Pseudomonas aeruginosa. Antimicrob Agents Chemother 43: 1362-1366.
135. Naas T, Poirel L, Karim A, Nordmann P (1999) Molecular characterization of In50, a class 1 integron encoding the gene for the extended-spectrum beta-lactamase VEB-1 in Pseudomonas aeruginosa. FEMS Microbiol Lett 176: 411-419.
136. Paterson DL, Bonomo RA (2005) Extended-spectrum beta-lactamases: a clinical update. Clin Microbiol Rev 18: 657-686.
137. Girlich D, Naas T, Nordmann P (2004) Biochemical characterization of the naturally occurring oxacillinase OXA-50 of Pseudomonas aeruginosa. Antimicrob Agents Chemother 48: 2043-2048.
138. Sanders CC, Sanders WE, Jr. (1986) Type I beta-lactamases of gram-negative bacteria: interactions with beta-lactam antibiotics. J Infect Dis 154: 792-800.
139. Rodriguez-Martinez JM, Poirel L, Nordmann P (2009) Extended-spectrum cephalosporinases in Pseudomonas aeruginosa. Antimicrob Agents Chemother 53: 1766-1771.
140. Poole K (2011) Pseudomonas aeruginosa: resistance to the max. Front Microbiol 2: 65.
141. Livermore DM (1995) beta-Lactamases in laboratory and clinical resistance. Clin Microbiol Rev 8: 557-584.
142. Bagge N, Schuster M, Hentzer M, Ciofu O, Givskov M, et al. (2004) Pseudomonas aeruginosa biofilms exposed to imipenem exhibit changes in global gene expression and beta-lactamase and alginate production. Antimicrob Agents Chemother 48: 1175-1187.
143. Tam VH, Chang KT, Schilling AN, LaRocco MT, Genty LO, et al. (2009) Impact of AmpC overexpression on outcomes of patients with Pseudomonas aeruginosa bacteremia. Diagn Microbiol Infect Dis 63: 279-285.
144. Xavier DE, Picao RC, Girardello R, Fehlberg LC, Gales AC (2010) Efflux pumps expression and its association with porin down-regulation and beta-lactamase production among Pseudomonas aeruginosa causing bloodstream infections in Brazil. BMC Microbiol 10: 217.
145. Drissi M, Ahmed ZB, Dehecq B, Bakour R, Plesiat P, et al. (2008) Antibiotic susceptibility and mechanisms of beta-lactam resistance among clinical strains of Pseudomonas aeruginosa: first report in Algeria. Med Mal Infect 38: 187-191.
146. Cheng Q, Park JT (2002) Substrate specificity of the AmpG permease required for recycling of cell wall anhydro-muropeptides. J Bacteriol 184: 6434-6436.
147. Holtje JV, Kopp U, Ursinus A, Wiedemann B (1994) The negative regulator of beta-lactamase induction AmpD is a N-acetyl-anhydromuramyl-L-alanine amidase. FEMS Microbiol Lett 122: 159-164.
148. Langaee TY, Dargis M, Huletsky A (1998) An ampD gene in Pseudomonas aeruginosa encodes a negative regulator of AmpC beta-lactamase expression. Antimicrob Agents Chemother 42: 3296-3300.
149. Jacobs C, Frere JM, Normark S (1997) Cytosolic intermediates for cell wall biosynthesis and degradation control inducible beta-lactam resistance in gram-negative bacteria. Cell 88: 823-832.
150. Dietz H, Pfeifle D, Wiedemann B (1996) Location of N-acetylmuramyl-L-alanyl-D-glutamylmesodiaminopimelic acid, presumed signal molecule for beta-lactamase induction, in the bacterial cell. Antimicrob Agents Chemother 40: 2173-2177.
151. Bagge N, Ciofu O, Hentzer M, Campbell JI, Givskov M, et al. (2002) Constitutive high expression of chromosomal beta-lactamase in Pseudomonas aeruginosa caused by a new insertion sequence (IS1669) located in ampD. Antimicrob Agents Chemother 46: 3406-3411.
152. Schmidtke AJ, Hanson ND (2008) Role of ampD homologs in overproduction of AmpC in clinical isolates of Pseudomonas aeruginosa. Antimicrob Agents Chemother 52: 3922-3927.
153. Juan C, Moya B, Perez JL, Oliver A (2006) Stepwise upregulation of the Pseudomonas aeruginosa chromosomal cephalosporinase conferring high-level beta-lactam resistance involves three AmpD homologues. Antimicrob Agents Chemother 50: 1780-1787.

154. Juan C, Macia MD, Gutierrez O, Vidal C, Perez JL, et al. (2005) Molecular mechanisms of beta-lactam resistance mediated by AmpC hyperproduction in Pseudomonas aeruginosa clinical strains. Antimicrob Agents Chemother 49: 4733-4738.
155. Moya B, Dötsch A, Juan C, Blazquez J, Zamorano L, et al. (2009) Beta-lactam resistance response triggered by inactivation of a nonessential penicillin-binding protein. PLoS Pathog 5: e1000353.
156. Fajardo A, Martinez-Martin N, Mercadillo M, Galan JC, Ghysels B, et al. (2008) The neglected intrinsic resistome of bacterial pathogens. PLoS One 3: e1619.
157. Breidenstein EB, Khaira BK, Wiegand I, Overhage J, Hancock RE (2008) Complex ciprofloxacin resistome revealed by screening a Pseudomonas aeruginosa mutant library for altered susceptibility. Antimicrob Agents Chemother 52: 4486-4491.
158. Schurek KN, Marr AK, Taylor PK, Wiegand I, Semenec L, et al. (2008) Novel genetic determinants of low-level aminoglycoside resistance in Pseudomonas aeruginosa. Antimicrob Agents Chemother 52: 4213-4219.
159. Alvarez-Ortega C, Wiegand I, Olivares J, Hancock RE, Martinez JL (2010) Genetic determinants involved in the susceptibility of Pseudomonas aeruginosa to beta-lactam antibiotics. Antimicrob Agents Chemother 54: 4159-4167.
160. Fernandez L, Alvarez-Ortega C, Wiegand I, Olivares J, Kocincova D, et al. (2013) Characterization of the polymyxin B resistome of Pseudomonas aeruginosa. Antimicrob Agents Chemother 57: 110-119.
161. Valentini M, Lapouge K (2013) Catabolite repression in Pseudomonas aeruginosa PAO1 regulates the uptake of C4 -dicarboxylates depending on succinate concentration. Environ Microbiol 15: 1707-1716.
162. Linares JF, Moreno R, Fajardo A, Martinez-Solano L, Escalante R, et al. (2010) The global regulator Crc modulates metabolism, susceptibility to antibiotics and virulence in Pseudomonas aeruginosa. Environ Microbiol 12: 3196-3212.
163. Zhang L, Chiang WC, Gao Q, Givskov M, Tolker-Nielsen T, et al. (2012) The catabolite repression control protein Crc plays a role in the development of antimicrobial-tolerant subpopulations in Pseudomonas aeruginosa biofilms. Microbiology 158: 3014-3019.
164. Kohanski MA, Dwyer DJ, Hayete B, Lawrence CA, Collins JJ (2007) A common mechanism of cellular death induced by bactericidal antibiotics. Cell 130: 797-810.
165. Liu Y, Imlay JA (2013) Cell death from antibiotics without the involvement of reactive oxygen species. Science 339: 1210-1213.
166. Keren I, Wu Y, Inocencio J, Mulcahy LR, Lewis K (2013) Killing by bactericidal antibiotics does not depend on reactive oxygen species. Science 339: 1213-1216.
167. Wang X, Zhao X, Malik M, Drlica K (2010) Contribution of reactive oxygen species to pathways of quinolone-mediated bacterial cell death. J Antimicrob Chemother 65: 520-524.
168. Grant SS, Kaufmann BB, Chand NS, Haseley N, Hung DT (2012) Eradication of bacterial persisters with antibiotic-generated hydroxyl radicals. Proc Natl Acad Sci U S A 109: 12147-12152.
169. Foti JJ, Devadoss B, Winkler JA, Collins JJ, Walker GC (2012) Oxidation of the guanine nucleotide pool underlies cell death by bactericidal antibiotics. Science 336: 315-319.
170. Fleischmann RD, Adams MD, White O, Clayton RA, Kirkness EF, et al. (1995) Whole-genome random sequencing and assembly of Haemophilus influenzae Rd. Science 269: 496-512.
171. Metzker ML (2005) Emerging technologies in DNA sequencing. Genome Res 15: 1767-1776.
172. Collins FS, Morgan M, Patrinos A (2003) The Human Genome Project: lessons from large-scale biology. Science 300: 286-290.
173. Loman NJ, Constantinidou C, Chan JZ, Halachev M, Sergeant M, et al. (2012) High-throughput bacterial genome sequencing: an embarrassment of choice, a world of opportunity. Nat Rev Microbiol 10: 599-606.
174. Kurzweil R (2001) The 21st Century: a Confluence of Accelerating Revolutions. KurzweilAI.net.
175. NCBI-Genome-Reports ftp://ftp.ncbi.nlm.nih.gov/genomes/GENOME_REPORTS/prokaryotes.txt. Accessed 31st of January 2014.

176. Bentley DR, Balasubramanian S, Swerdlow HP, Smith GP, Milton J, et al. (2008) Accurate whole human genome sequencing using reversible terminator chemistry. Nature 456: 53-59.
177. Ronaghi M, Uhlen M, Nyren P (1998) A sequencing method based on real-time pyrophosphate. Science 281: 363, 365.
178. Shendure J, Porreca GJ, Reppas NB, Lin X, McCutcheon JP, et al. (2005) Accurate multiplex polony sequencing of an evolved bacterial genome. Science 309: 1728-1732.
179. Metzker ML (2010) Sequencing technologies - the next generation. Nat Rev Genet 11: 31-46.
180. Sorek R, Cossart P (2010) Prokaryotic transcriptomics: a new view on regulation, physiology and pathogenicity. Nat Rev Genet 11: 9-16.
181. Wang Z, Gerstein M, Snyder M (2009) RNA-Seq: a revolutionary tool for transcriptomics. Nat Rev Genet 10: 57-63.
182. Croucher NJ, Thomson NR (2010) Studying bacterial transcriptomes using RNA-seq. Curr Opin Microbiol 13: 619-624.
183. Yoder-Himes DR, Chain PS, Zhu Y, Wurtzel O, Rubin EM, et al. (2009) Mapping the Burkholderia cenocepacia niche response via high-throughput sequencing. Proc Natl Acad Sci U S A 106: 3976-3981.
184. Cho BK, Zengler K, Qiu Y, Park YS, Knight EM, et al. (2009) The transcription unit architecture of the Escherichia coli genome. Nat Biotechnol 27: 1043-1049.
185. Albrecht M, Sharma CM, Reinhardt R, Vogel J, Rudel T (2010) Deep sequencing-based discovery of the Chlamydia trachomatis transcriptome. Nucleic Acids Res 38: 868-877.
186. Katsanis SH, Katsanis N (2013) Molecular genetic testing and the future of clinical genomics. Nat Rev Genet 14: 415-426.
187. Didelot X, Bowden R, Wilson DJ, Peto TE, Crook DW (2012) Transforming clinical microbiology with bacterial genome sequencing. Nat Rev Genet 13: 601-612.
188. Palmer AC, Kishony R (2013) Understanding, predicting and manipulating the genotypic evolution of antibiotic resistance. Nat Rev Genet 14: 243-248.
189. Winsor GL, Lam DK, Fleming L, Lo R, Whiteside MD, et al. (2011) Pseudomonas Genome Database: improved comparative analysis and population genomics capability for Pseudomonas genomes. Nucleic Acids Res 39: D596-600.
190. Woodcock DM, Crowther PJ, Doherty J, Jefferson S, DeCruz E, et al. (1989) Quantitative evaluation of Escherichia coli host strains for tolerance to cytosine methylation in plasmid and phage recombinants. Nucleic Acids Res 17: 3469-3478.
191. Simon R PU, Pühler A (1983) A broad host range mobilization system for in vivo genetic engineering: Transposon mutagenesis in gram negative bacteria. Biotechnology.
192. Liberati NT, Urbach JM, Miyata S, Lee DG, Drenkard E, et al. (2006) An ordered, nonredundant library of Pseudomonas aeruginosa strain PA14 transposon insertion mutants. Proc Natl Acad Sci U S A 103: 2833-2838.
193. Dötsch A, Eckweiler D, Schniederjans M, Zimmermann A, Jensen V, et al. (2012) The Pseudomonas aeruginosa transcriptome in planktonic cultures and static biofilms using RNA sequencing. PLoS One 7: e31092.
194. Yi H, Cho YJ, Won S, Lee JE, Jin Yu H, et al. (2011) Duplex-specific nuclease efficiently removes rRNA for prokaryotic RNA-seq. Nucleic Acids Res 39: e140.
195. Dabney J, Meyer M (2012) Length and GC-biases during sequencing library amplification: a comparison of various polymerase-buffer systems with ancient and modern DNA sequencing libraries. Biotechniques 52: 87-94.
196. Lunter G, Goodson M (2011) Stampy: a statistical algorithm for sensitive and fast mapping of Illumina sequence reads. Genome Res 21: 936-939.
197. Li H, Handsaker B, Wysoker A, Fennell T, Ruan J, et al. (2009) The Sequence Alignment/Map format and SAMtools. Bioinformatics 25: 2078-2079.
198. Anders S, Huber W (2010) Differential expression analysis for sequence count data. Genome Biol 11: R106.
199. Zerbino DR (2010) Using the Velvet de novo assembler for short-read sequencing technologies. Curr Protoc Bioinformatics Chapter 11: Unit 11 15.

200. Corpet F (1988) Multiple sequence alignment with hierarchical clustering. Nucleic Acids Res 16: 10881-10890.
201. Paradis E, Claude J, Strimmer K (2004) APE: Analyses of Phylogenetics and Evolution in R language. Bioinformatics 20: 289-290.
202. Huson DH, Scornavacca C (2012) Dendroscope 3: an interactive tool for rooted phylogenetic trees and networks. Syst Biol 61: 1061-1067.
203. Letunic I, Bork P (2011) Interactive Tree Of Life v2: online annotation and display of phylogenetic trees made easy. Nucleic Acids Res 39: W475-478.
204. Pruitt KD, Tatusova T, Maglott DR (2005) NCBI Reference Sequence (RefSeq): a curated non-redundant sequence database of genomes, transcripts and proteins. Nucleic Acids Res 33: D501-504.
205. NCBI Resource Coordinators (2013) Database resources of the National Center for Biotechnology Information. Nucleic Acids Res 41: D8-D20.
206. UniProt Consortium (2011) Ongoing and future developments at the Universal Protein Resource. Nucleic Acids Res 39: D214-219.
207. Punta M, Coggill PC, Eberhardt RY, Mistry J, Tate J, et al. (2012) The Pfam protein families database. Nucleic Acids Res 40: D290-301.
208. Lauretti L, Riccio ML, Mazzariol A, Cornaglia G, Amicosante G, et al. (1999) Cloning and characterization of blaVIM, a new integron-borne metallo-beta-lactamase gene from a Pseudomonas aeruginosa clinical isolate. Antimicrob Agents Chemother 43: 1584-1590.
209. Hoang TT, Karkhoff-Schweizer RR, Kutchma AJ, Schweizer HP (1998) A broad-host-range Flp-FRT recombination system for site-specific excision of chromosomally-located DNA sequences: application for isolation of unmarked Pseudomonas aeruginosa mutants. Gene 212: 77-86.
210. Ho SN, Hunt HD, Horton RM, Pullen JK, Pease LR (1989) Site-directed mutagenesis by overlap extension using the polymerase chain reaction. Gene 77: 51-59.
211. Larsen JE, Lund O, Nielsen M (2006) Improved method for predicting linear B-cell epitopes. Immunome Res 2: 2.
212. Brown TA (2002) Genomes: Garland Science, New York.
213. Peano C, Pietrelli A, Consolandi C, Rossi E, Petiti L, et al. (2013) An efficient rRNA removal method for RNA sequencing in GC-rich bacteria. Microb Inform Exp 3: 1.
214. He S, Wurtzel O, Singh K, Froula JL, Yilmaz S, et al. (2010) Validation of two ribosomal RNA removal methods for microbial metatranscriptomics. Nat Methods 7: 807-812.
215. Rutherford K, Parkhill J, Crook J, Horsnell T, Rice P, et al. (2000) Artemis: sequence visualization and annotation. Bioinformatics 16: 944-945.
216. Lee DG, Urbach JM, Wu G, Liberati NT, Feinbaum RL, et al. (2006) Genomic analysis reveals that Pseudomonas aeruginosa virulence is combinatorial. Genome Biol 7: R90.
217. Mathee K, Narasimhan G, Valdes C, Qiu X, Matewish JM, et al. (2008) Dynamics of Pseudomonas aeruginosa genome evolution. Proc Natl Acad Sci U S A 105: 3100-3105.
218. Winstanley C, Langille MG, Fothergill JL, Kukavica-Ibrulj I, Paradis-Bleau C, et al. (2009) Newly introduced genomic prophage islands are critical determinants of in vivo competitiveness in the Liverpool Epidemic Strain of Pseudomonas aeruginosa. Genome Res 19: 12-23.
219. Spencer DH, Kas A, Smith EE, Raymond CK, Sims EH, et al. (2003) Whole-genome sequence variation among multiple isolates of Pseudomonas aeruginosa. J Bacteriol 185: 1316-1325.
220. Kung VL, Ozer EA, Hauser AR (2010) The accessory genome of Pseudomonas aeruginosa. Microbiol Mol Biol Rev 74: 621-641.
221. Romling U, Wingender J, Muller H, Tümmler B (1994) A major Pseudomonas aeruginosa clone common to patients and aquatic habitats. Appl Environ Microbiol 60: 1734-1738.
222. Sefraoui I, Berrazeg M, Drissi M, Rolain JM (2013) Molecular Epidemiology of Carbapenem-Resistant Pseudomonas aeruginosa Clinical Strains Isolated from Western Algeria Between 2009 and 2012. Microb Drug Resist.
223. Wiehlmann L, Wagner G, Cramer N, Siebert B, Gudowius P, et al. (2007) Population structure of Pseudomonas aeruginosa. Proc Natl Acad Sci U S A 104: 8101-8106.
224. Oliveros JC (2007) VENNY. An interactive tool for comparing lists with Venn Diagrams.

225. Krzywinski M, Schein J, Birol I, Connors J, Gascoyne R, et al. (2009) Circos: an information aesthetic for comparative genomics. Genome Res 19: 1639-1645.
226. Llanes C, Köhler T, Patry I, Dehecq B, van Delden C, et al. (2011) Role of the MexEF-OprN efflux system in low-level resistance of Pseudomonas aeruginosa to ciprofloxacin. Antimicrob Agents Chemother 55: 5676-5684.
227. Zaoui C, Overhage J, Löns D, Zimmermann A, Müsken M, et al. (2012) An orphan sensor kinase controls quinolone signal production via MexT in Pseudomonas aeruginosa. Mol Microbiol 83: 536-547.
228. Westfall LW, Carty NL, Layland N, Kuan P, Colmer-Hamood JA, et al. (2006) mvaT mutation modifies the expression of the Pseudomonas aeruginosa multidrug efflux operon mexEF-oprN. FEMS Microbiol Lett 255: 247-254.
229. Balasubramanian D, Schneper L, Merighi M, Smith R, Narasimhan G, et al. (2012) The regulatory repertoire of Pseudomonas aeruginosa AmpC β-lactamase regulator AmpR includes virulence genes. PLoS One 7: e34067.
230. Nakada Y, Itoh Y (2002) Characterization and regulation of the gbuA gene, encoding guanidinobutyrase in the arginine dehydrogenase pathway of Pseudomonas aeruginosa PAO1. J Bacteriol 184: 3377-3384.
231. Avison MB, Horton RE, Walsh TR, Bennett PM (2001) Escherichia coli CreBC is a global regulator of gene expression that responds to growth in minimal media. J Biol Chem 276: 26955-26961.
232. Lin CW, Lin HC, Huang YW, Chung TC, Yang TC (2011) Inactivation of mrcA gene derepresses the basal-level expression of L1 and L2 beta-lactamases in Stenotrophomonas maltophilia. J Antimicrob Chemother 66: 2033-2037.
233. Abdelraouf K, Kabbara S, Ledesma KR, Poole K, Tam VH (2011) Effect of multidrug resistance-conferring mutations on the fitness and virulence of Pseudomonas aeruginosa. J Antimicrob Chemother 66: 1311-1317.
234. Olivares J, Bernardini A, Garcia-Leon G, Corona F, M BS, et al. (2013) The intrinsic resistome of bacterial pathogens. Front Microbiol 4: 103.
235. Lopez E, Elez M, Matic I, Blazquez J (2007) Antibiotic-mediated recombination: ciprofloxacin stimulates SOS-independent recombination of divergent sequences in Escherichia coli. Mol Microbiol 64: 83-93.
236. Zamorano L, Reeve TM, Deng L, Juan C, Moya B, et al. (2010) NagZ inactivation prevents and reverts beta-lactam resistance, driven by AmpD and PBP 4 mutations, in Pseudomonas aeruginosa. Antimicrob Agents Chemother 54: 3557-3563.
237. Blake KL, O'Neill AJ (2013) Transposon library screening for identification of genetic loci participating in intrinsic susceptibility and acquired resistance to antistaphylococcal agents. J Antimicrob Chemother 68: 12-16.
238. Parkins MD, Ceri H, Storey DG (2001) Pseudomonas aeruginosa GacA, a factor in multihost virulence, is also essential for biofilm formation. Mol Microbiol 40: 1215-1226.
239. Kanehisa M, Goto S, Sato Y, Kawashima M, Furumichi M, et al. (2014) Data, information, knowledge and principle: back to metabolism in KEGG. Nucleic Acids Res 42: D199-205.
240. Fuhrer T, Fischer E, Sauer U (2005) Experimental identification and quantification of glucose metabolism in seven bacterial species. J Bacteriol 187: 1581-1590.
241. Romero P, Karp P (2003) PseudoCyc, a pathway-genome database for Pseudomonas aeruginosa. J Mol Microbiol Biotechnol 5: 230-239.
242. World Health Organization (2012) The evolving threat of antimicrobial resistance: options for action.
243. Hegreness M, Shoresh N, Damian D, Hartl D, Kishony R (2008) Accelerated evolution of resistance in multidrug environments. Proc Natl Acad Sci U S A 105: 13977-13981.
244. MacKenzie FM, Bruce J, Struelens MJ, Goossens H, Mollison J, et al. (2007) Antimicrobial drug use and infection control practices associated with the prevalence of methicillin-resistant Staphylococcus aureus in European hospitals. Clin Microbiol Infect 13: 269-276.

245. Furtado GH, Perdiz LB, Onita JH, Wey SB, Medeiros EA (2010) Correlation between rates of carbapenem consumption and the prevalence of carbapenem-resistant Pseudomonas aeruginosa in a tertiary care hospital in Brazil: a 4-year study. Infect Control Hosp Epidemiol 31: 664-666.
246. Meyer E, Schwab F, Schroeren-Boersch B, Gastmeier P (2010) Dramatic increase of third-generation cephalosporin-resistant E. coli in German intensive care units: secular trends in antibiotic drug use and bacterial resistance, 2001 to 2008. Crit Care 14: R113.
247. Polk RE, Johnson CK, McClish D, Wenzel RP, Edmond MB (2004) Predicting hospital rates of fluoroquinolone-resistant Pseudomonas aeruginosa from fluoroquinolone use in US hospitals and their surrounding communities. Clin Infect Dis 39: 497-503.
248. Weng TC, Chen YH, Lee CC, Wang CY, Lai CC, et al. (2011) Correlation between fluoroquinolone consumption in hospitals and ciprofloxacin resistance amongst Pseudomonas aeruginosa isolates causing healthcare-associated infections, Taiwan, 2000-2009. Int J Antimicrob Agents 37: 581-584.
249. Hsueh PR, Chen WH, Luh KT (2005) Relationships between antimicrobial use and antimicrobial resistance in Gram-negative bacteria causing nosocomial infections from 1991-2003 at a university hospital in Taiwan. Int J Antimicrob Agents 26: 463-472.
250. Gasink LB, Edelstein PH, Lautenbach E, Synnestvedt M, Fishman NO (2009) Risk factors and clinical impact of Klebsiella pneumoniae carbapenemase-producing K. pneumoniae. Infect Control Hosp Epidemiol 30: 1180-1185.
251. Lepelletier D, Cady A, Caroff N, Marraillac J, Reynaud A, et al. (2010) Imipenem-resistant Pseudomonas aeruginosa gastrointestinal carriage among hospitalized patients: risk factors and resistance mechanisms. Diagn Microbiol Infect Dis 66: 1-6.
252. Enne VI, Livermore DM, Stephens P, Hall LM (2001) Persistence of sulphonamide resistance in Escherichia coli in the UK despite national prescribing restriction. Lancet 357: 1325-1328.
253. Sundqvist M, Geli P, Andersson DI, Sjolund-Karlsson M, Runehagen A, et al. (2010) Little evidence for reversibility of trimethoprim resistance after a drastic reduction in trimethoprim use. J Antimicrob Chemother 65: 350-360.
254. Canton R, Morosini MI (2011) Emergence and spread of antibiotic resistance following exposure to antibiotics. FEMS Microbiol Rev 35: 977-991.
255. Kummerer K (2009) Antibiotics in the aquatic environment--a review--part I. Chemosphere 75: 417-434.
256. European Surveillance of Antibiotic Consumption ESAC (2009) Final management report 2009-2010.
257. Goossens H, Ferech M, Vander Stichele R, Elseviers M, Group EP (2005) Outpatient antibiotic use in Europe and association with resistance: a cross-national database study. Lancet 365: 579-587.
258. Baquero F (2001) Low-level antibacterial resistance: a gateway to clinical resistance. Drug Resist Updat 4: 93-105.
259. Kummerer K, Henninger A (2003) Promoting resistance by the emission of antibiotics from hospitals and households into effluent. Clin Microbiol Infect 9: 1203-1214.
260. Larsson DG, de Pedro C, Paxeus N (2007) Effluent from drug manufactures contains extremely high levels of pharmaceuticals. J Hazard Mater 148: 751-755.
261. Christiana T, Schneidera RJ, Färberb HA, Skutlarekb D, Meyerc MT, et al. (2003) Determination of Antibiotic Residues in Manure, Soil, and Surface Waters. Acta hydrochim hydrobiol 31: 36–44.
262. Subbiah M, Mitchell SM, Ullman JL, Call DR (2011) beta-lactams and florfenicol antibiotics remain bioactive in soils while ciprofloxacin, neomycin, and tetracycline are neutralized. Appl Environ Microbiol 77: 7255-7260.
263. Andrews JM (2001) Determination of minimum inhibitory concentrations. J Antimicrob Chemother 48 Suppl 1: 5-16.
264. Turnidge J, Paterson DL (2007) Setting and revising antibacterial susceptibility breakpoints. Clin Microbiol Rev 20: 391-408, table of contents.

265. CLSI (2013) Performance Standards for Antimicrobial Susceptibility Testing; Twenty-Third Informational Supplement. Wayne, PA: Clinical and Laboratory Standards Institute.
266. Juan C, Conejo MC, Tormo N, Gimeno C, Pascual A, et al. (2013) Challenges for accurate susceptibility testing, detection and interpretation of beta-lactam resistance phenotypes in Pseudomonas aeruginosa: results from a Spanish multicentre study. J Antimicrob Chemother 68: 619-630.
267. European Committee on Antimicrobial Susceptibility Testing E (2014) Clinical breakpoints - bacteria. European Society of Clinical Microbiology and Infectous Diseases.
268. Rodriguez-Martinez JM, Briales A, Velasco C, Diaz de Alba P, Martinez-Martinez L, et al. (2011) Discrepancies in fluoroquinolone clinical categories between the European Committee on Antimicrobial Susceptibility Testing (EUCAST) and CLSI for Escherichia coli harbouring qnr genes and mutations in gyrA and parC. J Antimicrob Chemother 66: 1405-1407.
269. Zhao X, Drlica K (2008) A unified anti-mutant dosing strategy. J Antimicrob Chemother 62: 434-436.
270. Rodriguez-Martinez JM, Velasco C, Garcia I, Cano ME, Martinez-Martinez L, et al. (2007) Mutant prevention concentrations of fluoroquinolones for Enterobacteriaceae expressing the plasmid-carried quinolone resistance determinant qnrA1. Antimicrob Agents Chemother 51: 2236-2239.
271. Luo Y, Li J, Meng Y, Ma Y, Hu C, et al. (2011) Joint effects of topoisomerase alterations and plasmid-mediated quinolone-resistant determinants in Salmonella enterica Typhimurium. Microb Drug Resist 17: 1-5.
272. Briales A, Rodriguez-Martinez JM, Velasco C, Diaz de Alba P, Dominguez-Herrera J, et al. (2011) In vitro effect of qnrA1, qnrB1, and qnrS1 genes on fluoroquinolone activity against isogenic Escherichia coli isolates with mutations in gyrA and parC. Antimicrob Agents Chemother 55: 1266-1269.
273. Morar M, Wright GD (2010) The genomic enzymology of antibiotic resistance. Annu Rev Genet 44: 25-51.
274. Perkins TT, Kingsley RA, Fookes MC, Gardner PP, James KD, et al. (2009) A strand-specific RNA-Seq analysis of the transcriptome of the typhoid bacillus Salmonella typhi. PLoS Genet 5: e1000569.
275. Dötsch A, Becker T, Pommerenke C, Magnowska Z, Jansch L, et al. (2009) Genomewide identification of genetic determinants of antimicrobial drug resistance in Pseudomonas aeruginosa. Antimicrob Agents Chemother 53: 2522-2531.
276. Giannoukos G, Ciulla DM, Huang K, Haas BJ, Izard J, et al. (2012) Efficient and robust RNA-seq process for cultured bacteria and complex community transcriptomes. Genome Biol 13: R23.
277. Haas BJ, Chin M, Nusbaum C, Birren BW, Livny J (2012) How deep is deep enough for RNA-Seq profiling of bacterial transcriptomes? BMC Genomics 13: 734.
278. Wang D, Seeve C, Pierson LS, 3rd, Pierson EA (2013) Transcriptome profiling reveals links between ParS/ParR, MexEF-OprN, and quorum sensing in the regulation of adaptation and virulence in Pseudomonas aeruginosa. BMC Genomics 14: 618.
279. Minoche AE, Dohm JC, Himmelbauer H (2011) Evaluation of genomic high-throughput sequencing data generated on Illumina HiSeq and genome analyzer systems. Genome Biol 12: R112.
280. Priest FG, Barker M, Baillie LW, Holmes EC, Maiden MC (2004) Population structure and evolution of the Bacillus cereus group. J Bacteriol 186: 7959-7970.
281. Jolley KA, Bliss CM, Bennett JS, Bratcher HB, Brehony C, et al. (2012) Ribosomal multilocus sequence typing: universal characterization of bacteria from domain to strain. Microbiology 158: 1005-1015.
282. Hocquet D, Plesiat P, Dehecq B, Mariotte P, Talon D, et al. (2010) Nationwide investigation of extended-spectrum beta-lactamases, metallo-beta-lactamases, and extended-spectrum oxacillinases produced by ceftazidime-resistant Pseudomonas aeruginosa strains in France. Antimicrob Agents Chemother 54: 3512-3515.

283. Kaase M (2012) [Carbapenemases in gram-negative bacteria. Current data and trends of resistance resulting from the work of national reference centres]. Bundesgesundheitsblatt Gesundheitsforschung Gesundheitsschutz 55: 1401-1404.
284. Castanheira M, Deshpande LM, Costello A, Davies TA, Jones RN (2014) Epidemiology and carbapenem resistance mechanisms of carbapenem-non-susceptible Pseudomonas aeruginosa collected during 2009-11 in 14 European and Mediterranean countries. J Antimicrob Chemother.
285. Peter S, Lacher A, Marschal M, Holzl F, Buhl M, et al. (2014) Evaluation of phenotypic detection methods for metallo-beta-lactamases (MBLs) in clinical isolates of Pseudomonas aeruginosa. Eur J Clin Microbiol Infect Dis.
286. Zander E, Fernandez-Gonzalez A, Schleicher X, Dammhayn C, Kamolvit W, et al. (2014) Worldwide dissemination of acquired carbapenem-hydrolysing class D beta-lactamases in Acinetobacter spp. other than Acinetobacter baumannii. Int J Antimicrob Agents 43: 375-377.
287. Mark BL, Vocadlo DJ, Oliver A (2011) Providing beta-lactams a helping hand: targeting the AmpC beta-lactamase induction pathway. Future Microbiol 6: 1415-1427.
288. Vettoretti L, Plesiat P, Muller C, El Garch F, Phan G, et al. (2009) Efflux unbalance in Pseudomonas aeruginosa isolates from cystic fibrosis patients. Antimicrob Agents Chemother 53: 1987-1997.
289. Satake S, Yoshihara E, Nakae T (1990) Diffusion of beta-lactam antibiotics through liposome membranes reconstituted from purified porins of the outer membrane of Pseudomonas aeruginosa. Antimicrob Agents Chemother 34: 685-690.
290. Balasubramanian D, Kumari H, Jaric M, Fernandez M, Turner KH, et al. (2014) Deep sequencing analyses expands the Pseudomonas aeruginosa AmpR regulon to include small RNA-mediated regulation of iron acquisition, heat shock and oxidative stress response. Nucleic Acids Res 42: 979-998.
291. Kumari H, Balasubramanian D, Zincke D, Mathee K (2014) Role of Pseudomonas aeruginosa AmpR on beta-lactam and non-beta-lactam transient cross-resistance upon pre-exposure to subinhibitory concentrations of antibiotics. J Med Microbiol 63: 544-555.
292. Okamoto K, Gotoh N, Tsujimoto H, Yamada H, Yoshihara E, et al. (1999) Molecular cloning and characterization of the oprQ gene coding for outer membrane protein OprE3 of Pseudomonas aeruginosa. Microbiol Immunol 43: 297-301.
293. Lieberman TD, Michel JB, Aingaran M, Potter-Bynoe G, Roux D, et al. (2011) Parallel bacterial evolution within multiple patients identifies candidate pathogenicity genes. Nat Genet 43: 1275-1280.
294. McAdam PR, Holmes A, Templeton KE, Fitzgerald JR (2011) Adaptive evolution of Staphylococcus aureus during chronic endobronchial infection of a cystic fibrosis patient. PLoS One 6: e24301.
295. Mwangi MM, Wu SW, Zhou Y, Sieradzki K, de Lencastre H, et al. (2007) Tracking the in vivo evolution of multidrug resistance in Staphylococcus aureus by whole-genome sequencing. Proc Natl Acad Sci U S A 104: 9451-9456.
296. Gordon NC, Price JR, Cole K, Everitt R, Morgan M, et al. (2014) Prediction of Staphylococcus aureus Antimicrobial Resistance by Whole-Genome Sequencing. J Clin Microbiol 52: 1182-1191.
297. Stanssens P, Zabeau M, Meersseman G, Remes G, Gansemans Y, et al. (2004) High-throughput MALDI-TOF discovery of genomic sequence polymorphisms. Genome Res 14: 126-133.
298. Johansen P, Andersen JD, Borsting C, Morling N (2013) Evaluation of the iPLEX(R) Sample ID Plus Panel designed for the Sequenom MassARRAY(R) system. A SNP typing assay developed for human identification and sample tracking based on the SNPforID panel. Forensic Sci Int Genet 7: 482-487.
299. Lee SH, Li CF, Lin HY, Lin CH, Liu HC, et al. (2014) High-throughput detection of common sequence variations of Fabry disease in Taiwan using DNA mass spectrometry. Mol Genet Metab 111: 507-512.

300. Wu Z, Zheng W, Xu J, Sun F, Chen H, et al. (2014) IL10 polymorphisms associated with Behcet's disease in Chinese Han. Hum Immunol 75: 271-276.
301. Earp MA, Brooks-Wilson A, Cook L, Le N (2013) Inherited common variants in mitochondrial DNA and invasive serous epithelial ovarian cancer risk. BMC Res Notes 6: 425.
302. Guan YP, Yang XX, Yao GY, Qiu F, Chen J, et al. (2014) Breast cancer association studies in a Han Chinese population using 10 European-ancestry-associated breast cancer susceptibility SNPs. Asian Pac J Cancer Prev 15: 85-91.
303. Trembizki E, Smith H, Lahra MM, Chen M, Donovan B, et al. (2014) High-throughput informative single nucleotide polymorphism-based typing of Neisseria gonorrhoeae using the Sequenom MassARRAY iPLEX platform. J Antimicrob Chemother.
304. Sparbier K, Schubert S, Weller U, Boogen C, Kostrzewa M (2012) Matrix-assisted laser desorption ionization-time of flight mass spectrometry-based functional assay for rapid detection of resistance against beta-lactam antibiotics. J Clin Microbiol 50: 927-937.
305. Wang L, Han C, Sui W, Wang M, Lu X (2013) MALDI-TOF MS applied to indirect carbapenemase detection: a validated procedure to clearly distinguish between carbapenemase-positive and carbapenemase-negative bacterial strains. Anal Bioanal Chem 405: 5259-5266.
306. Jung JS, Popp C, Sparbier K, Lange C, Kostrzewa M, et al. (2014) Evaluation of matrix-assisted laser desorption ionization-time of flight mass spectrometry for rapid detection of beta-lactam resistance in Enterobacteriaceae derived from blood cultures. J Clin Microbiol 52: 924-930.
307. Hrabak J, Chudackova E, Walkova R (2013) Matrix-assisted laser desorption ionization-time of flight (maldi-tof) mass spectrometry for detection of antibiotic resistance mechanisms: from research to routine diagnosis. Clin Microbiol Rev 26: 103-114.
308. Drlica K (2003) The mutant selection window and antimicrobial resistance. J Antimicrob Chemother 52: 11-17.
309. Drlica K, Zhao X (2007) Mutant selection window hypothesis updated. Clin Infect Dis 44: 681-688.
310. Negri MC, Lipsitch M, Blazquez J, Levin BR, Baquero F (2000) Concentration-dependent selection of small phenotypic differences in TEM beta-lactamase-mediated antibiotic resistance. Antimicrob Agents Chemother 44: 2485-2491.
311. Liu A, Fong A, Becket E, Yuan J, Tamae C, et al. (2011) Selective advantage of resistant strains at trace levels of antibiotics: a simple and ultrasensitive color test for detection of antibiotics and genotoxic agents. Antimicrob Agents Chemother 55: 1204-1210.
312. Gullberg E, Cao S, Berg OG, Ilback C, Sandegren L, et al. (2011) Selection of resistant bacteria at very low antibiotic concentrations. PLoS Pathog 7: e1002158.
313. Demple B, Harrison L (1994) Repair of oxidative damage to DNA: enzymology and biology. Annu Rev Biochem 63: 915-948.
314. Lapouge K, Schubert M, Allain FH, Haas D (2008) Gac/Rsm signal transduction pathway of gamma-proteobacteria: from RNA recognition to regulation of social behaviour. Mol Microbiol 67: 241-253.
315. Goodman AL, Kulasekara B, Rietsch A, Boyd D, Smith RS, et al. (2004) A signaling network reciprocally regulates genes associated with acute infection and chronic persistence in Pseudomonas aeruginosa. Dev Cell 7: 745-754.
316. Brencic A, McFarland KA, McManus HR, Castang S, Mogno I, et al. (2009) The GacS/GacA signal transduction system of Pseudomonas aeruginosa acts exclusively through its control over the transcription of the RsmY and RsmZ regulatory small RNAs. Mol Microbiol 73: 434-445.
317. Arai H, Kodama T, Igarashi Y (1997) Cascade regulation of the two CRP/FNR-related transcriptional regulators (ANR and DNR) and the denitrification enzymes in Pseudomonas aeruginosa. Mol Microbiol 25: 1141-1148.
318. Zimmermann A, Reimmann C, Galimand M, Haas D (1991) Anaerobic growth and cyanide synthesis of Pseudomonas aeruginosa depend on anr, a regulatory gene homologous with fnr of Escherichia coli. Mol Microbiol 5: 1483-1490.

319. Schobert M, Jahn D (2010) Anaerobic physiology of Pseudomonas aeruginosa in the cystic fibrosis lung. Int J Med Microbiol 300: 549-556.
320. Unden G, Schirawski J (1997) The oxygen-responsive transcriptional regulator FNR of Escherichia coli: the search for signals and reactions. Mol Microbiol 25: 205-210.
321. Imlay JA, Chin SM, Linn S (1988) Toxic DNA damage by hydrogen peroxide through the Fenton reaction in vivo and in vitro. Science 240: 640-642.
322. Imlay JA, Linn S (1988) DNA damage and oxygen radical toxicity. Science 240: 1302-1309.
323. Yeom J, Imlay JA, Park W (2010) Iron homeostasis affects antibiotic-mediated cell death in Pseudomonas species. J Biol Chem 285: 22689-22695.
324. Liu Y, Liu X, Qu Y, Wang X, Li L, et al. (2012) Inhibitors of reactive oxygen species accumulation delay and/or reduce the lethality of several antistaphylococcal agents. Antimicrob Agents Chemother 56: 6048-6050.
325. Sampson TR, Liu X, Schroeder MR, Kraft CS, Burd EM, et al. (2012) Rapid killing of Acinetobacter baumannii by polymyxins is mediated by a hydroxyl radical death pathway. Antimicrob Agents Chemother 56: 5642-5649.
326. Wang X, Zhao X (2009) Contribution of oxidative damage to antimicrobial lethality. Antimicrob Agents Chemother 53: 1395-1402.
327. Livermore DM (2003) Bacterial resistance: origins, epidemiology, and impact. Clin Infect Dis 36: S11-23.
328. Lee HH, Molla MN, Cantor CR, Collins JJ (2010) Bacterial charity work leads to population-wide resistance. Nature 467: 82-85.
329. Hughes D, Andersson DI (2012) Selection of resistance at lethal and non-lethal antibiotic concentrations. Curr Opin Microbiol 15: 555-560.
330. Vlasits J, Jakopitsch C, Schwanninger M, Holubar P, Obinger C (2007) Hydrogen peroxide oxidation by catalase-peroxidase follows a non-scrambling mechanism. FEBS Lett 581: 320-324.
331. Nguyen D, Joshi-Datar A, Lepine F, Bauerle E, Olakanmi O, et al. (2011) Active starvation responses mediate antibiotic tolerance in biofilms and nutrient-limited bacteria. Science 334: 982-986.
332. Jensen PO, Briales A, Brochmann RP, Wang H, Kragh KN, et al. (2013) Formation of hydroxyl radicals contributes to the bactericidal activity of ciprofloxacin against Pseudomonas aeruginosa biofilms. Pathog Dis.

Danksagung

Zuerst möchte ich mich bei Prof. Dr. Susanne Häußler für die Möglichkeit, dieses spannende Projekt in ihrer Abteilung bearbeiten zu dürfen sowie für die Übernahme des Korreferates und die intensive und stets enthusiastische Betreuung während meiner Doktorandenzeit bedanken.

Weiterer Dank geht an Prof. Dr. Michael Steinert für die Übernahme des Hauptreferates und der Mentorenschaft sowie Prof. Dr. Dietmar Schomburg für die Übernahme des Prüfungsvorsitzes.

Außerdem möchte ich mich bei der gesamten Arbeitsgruppe Molekulare Bakteriologie für die ausgesprochen gute Arbeitsatmosphäre und stete Hilfsbereitschaft bedanken.
Vor allem Piotr Bielecki, Monika Schniederjans, Sebastian Bruchmann und Agata Bielecka für viele anregende Diskussionen sowie unseren Bioinformatikern Andreas Dötsch, Denitsa Eckweiler, Sarah Pohl, Klaus Hornischer und Uthayakumar Muthukumarasamy für ihre Unterstützung bei der Datenanalyse.

Vielen Dank auch an Frank Klawonn für die hilfreichen Vorschläge zur statistischen Betrachtung meiner Daten sowie Wolf-Rainer Abraham und Esther Surges für die intensive Kooperation zur Untersuchung metabolischer Effekte durch geringe Antibiotikakonzentrationen.
Ebenso danke ich Lothar Jänsch und Josef Wissing für ihre Zusammenarbeit zur Durchführung der massensprektrometrischen Analysen.

Ein weiterer Dank geht an die HZI Graduiertenschule, welche die Weiterbildung während meiner Doktorandenzeit sowohl finanziell als auch durch viele interessante Tagungen, Kursangebote, Seminare und Vernetzungen sehr bereichert hat.

Ein letzter, aber besonders wichtiger Dank gilt meiner Familie und meinem Mann Frederik für die uneingeschränkte Unterstützung während der letzten dreieinhalb Jahre sowie meiner TU-Connection Dagmar für den regen biologischen und nicht-biologischen Austausch.